NAVAL POSTGRADUATE SCHOOL
Monterey, California

DISSERTATION

THEORY OF MULTIRATE SIGNAL PROCESSING WITH APPLICATION TO SIGNAL AND IMAGE RECONSTRUCTION

by

James W. Scrofani

September 2005

Dissertation Supervisor: Charles W. Therrien

Approved for public release; distribution is unlimited.

THIS PAGE INTENTIONALLY LEFT BLANK

REPORT DOCUMENTATION PAGE

Form Approved OMB No. 0704-0188

1. AGENCY USE ONLY (*Leave blank*)	2. REPORT DATE	3. REPORT TYPE AND DATES COVERED
	September 2005	Doctoral Dissertation

4. TITLE AND SUBTITLE Theory of Multirate Signal Processing with Application to Signal and Image Reconstruction

5. FUNDING NUMBERS

6. AUTHORS Scrofani, James W.

7. PERFORMING ORGANIZATION NAME(S) AND ADDRESS(ES)
Naval Postgraduate School
Monterey CA 93943-5000

8. PERFORMING ORGANIZATION REPORT NUMBER

9. SPONSORING/MONITORING AGENCY NAME(S) AND ADDRESS(ES)

10. SPONSORING/MONITORING AGENCY REPORT NUMBER

11. SUPPLEMENTARY NOTES The views expressed in this thesis are those of the author and do not reflect the official policy or position of the Department of Defense or the U.S. Government.

12a. DISTRIBUTION/AVAILABILITY STATEMENT
Approved for public release; distribution is unlimited.

12b. DISTRIBUTION CODE

13. ABSTRACT(*maximum 200 words*)

Signal processing methods for signals sampled at different rates are investigated and applied to the problem of signal and image reconstruction or super-resolution reconstruction. The problem is approached from the viewpoint of linear mean-square estimation theory and multirate signal processing for one- and two-dimensional signals. A new look is taken at multirate system theory in one and two dimensions which provides the framework for these methodologies. A careful analysis of linear optimal filtering for problems involving different input and output sampling rates is conducted. This results in the development of index mapping techniques that simplify the formulation of Wiener-Hopf equations whose solution determine the optimal filters. The required filters exhibit periodicity in both one and two dimensions, due to the difference in sampling rates. The reconstruction algorithms developed are applied to one- and two-dimensional reconstruction problems.

14. SUBJECT TERMS Multirate Signal Processing, Linear Estimation, Signal Reconstruction, Number Theory

15. NUMBER OF PAGES 155

16. PRICE CODE

17. SECURITY CLASSIFICATION OF REPORT	18. SECURITY CLASSIFICATION OF THIS PAGE	19. SECURITY CLASSIFICATION OF ABSTRACT	20. LIMITATION OF ABSTRACT
Unclassified	Unclassified	Unclassified	UL

NSN 7540-01-280-5500 Standard Form 298 (Rev. 2-89)
Prescribed by ANSI Std. 239-18 298-102

THIS PAGE INTENTIONALLY LEFT BLANK

Approved for public release; distribution is unlimited

THEORY OF MULTIRATE SIGNAL PROCESSING WITH APPLICATION TO SIGNAL AND IMAGE RECONSTRUCTION

James W. Scrofani
Commander, United States Navy
B.S., University of Florida, 1987
M.S., Naval Postgraduate School, 1997

Submitted in partial fulfillment of the
requirements for the degree of

DOCTOR OF PHILOSOPHY IN ELECTRICAL ENGINEERING

from the

NAVAL POSTGRADUATE SCHOOL
September 2005

Author: James W. Scrofani

Approved by: Charles W. Therrien, Professor of Electrical Engineering
Dissertation Supervisor and Committee Chair

Roberto Cristi Professor of Electrical Engineering	Murali Tummala Professor of Electrical Engineering
Carlos F. Borges Associate Professor of Mathematics	Robert G. Hutchins Associate Professor of Electrical Engineering

Approved by: Jeffrey B. Knorr, Chair, Department of Electrical and Computer Engineering

Approved by: Knox T .Millsaps, Associate Provost for Academic Affairs

THIS PAGE INTENTIONALLY LEFT BLANK

ABSTRACT

Signal processing methods for signals sampled at different rates are investigated and applied to the problem of signal and image reconstruction or super-resolution reconstruction. The problem is approached from the viewpoint of linear mean-square estimation theory and multirate signal processing for one- and two-dimensional signals. A new look is taken at multirate system theory in one and two dimensions which provides the framework for these methodologies. A careful analysis of linear optimal filtering for problems involving different input and output sampling rates is conducted. This results in the development of index mapping techniques that simplify the formulation of Wiener-Hopf equations whose solution determine the optimal filters. The required filters exhibit periodicity in both one and two dimensions, due to the difference in sampling rates. The reconstruction algorithms developed are applied to one- and two-dimensional reconstruction problems.

THIS PAGE INTENTIONALLY LEFT BLANK

TABLE OF CONTENTS

LIST OF FIGURES

LIST OF TABLES

THIS PAGE INTENTIONALLY LEFT BLANK

EXECUTIVE SUMMARY

As physical and manufacturing limitations are reached in state-of-the-art image acquisition systems, there is increased motivation to improve the resolution of imagery through signal processing methods. High-resolution (HR) imagery is desirable because it can offer more detail about the object associated with the imagery. The "extra" information is of critical importance in many applications. For example, HR reconnaissance images can provide intelligence analysts, greater information about a military target, including its capabilities, operability and vulnerabilities, and increase analysts' confidence in such assessments. Likewise, HR medical images can be crucial to a physician in making a proper diagnosis or developing a suitable treatment regimen.

Super-resolution (SR) image reconstruction is an approach to this problem, and this area of research encompasses those signal processing techniques that use multiple low-resolution (LR) images to form a HR image of some related object. In this work, a super-resolution image reconstruction approach is proposed from the viewpoint of estimation and multirate signal processing for two-dimensional signals or images.

Multirate signal processing theory deals with the analysis of a system comprised of multiple signals at different sampling rates and is fundamental to this research. An example of such a system is a sensor network that collects and processes data from various sensors, where the information from each sensor might be collected at a different rate. In developing this theory, a number of relationships between signals in a multirate system are identified. The critical finding is that all of the signals in a multirate system can be referred to a single "universal" rate for that system; therefore, many of the results of standard signal processing theory can be adapted to multirate systems through this observation.

The multirate theory developed here is applied to signal estimation, where one signal is estimated from some other related signal or signals. The desired signal may be corrupted by distortion or interference and is usually unobservable (at least at the moment when the estimate is desired). A typical signal estimation application is the recovery of a transmitted signal from a received signal that has been subject to distortion and is corrupted by noise.

SR image reconstruction can be viewed as a problem in signal estimation, where a related LR signal or signals is used to estimate an underlying HR signal. From this perspective, the observation signal or signals, and desired signal form a multirate system. This motivates the application of the theory of multirate systems to signal estimation and the resultant extension of single-rate signal estimation theory to the multirate case.

The particular branch of estimation theory applied in this work is optimal filtering, where the error in estimation is minimized by using a weighted set of the LR observation images to filter and estimate the HR image. The weights used in this linear estimate are called filter coefficients and application of this theory results in a set of equations that are solved to obtain these coefficients known as the Wiener-Hopf (WH) equations. In this research, the multirate WH equations are developed and shown to have a periodically time-dependent solution. Additionally, the concept of index mapping, an extension of the multirate theory, is developed to determine the required regions of the LR images required for estimation.

A new methodology is developed and presented, by application and extension of the results of multirate and optimal estimation theory to the problem of SR image reconstruction. This new method is applied to a set of LR images, and the resultant HR image is compared with results from standard interpolation methods. In every case, this method performed better than the standard methods.

ACKNOWLEDGMENTS

First, I thank my wife, Lori, the love of my life, who kept everything in order, while I was buried in books. My gratitude is deep, my love even deeper.

An excellent wife who can find?
She is far more precious than jewels.
The heart of her husband trusts in her.

I also thank my children, Sydni and Christian, for making me a proud father, I love you both, more than I say.

May our sons in their youth be like plants full grown
our daughters like corner pillars cut for the structure of a palace;

I am deeply indebted to my advisor, Dr. Charles Therrien, who inspired me toward loftier ideas and encouraged me to work even harder. I am thankful for his wisdom and insights during this research.

I also extend my appreciation to the other members of my committee: Dr. Carlos Borges, Dr. Roberto Cristi, Dr. Robert Hutchins, and Dr. Murali Tummala, all of whom challenged me and also encouraged me along the way, making this work much better than it would have been.

Finally, I am forever thankful for the faithful congregation of Covenant Orthodox Presbyterian Church, whose prayers and encouragement were greatly appreciated, and whose love will stay with us. Joel, thank you for faithfully preaching the gospel. Marty, thanks for all the coffees and talks "on what really matters." Richard, thanks for your encouragement, big smile and Matlab talk!

To God only wise, be glory through Jesus Christ forever. Amen.
Romans 16:26-28

THIS PAGE INTENTIONALLY LEFT BLANK

I. INTRODUCTION

As physical and manufacturing limitations are reached in state-of-the-art image acquisition systems, there is increased motivation to improve the resolution of imagery through signal processing methods. Improvements in this area have significant commercial and military application, and in this work a super-resolution image reconstruction approach is proposed from the viewpoint of estimation and multirate signal processing for two-dimensional signals.

A. PROBLEM STATEMENT/MOTIVATION

Super-resolution (SR) imaging has recently become an area of great interest in the image processing research community (see Section I.B.2). The ability to form a high-resolution (HR) image from a collection of subsampled images has a broad range of applications and has largely been motivated by physical and production limitations on existing image acquisition systems and the marginal costs associated with increased spatial resolution. Figure 1.1 depicts the SR concept where a collection of low-resolution (LR) images of a scene are superimposed on a HR grid, available for subsequent HR image reconstruction.

In this work, we propose a stochastic multirate approach to this problem, adapting and extending the work in [Ref. 6, 7, 8, 9] to one- and two-dimensional signals. The earlier work has focused on information fusion applications, i.e., on the combination of observations from multiple sensors to perform tracking, surveillance, classification or some other task. This work extends these concepts to reconstruction of one-dimensional signals and SR image reconstruction.

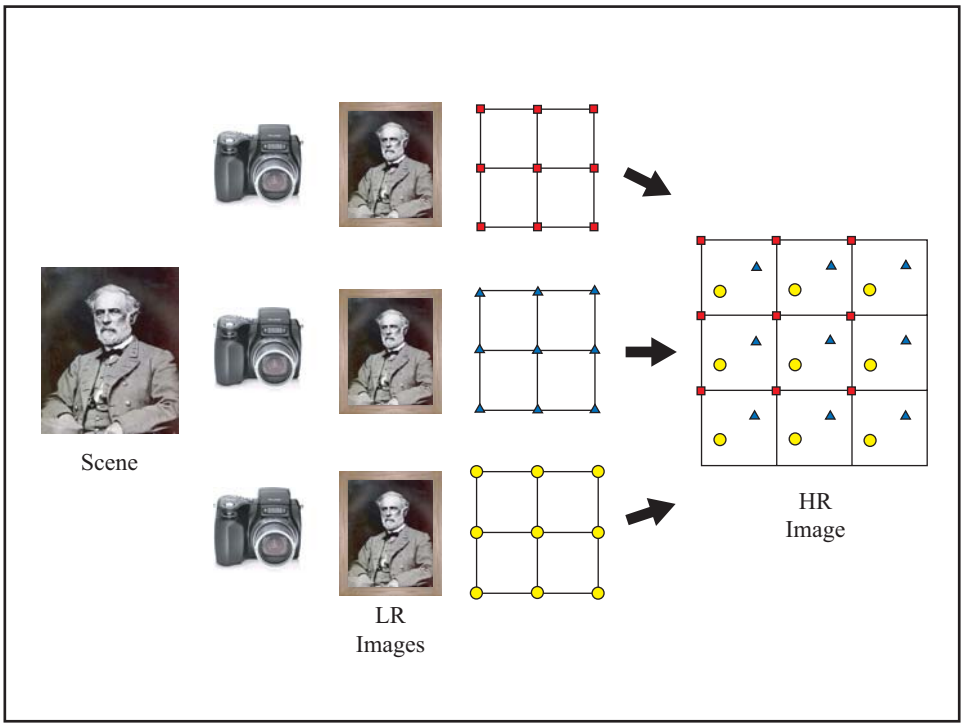

Figure 1.1. Super-resolution imaging concept, (After [Ref. 1]).

B. PREVIOUS WORK

1. Stochastic Multirate Signal Processing

Research in the area of stochastic multirate signal processing has been limited to a handful of investigators whose work has focused mainly on second moment analysis of stochastic systems, from both temporal and spectral points of view, and optimal estimation theory, including both Kalman and Weiner filtering theory.

Vaidyanathan *et al.* [Ref. 10, 11, 12] investigate how the statistical properties of stochastic signals are altered through multirate systems. In [Ref. 10], several facts and theorems are presented regarding the statistical behavior of signals as they are passed through decimators, interpolators, modulators, and more complicated inter-

connections. For example, the necessary and sufficient condition for the output of an L-fold interpolation filter to be wide-sense stationary (WSS), given a WSS input, is that the L-fold decimation of the filter coefficients results in no aliasing, i. e., the filter must have an alias-free (L) support. Additionally, the authors illustrate an application of this theoretical analysis to a multirate adaptive filtering scheme for identification of band-limited channels. In [Ref. 11], this work is continued but addressed using bifrequency maps and bispectra. These two-dimensional (2-D) Fourier transforms characterize all linear time-varying (LTV) systems and nonstationary random processes, respectively. In fact, by using these concepts, the previous results are simplified and even generalized to handle the case of vector systems. Finally, in [Ref. 12], further analysis is conducted using bifrequency maps and bispectra, and a bifrequency characterization of lossless LTV systems is derived.

Jahromi *et al.* [Ref. 13, 14, 15] consider methods to optimally estimate samples of a random signal based on observations made by multiple observers at different sampling rates (lower than the original rate). In particular, in [Ref. 13], the problem of fusing two low-rate sensors in the reconstruction of one high-resolution signal is considered when time delay of arrival (TDOA) is present. Using the "generalized cross-correlation" technique, the delay is estimated and then signal reconstruction is accomplished using perfect reconstruction synthesis filter bank theory. In [Ref. 14] and [Ref. 15], optimal least mean-square estimation is used to develop an estimate for samples of a high-rate signal. The estimator is a function of the power spectral density of the original random signal, which is obtained using a method for inductive inference of probability distribution referred to as the "maximum entropy principle" [Ref. 16].

Chen *et al.* [Ref. 17, 18, 19, 20] investigate use of the Kalman filter and Weiner filter in the reconstruction of a stochastic signal when only a noisy, downsampled version of the signal can be measured. In [Ref. 17], the use of the Kalman filter is investigated for interpolating and estimating values of an autoregressive or moving

average stochastic signal when only a noisy, downsampled version of the signal can be measured. The signal reconstruction problem is converted into a state estimation problem for which the Kalman filter is optimal. Some extensions are discussed, including the application of the Kalman reconstruction filter in recovering missing speech packets in a packet switching network with packet interleaving. Simulation results are presented, which indicate that the multirate Kalman reconstruction filters possess better reconstruction performance than a Wiener reconstruction filter under comparable numerical complexity. In [Ref. 18], a multirate deconvolution filter is proposed for signal reconstruction in multirate systems with channel noise. Both filter bank and transmultiplexer architectures are used to demonstrate the design procedure. In [Ref. 19], a block state-space model is introduced where transmultiplexer systems unify the multirate signals and channel noise. In [Ref. 20], the optimal signal reconstruction problem is considered in transmultiplexer systems under channel noise from the viewpoint of Wiener-Hopf theory. A calculus of variation method and a spectral factorization technique are used to develop an appropriate separation filter bank design.

Scharf *et al.* [Ref. 21] introduce a least squares design methodology for filtering periodically correlated (PC) scalar time series. Since any PC time series can be represented as a WSS vector time series where each constituent subsequence is a decimated version of the original shifted in time, and vice versa, multirate filter banks and equivalent polyphase realizations provide a natural representation for this bidirectional relationship. This relationship affords means to develop a spectral representation for the PC time series and hence develop causal synthesis and causal whitening filters for the PC scalar time series. These techniques are used to solve generalized linear minimum mean-square error (MMSE) filter design problems for PC scalar time series. Note that this viewpoint can be extended to multirate systems where the correlation between observation sequences is periodically correlated.

Therrien *et al.* [Ref. 6, 22, 7, 8, 9, 23] develop theory and methodology required for employing optimal linear filtering in estimating an underlying signal from observation sequences at different sampling rates. The focus of these efforts is on information fusion, i.e., on the combination of observations from multiple sensors to perform tracking, surveillance, classification or some other task. In particular, [Ref. 6], [Ref. 22] and [Ref. 7] consider a simplified problem where an underlying signal is estimated from two sequences, one observed at full rate and the other at half the rate. In [Ref. 8], least squares formulations are examined where the second sequence has an arbitrary sampling rate. In [Ref. 9], a general approach is suggested for any number of observation signals at arbitrary sampling rates. Finally, in [Ref. 23], previous theory and methods are developed to consider the problem of HR signal and image reconstruction. This work forms the basis for the proposed research and represents an advance in the area of super-resolution image reconstruction.

2. Super-Resolution Reconstruction/Imaging

Generally, super-resolution (SR) image reconstruction refers to signal processing methods in which a high-resolution (HR) image is obtained from a set or ensemble of observed low-resolution (LR) images [Ref. 1]. If each observed LR image is subsampled (and aliased) and is translated by a different subpixel amount, this set of unique observation images can be used for reconstruction. Figure 1.1 demonstrates this conceptually. Both [Ref. 1] and [Ref. 2] provide general surveys of research to date regarding this topic, and the following major areas of research are identified: nonuniform interpolation, frequency domain, regularized SR reconstruction, projection onto convex sets (POCS), maximum likelihood (ML) projection onto convex sets (ML-POCS) hybrid reconstruction, and other approaches [Ref. 1].

The most prevalent approaches in the literature are those based on nonuniform interpolation. These approaches typically use a three-stage sequential process, comprised of registration, interpolation, and restoration. The registration step is a mapping of pixels from each LR image to a reference grid, which results in a HR grid

comprised of a set of nonuniformly spaced pixels. The interpolation step conforms these nonuniformly spaced pixels to a uniform sampling grid, which results in the upsampled HR image. Finally, restoration removes the effects of sensor distortion and noise. This scheme is depicted in Figure 1.2. Representative works include [Ref. 24, 25, 26, 27].

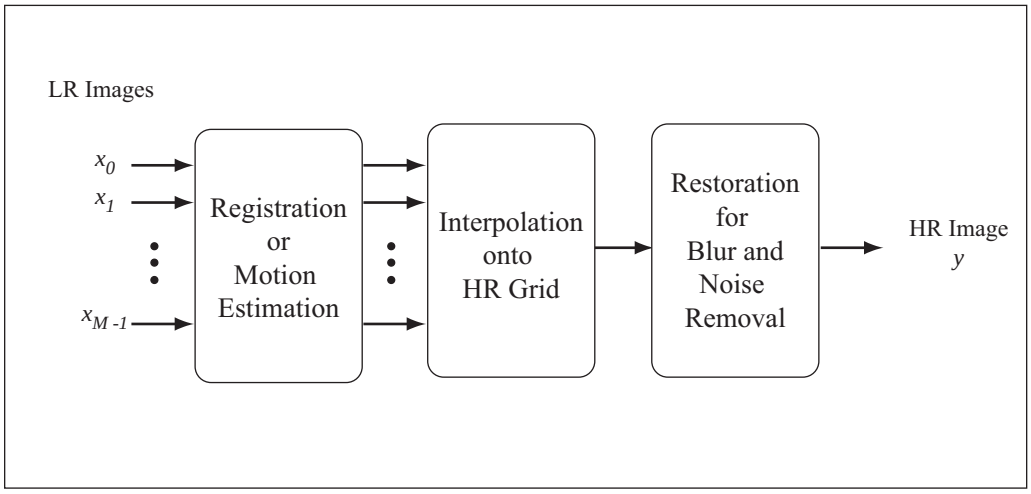

Figure 1.2. Typical model for nonuniform interpolation approach to SR, (From [Ref. 2]).

The frequency-domain approaches exploit the relationship between the discrete Fourier transforms (DFT) of the LR images and the continuous Fourier transform (CFT) of the desired HR image by using the information generated through relative motion between the LR images, the aliasing generated by downsampling relative to the desired HR image, and the assumption that the original HR image is bandlimited. A set of linear system equations are developed, and the continuous Fourier coefficients are found. The desired HR image is estimated from the CFT synthesis equation. Tsai and Huang [Ref. 28] were the first to introduce this method and were also the first researchers to address the problem of reconstructing a HR image from a set of translated LR images. Kim *et al.* [Ref. 29] extended this approach to include the presence of noise in the LR images using a recursive procedure based on weighted least squares theory. Kim and Su [Ref. 30] further extended this approach by consid-

ering noise and different blur distortions in the LR images. Vandewalle *et al.* [Ref. 31] consider offset estimation using a subspace minimization method followed by a frequency-based reconstruction method based on the continuous and discrete Fourier series.

The regularized SR reconstruction methods use regularization methods to solve the often ill-posed inverse problem introduced in the frequency-domain approaches. Typically, the ill-posed problems are a result of an insufficient number of LR images or ill-conditioned blur operators [Ref. 1]. Generally, two approaches have been considered: deterministic and stochastic regularization. Deterministic approaches [Ref. 32, 33, 34, 35] typically use constrained least squares methods (CLS) while stochastic approaches [Ref. 36, 37, 38] typically use maximum *a posteriori* (MAP) or maximum likelihood (ML) methods.

POCS methods are based on set theoretic estimation theory [Ref. 39]. Rather than using conventional estimation theory, the POCS formulations incorporate *a priori* knowledge into the solution and yield a solution consistent with user-furnished constraints. Application of this method as applied to SR was introduced by Stark and Oskoui [Ref. 40] and extended by Tekalp *et al.* in [Ref. 41, 42], which takes into account the presence of both sensor blurring and observation noise, and suggests POCS as a new method for restoration of spatially-variant blurred images.

ML-POCS hybrid reconstruction approaches estimate desired HR images by minimizing the ML or MAP cost functional while constraining the solution within certain closed convex sets in accordance with POCS methodology [Ref. 37].

There are a number of other areas that are considered in the literature, and some examples are presented here. One approach attempts to reconstruct a HR image from a single LR image and is referred to as improved definition image interpolation [Ref. 43]. Another area of study, referred to as iterative back-projection [Ref. 44, 45, 46], uses tomographic projection methods to estimate a HR image. Researchers are also considering the SR problem when no relative subpixel motion exists between LR

images. By considering differently blurred LR images, motionless SR reconstruction can be demonstrated [Ref. 47, 48]. Milanfar *et al.* analyze the joint problem of image registration and HR reconstruction in the context of fundamental statistical performance limits. By using the Cramér-Rao bound, they demonstrate ability to bound estimator performance in terms of MSE, examining performance limits as they relate to such imaging system parameters as the downsampling factor, signal-to-noise ratio, and point spread function. Finally, researchers are considering adaptive filtering approaches to the SR problem, considering modified recursive least squares (RLS), linear mean-square (LMS) and steepest descent methods [Ref. 49].

C. THESIS ORGANIZATION

This manuscript is organized as follows. The current chapter is introductory and presents the motivation for this work, defining the problem and outlining the approach used to solve it. Additionally, a review of the relevant literature is included, both in the area of stochastic multirate signal processing and super-resolution image reconstruction.

The second chapter introduces various fundamental signal processing and mathematical concepts required for theoretic and application-related developments in future chapters. These include various signal taxonomies and representations, a review of relevant topics in second-moment analysis, and required number theory and linear algebra concepts. Further, this chapter, establishes notation and conventions for purposes of consistency throughout this work.

In the third chapter, the theory of multirate systems is established. In this analysis, the relationships between a multirate system and its constituent signals are characterized, the system theory for multirate systems is developed, and the

representation of discrete linear systems is presented from a system theoretic point of view. Finally, a linear algebraic approach is introduced to model various multirate operations for use in reconstruction applications.

Chapter IV develops the concept of multirate signal estimation and is foundational in developing stochastic approaches to solving the signal reconstruction problem. The optimal filtering problem is introduced in terms of the ordinary Wiener-Hopf equation and is then expanded, first to the single-channel, multirate estimation problem and then to the multi-channel, multirate problem. Also in this chapter, the relationship between samples in one signal domain to those in a different signal domain (signals at different rates) is established through the concept of index mapping, which allows for a very general representation of the multirate Wiener-Hopf equations.

Chapter V considers the problem of signal reconstruction in the one- and two-dimensions. In this chapter, the problem is stated for both cases, observation models are established, reconstruction approaches and algorithms are developed, and then the results of each algorithm are presented.

Finally, Chapter VI provides conclusory remarks on the findings of this research and establishes direction for future work related to this research.

THIS PAGE INTENTIONALLY LEFT BLANK

II. PRELIMINARIES, CONVENTIONS, AND NOTATION

In the development of approaches to signal and image reconstruction, a number of fundamental concepts from the areas of signal processing and mathematics are required. In this chapter, a foundation is set in these areas upon which the theory of multirate signals and multirate estimation will be built. In doing so, we present the underlying concepts, but also emphasize required definitions, notations and conventions, in order to ensure consistency and accuracy, and to facilitate understanding.

A. SIGNALS

1. Etymology

Etymologically speaking, the word *signal* is derived from the Latin *signum*, which can be rendered as "a sign, mark, or token;" or in a military sense, "a standard, banner, or ensign;" or "a physical representation of a person or thing, like a figure, image, or statue [Ref. 50]." Generally, the Latin seems to imply that a *signum* is something that conveys information about or from someone or something else. The relevant modern dictionary definition of *signal* carries this idea further: "a detectable physical quantity or impulse by which messages or information can be transmitted [Ref. 51]."

In the area of electrical engineering known as digital signal processing, a related but more helpful definition of a *signal* is a collection of information, usually a pattern of variation [Ref. 52], that describes some physical phenomenon. In other words, a signal conveys relevant information about some physical phenomena (*signum*). The variation in electrical voltage measured at the input of an electronic circuit, the

variation in acoustic pressure sensed by a microphone recording a musical concert, or the variation in light intensity captured by a camera recording a scene are all examples of signals treated in modern signal processing.

2. Signal Definitions

Throughout this presentation, various types of signals and sequences are introduced and analyzed. In this section, for the sake of clarity, the definition of such signals and sequences are established, as are the associated conventions and notations. Let us begin with one-dimensional signals that are scalar-valued. We define these more precisely below.

a. Deterministic Signals and Sequences

A *deterministic analog signal* or simply an *analog signal* is defined as follows.

Definition 1. A *deterministic analog signal*, denoted by $\{x(t)\}$, or when it is clear from context $x(t)$, is a set of ordered measurements such that for every $t \in \mathbb{R}$, there exists a corresponding measurement $m = x(t)$. If all such measurements are members of the extended real numbers[1], then $x(t)$ is said to be a *real-valued* (or *real*) analog signal. If the measurements are members of the complex numbers, then the signal is said to be a *complex-valued* (or *complex*) analog signal.

An analog signal is frequently represented by a mathematical function, which may or may not be continuous. For example, the signal known as the *unit-step*, defined by

$$u(t) = \begin{cases} 1 & t \geq 0 \\ 0 & t < 0 \end{cases} \tag{2.1}$$

is well known in signal processing, but the function representing it is not continuous (at $t = 0$).

[1]The extended real numbers are defined as $\bar{\mathbb{R}} = \mathbb{R} \cup \{-\infty, \infty\}$.

Although many signals are represented by functions defined on the real number line, our definition of a signal is not necessarily the same as the mathematical definition of a function. The set of analog signals commonly includes the unit impulse, which (strictly speaking) is not a function at all but a distribution or "generalized function," described by a careful limiting process [Ref. 53, 54] to insure that the resulting entity satisfies certain conditions when it appears in an integral.

Signals may have many other properties that provide for further characterization. One property of concern in this work is that of *periodicity*. A signal is said to be *periodic* if there exists a positive real number P such that

$$x(t) = x(t+P) \quad \text{for all } t. \tag{2.2}$$

The smallest such P is called the *period*.

A *deterministic sequence* (or simply a *sequence*) is defined as follows.

Definition 2. A *deterministic sequence*, denoted by $\{x[n]\}$, or when clear from context $x[n]$, is a countable set of ordered measurements such that for every $n \in \mathbb{Z}$, there exists a corresponding measurement $m = x[n]$. If all such measurements are members of the extended real numbers, then $x[n]$ is said to be a *real-valued* (or *real*) sequence. If the measurements are members of the complex numbers, then the sequence is said to be a *complex-valued* (or *complex*) sequence.

A sequence $x[n]$ is said to be periodic if there exists a positive integer N such that

$$x[n] = x[n+N] \quad \text{for all } n, \tag{2.3}$$

and the smallest such N is called the period. Note that not all sequences derived by sampling a periodic analog signal are periodic. For example, the analog signal $x(t) = \cos(2\pi f_0 t + \phi)$ is periodic for any real number f_0, while the sequence $x[n]$ defined by $x[n] = x(nT_s) = \cos(2\pi f_0 n T_s + \phi)$ is periodic only if $f_0 T_s$ is a rational number.

Observe that both a signal and a sequence are defined by an ordered set of measurements, but over a different *domain* ($\mathbb{R}$ or $\mathbb{Z}$). Further, parentheses are used in the notation for an analog signal $x(\cdot)$ while square brackets are used for a sequence $x[\cdot]$ (to indicate the discrete nature of its domain). The variable t or n is frequently used to represent time, although the units of "time" need to be specified in any real-world problem. In the case of a sequence, n is just an index variable used to order the measurements, and there is need in signal processing to define what will be called a *deterministic discrete-domain signal* or simply *discrete-domain signal* .

Definition 3. A *deterministic discrete-domain signal*, denoted by $\{x_T(t)\}$, or when it is clear from context $x_T(t)$, is a set of ordered measurements such that for every $t \in \Psi_T$, there exists a corresponding measurement $m = x_T(t)$, where
$\Psi_T = \{nT; n \in \mathbb{Z}\}$, and T is a positive real number called the *sampling interval*. The signal *domain* is defined as the set Ψ_T. If all such measurements are members of the extended real numbers, then $x_T(t)$ is said to be a *real-valued* (or *real*) discrete-domain signal. If the measurements are members of the complex numbers, then the signal is said to be a *complex-valued* (or *complex*) discrete-domain signal. When t represents time, a discrete-domain signal may be called a *discrete-time* signal.

This definition of a discrete-domain signal is similar to that of an analog signal except that the signal is defined on a countable set Ψ_T. An important observation is that a discrete-domain signal is equivalent to a sequence and an associated sampling interval T or its reciprocal $F = 1/T$,

$$x_T(t) \equiv \{x[n], T\} \equiv \{x[n], F\} \text{ for } n \in \mathbb{Z}. \tag{2.4}$$

The quantity F is called the sampling rate (in samples/sec or Hz) and in discussing discrete-domain signals, it is common to refer to the sequence and its sampling rate. For example, we may use the expression "$x[n]$ *at a rate* of 20 kHz" to describe a discrete-domain signal, which has a sampling interval of $T = 0.05$ msec.

It is also common not to mention the sampling rate if the sampling rate is common throughout a system (single-rate system). On the other hand, when dealing with a multirate system, it is common to use different letters, such as n and m, to designate sequences, for example, $x[n]$ and $y[m]$, to indicate that these sequences represent discrete-domain signals with different sampling rates.

Figure 2.1 illustrates a discrete-domain signal. Note that the signal is defined only on the points $t = nT$ and is *undefined* everywhere else. Note, also, that while a discrete-domain signal may be derived by sampling an analog signal, this is not always the case. Any sequence, regardless of how it is computed (say in MATLAB or on an ASIC chip) when combined with a sampling interval, defines a discrete-domain signal. The corresponding analog signal need not exist unless (as in the output of a digital signal processing chain) some special action is taken to construct it.

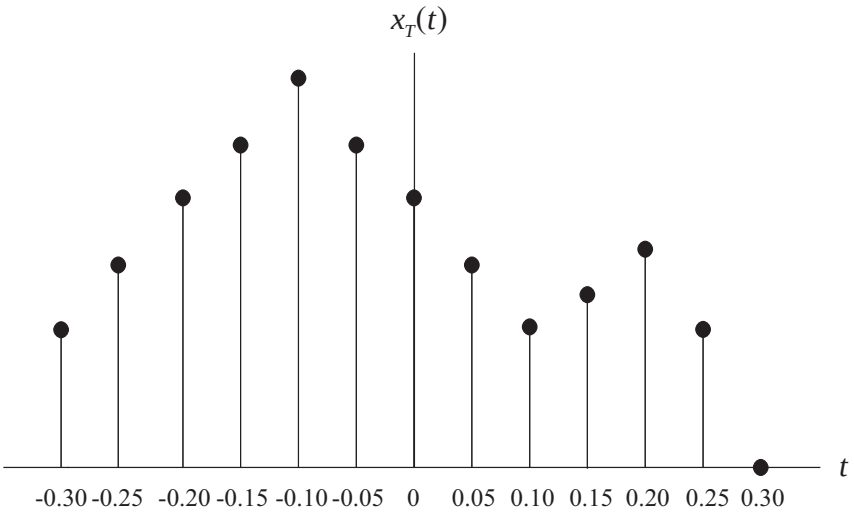

Figure 2.1. Graphical representation of a discrete-domain signal $x_T(t)$ with sampling interval $T = 0.05$. Note that the signal is defined only at $t = nT; n \in \mathbb{Z}$.

b. Random Signals and Sequences

In statistical signal processing, a probabilistic model is necessary for signals. This model is embedded in the concept of a *random signal* or a *stochastic signal*. A *real random signal* or (*real stochastic signal*) is defined as follows.

Definition 4. A *real random signal*, denoted by $\{X(t)\}$, or when it is clear from context $X(t)$, is a set of ordered random variables (representing measurements) such that for every $t \in \mathbb{R}$, there exists a corresponding random variable $X(t)$.

Note that when the context is clear, a random signal may be designated by a lower case variable, i.e., $x(t), d(t), etc.$

Since a random variable is a mapping from some sample space to the real line, the definition for a *complex random signal* requires special caution. The following definition is therefore provided.

Definition 5. A *complex random signal* or (*complex stochastic signal*), denoted by $\{Z(t)\}$, is defined by $Z(t) = X(t)+jY(t)$, where $X(t)$ and $Y(t)$ are real random analog signals defined on a common domain. In other words, for every $t \in \mathbb{R}$, there exists a pair of corresponding random variables $X(t)$ and $Y(t)$ such that $Z(t) = X(t)+jY(t)$. Again, we may use $Z(t)$ instead of $\{Z(t)\}$ when the meaning is clear from context.

Random sequences and random discrete-domain signals can be defined in a similar manner.

Definition 6. A *real random sequence* or (*real stochastic sequence*), denoted by $\{X[n]\}$, is a countable set of ordered random variables (representing measurements) such that for every $n \in \mathbb{Z}$, there exists a corresponding random variable $X[n]$. A *complex random sequence* can be defined in a manner similar to that of a complex random signal.

Note that when the context is clear, a random sequence may be designated by a lower case variable, i.e., $x[n], d[n], etc.$

Definition 7. A *random discrete-domain signal*, denoted by $\{X_T(t)\}$, or when it is clear from context $X_T(t)$, is a set of ordered random variables (representing measurements) such that for every $t \in \Psi_T$, there exists a corresponding random variable $X_T(t)$, where $\Psi_T = \{nT; n \in \mathbb{Z}\}$, and T is the sampling interval.

A random discrete-domain signal is sometimes also referred to as a *time series*; however, the use of that term in the literature is not always consistent.

c. Multi-channel Signals and Sequences

In signal processing, it is often the case that a system may contain signals or sequences that are derived from multiple sources or multiple sensors. In order to represent such signals and sequences, multi-channel signals and sequences are defined. A *multi-channel signal* is a set of (single-channel) signals that share a common domain and is represented by a vector

$$\mathbf{x}(t) = \begin{bmatrix} x_1(t) \\ x_2(t) \\ \vdots \\ x_N(t) \end{bmatrix},$$

whose components $x_1(t), x_2(t), \ldots, x_N(t)$ are (analog or discrete-domain) signals as defined earlier. The signals may be real or complex, deterministic or random. By convention, bold face and vector notation are used to represent such signals as in

$$\mathbf{x}(t) = \begin{bmatrix} \cos \omega t \\ -\sin \omega t \end{bmatrix},$$

or in

$$\mathbf{X}(t) = \begin{bmatrix} A\cos(\omega t + \Phi) \\ -A\sin(\omega t + \Phi) \end{bmatrix},$$

where $X(t)$ represents a random signal defined by random variables A and Φ.

A *multi-channel* sequence

$$\mathbf{x}[n] = \begin{bmatrix} x_1[n] \\ x_2[n] \\ \vdots \\ x_N[n] \end{bmatrix}$$

is represented by a vector whose components $x_1[n], x_2[n], \ldots, x_N[n]$ are sequences as defined earlier. Again, all of the terms describing an individual sequence (e.g., real, complex, etc.) can be applied to a multi-channel sequence.

d. Two-dimensional Signals and Sequences

Since two-dimensional signals and sequences are at the heart of image processing, it is helpful to characterize the 2-D counterparts to the familiar one-dimensional signals and sequences already presented. A *two-dimensional (2-D) analog signal* is defined as follows.

Definition 8. A *two-dimensional (2-D) analog signal*, denoted by $\{x(t_1, t_2)\}$, or when it is clear from context $x(t_1, t_2)$, is a set of ordered measurements such that for every pair $(t_1, t_2) \in \mathbb{R}^2$, there exists a corresponding measurement $m = x(t_1, t_2)$. Two-dimensional signals can be real or complex, deterministic or random. It is sometimes convenient to represent a 2-D signal with a bold face argument $\mathbf{t} = (t_1, t_2) \in \mathbb{R}^2$. Thus, the 2-D signal would be denoted by $\{x(\mathbf{t})\}$ or $x(\mathbf{t})$ when clear from the context.

Although a *sequence* seems to imply an ordered set of terms in one dimension, it is common in signal processing to extend the meaning to apply to signal defined on a two-dimensional domain. A *two-dimensional sequence* and two-dimensional discrete-domain signal are thus defined as follows.

Definition 9. A *two-dimensional sequence*, denoted by $\{x[n_1, n_2]\}$, or when it is clear from context $x[n_1, n_2]$, is a set of ordered measurements such that for every pair $(n_1, n_2) \in \mathbb{Z}^2$, there exists a corresponding measurement $m = x[n_1, n_2]$. 2-D sequences can be real or complex, deterministic or random; they may also be represented as $\{x[\mathbf{n}]\}$ or $x[\mathbf{n}]$, where the boldface argument denotes the ordered pair $(n_1, n_2) \in \mathbb{Z}^2$.

Definition 10. A *two-dimensional discrete-domain signal*, denoted by $\{x_{T_1T_2}(t_1, t_2)\}$ or $x_{T_1T_2}(t_1, t_2)$, is a set of ordered measurements such that for every pair (t_1, t_2) in the domain $\Psi_{T_1T_2} = \Psi_{T_1} \times \Psi_{T_2}$, where Ψ_T is as defined earlier, there exists a corresponding measurement $m = x_{T_1T_2}(t_1, t_2)$, and T_1 and T_2 are the associated sampling intervals.

For convenience in notation, we may use $x_{\mathbf{T}}(\mathbf{t})$ and $\Psi_{\mathbf{T}}$ to denote the 2-D signal and its domain, where $\mathbf{T}$ represents the ordered pair (T_1, T_2) of sampling intervals. Again, note that a two-dimensional discrete-domain signal can be real or complex, deterministic or random.

The image projected on the film plane of a camera is an example of a 2-D analog signal. If film is thought of as a continuous medium, then the image captured on the film is also a representation of a 2-D analog signal. If the image is projected onto a sensor array as in a digital camera, then the resulting sampled image is represented by a 2-D discrete-domain signal.

Signals can be both multi-dimensional and multi-channel. A common example is a color image where the domain is two-dimensional (horizontal and vertical spatial variables), and there are 3 channels corresponding to the three components of a color space, such as RGB (red, green, blue), CMY (cyan, magenta, yellow) or HSI (hue, saturation, intensity).

Two-dimensional random signals and sequences are similar to their corresponding deterministic representations except that the measurements are represented by random variables.

e. Summary of Notation and Convention

A summary of the various signal representations is provided in Table 2.1.

Representation	Name
$x(t)$	Deterministic analog signal, analog aignal
$x[n]$	Deterministic sequence
$x_T(t), x[n]_T$	Deterministic discrete-domain signal with sampling interval T, Discrete-domain signal
$x(t_1, t_2), x(\mathbf{t})$	Two-dimensional deterministic analog signal, 2-D analog signal
$x[n_1, n_2], x[\mathbf{n}]$	Two-dimensional deterministic sequence, 2-D deterministic sequence
$x_{T_1T_2}(t_1, t_2), x_{\mathbf{T}}(\mathbf{t})$	Two-dimensional deterministic discrete-domain signal with sampling intervals T_1 and T_2, 2-D discrete-domain signal
$X(t)$	Random analog signal
$X[n]$	Random sequence

Table 2.1. Summary of signal representations.

B. CONCEPTS IN LINEAR ALGEBRA

1. Random Vectors

Often, it is necessary to process some finite number of samples of a random sequence. Such a finite-length sequence can be conveniently represented by a *random vector* [Ref. 5]. This provides for compact notation and formulation and solution of problems in a linear algebra sense. A random sequence $X[n]$ restricted to some

interval $0 \leq n \leq N-1$ can be represented by an N-component random vector $\mathbf{x}$ as shown in Figure 2.2 and written as

$$\mathbf{x} = \begin{bmatrix} X[0] \\ X[1] \\ \vdots \\ X[N-1] \end{bmatrix}. \tag{2.5}$$

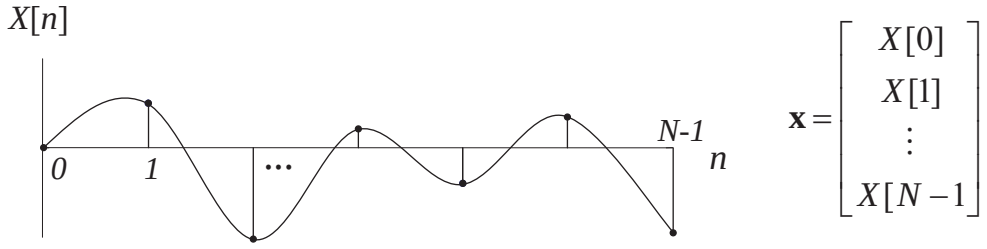

Figure 2.2. Graphical representation of a finite-length random sequence as a random vector.

2. Kronecker Products

The Kronecker product, also known as the direct product or tensor product, has its origins in group theory [Ref. 4] and has important applications in a number of technical disciplines. In this study, the Kronecker product is used to develop matrix representations of various multirate operations.

Definition 11. Let $\mathbf{A}$ be an $m \times n$ matrix (with entries a_{ij}) and let $\mathbf{B}$ be an $r \times s$ matrix. Then the Kronecker product of $\mathbf{A}$ and $\mathbf{B}$ is the $mr \times ns$ block matrix

$$\mathbf{A} \otimes \mathbf{B} = \begin{pmatrix} a_{11}\mathbf{B} & a_{12}\mathbf{B} & \dots & a_{1n}\mathbf{B} \\ a_{21}\mathbf{B} & a_{22}\mathbf{B} & \dots & a_{2n}\mathbf{B} \\ \vdots & \vdots & \ddots & \vdots \\ a_{m1}\mathbf{B} & a_{m2}\mathbf{B} & \dots & a_{mn}\mathbf{B} \end{pmatrix}. \tag{2.6}$$

Equation (2.6) is also called a *right* Kronecker product as opposed to the definition $\mathbf{A} \otimes' \mathbf{B} = \mathbf{B} \otimes \mathbf{A}$, which is called a *left* Kronecker product. Since there is no need to use both, we will stick with the more common definition (2.6).

A summary of some important properties of the Kronecker product is provided in Table 2.2.

$\mathbf{A} \otimes (\alpha\mathbf{B}) = \alpha(\mathbf{A} \otimes \mathbf{B})$
$(\mathbf{A} + \mathbf{B}) \otimes \mathbf{C} = \mathbf{A} \otimes \mathbf{C} + \mathbf{B} \otimes \mathbf{C}$
$\mathbf{A} \otimes (\mathbf{B} \otimes \mathbf{C}) = (\mathbf{A} \otimes \mathbf{B}) \otimes \mathbf{C}$
$(\mathbf{A} \otimes \mathbf{B})^T = \mathbf{A}^T \otimes \mathbf{B}^T$
$(\mathbf{A} \otimes \mathbf{B})(\mathbf{C} \otimes \mathbf{D}) = \mathbf{AC} \otimes \mathbf{BD}$
$(\mathbf{A} \otimes \mathbf{B})^{-1} = \mathbf{A}^{-1} \otimes \mathbf{B}^{-1}$

Table 2.2. Some Kronecker product properties and rules, (After [Ref. 4]).

3. Reversal of Matrices and Vectors

In signal processing, it is a common requirement to view signals as evolving either forward or backward in time. A well-known example is the convolution operation, where the linear combination of terms involves a time-reversed version of either the input signal or the system impulse response. Since, in discrete-time signal processing, signals are often represented by vectors, it is useful to define the operation of *reversal* for vectors and matrices.

The reversal of a vector $\mathbf{x}$ is the vector with its elements in reverse order. Given the vector

$$\mathbf{x} = \begin{bmatrix} x_1 \\ x_2 \\ \vdots \\ x_N \end{bmatrix}, \qquad \text{its reversal is} \qquad \tilde{\mathbf{x}} = \begin{bmatrix} x_N \\ x_{N-1} \\ \vdots \\ x_1 \end{bmatrix}. \tag{2.7}$$

Note that the notation for the reversal is $\tilde{\mathbf{x}}$, and it is used just like notation for the transposition of a vector or matrix.

The reversal of a matrix $\mathbf{A}$ is the matrix with its column and row elements in reverse order. Given the matrix $\mathbf{A} \in \mathbb{R}^{M \times N}$

$$\mathbf{A} = \begin{bmatrix} a_{11} & a_{12} & \dots & a_{1N} \\ a_{21} & a_{22} & \dots & a_{2N} \\ \vdots & \vdots & \ddots & \vdots \\ a_{M1} & a_{M2} & \dots & a_{MN} \end{bmatrix},$$

its reversal $\tilde{\mathbf{A}} \in \mathbb{R}^{M \times N}$ is given by

$$\tilde{\mathbf{A}} = \begin{bmatrix} a_{MN} & \dots & a_{M2} & a_{M1} \\ \vdots & \vdots & \ddots & \vdots \\ a_{2N} & \dots & a_{22} & a_{21} \\ a_{1N} & \dots & a_{12} & a_{11} \end{bmatrix}. \tag{2.8}$$

Note that the reversal of a vector or matrix can be formed by the product of a conformable counter identity and the vector or matrix itself.

Some common properties of the reversal operator are included in Table 2.3. In particular, the reversal of matrix and Kronecker products (see Section II.B.2) are products of the reversals, and the operation of reversal commutes with inversion, conjugation and transposition.

	Quantity	Reversal
Matrix product	$\mathbf{AB}$	$\tilde{\mathbf{A}}\tilde{\mathbf{B}}$
Matrix inverse	$\mathbf{A}^{-1}$	$(\tilde{\mathbf{A}})^{-1}$
Matrix conjugate	$\mathbf{A}^{*}$	$(\tilde{\mathbf{A}})^{*}$
Matrix transpose	$\mathbf{A}^{T}$	$(\tilde{\mathbf{A}})^{T}$
Kronecker product	$\mathbf{A} \otimes \mathbf{B}$	$\tilde{\mathbf{A}} \otimes \tilde{\mathbf{B}}$

Table 2.3. Some properties of the reversal operator, (After [Ref. 5]).

4. Frobenius Inner Product

In the development of approaches to two-dimensional signal reconstruction, it is convenient to express the related linear estimates in terms of the *Frobenius inner product*.

Definition 12. For any $\mathbf{A}, \mathbf{B} \in \mathbb{R}^{m \times n}$, with elements a_{ij}, b_{ij}, the Frobenius inner product of the matrices is defined as

$$\langle \mathbf{A}, \mathbf{B} \rangle = \mathrm{tr}(\mathbf{A}\mathbf{B}^T) = \sum_{i=1}^{m} \sum_{j=1}^{n} a_{ij} b_{ij}. \tag{2.9}$$

C. MOMENT ANALYSIS OF RANDOM PROCESSES

Generally, a complete statistical model is unavailable when analyzing systems of random processes. Either the required joint density functions are unavailable, or they are too complex to be of utility. If the random processes under consideration are Gaussian, then the system can be fully specified by only its first two moments [Ref. 5]. Even if the processes are not Gaussian, second moment analysis is often adequate in characterizing the statistical relationships between signals in such systems and forms the basis for any additional analyses. This section introduces the required definitions and relevant properties associated with second moment analysis [Ref. 5].

1. Definitions and Properties

Given the random process $X[n]$, the first moment or *mean* of the random process is defined by

$$m_X[n] = \mathcal{E}\{X[n]\}, \tag{2.10}$$

where $\mathcal{E}\{\cdot\}$ denotes expectation.

The correlation between any two samples of the random process $X[n_1]$ and $X[n_0]$ is described by the *correlation function* or *autocorrelation function*, which is

defined by

$$R_X[n_1, n_0] = \mathcal{E}\{X[n_1]X^*[n_0]\}. \tag{2.11}$$

In certain applications, and extensively in this work, it is convenient to define a *time-dependent correlation function* as

$$R_X[n; l] = \mathcal{E}\{X[n]X^*[n-l]\}, \tag{2.12}$$

and the various definitions and relationships introduced in this section will be based on this "time-dependent" representation.

The covariance between any two samples of the random process $X[n]$ and $X[n-l]$ is described by the *time-dependent covariance function*, which is defined by

$$C_X[n; l] = \mathcal{E}\{(X[n] - m_X[n])(X[n-l] - m_X[n-l])^*\}. \tag{2.13}$$

The relationship between the correlation function and the covariance function is

$$R_X[n; l] = C_X[n; l] + m_X[n]m_X^*[n-l], \tag{2.14}$$

hence when $X[n]$ is a zero-mean random process,

$$R_X[n; l] = C_X[n; l].$$

If we consider two random processes, $X[n]$ and $Y[n]$, the correlation between any two samples of the random processes is described by the *time-dependent cross-correlation function*, which is defined by

$$R_{XY}[n; l] = \mathcal{E}\{X[n]Y^*[n-l]\}. \tag{2.15}$$

An expression can be written for the *time-dependent cross-covariance function* as

$$C_{XY}[n; l] = \mathcal{E}\{(X[n] - m_X[n])(Y[n-l] - m_Y[n-l])^*\}. \tag{2.16}$$

The relationship between the cross-correlation function and the cross-covariance function is

$$R_{XY}[n; l] = C_{XY}[n; l] + m_X[n]m_Y^*[n-l], \tag{2.17}$$

hence when $X[n]$ and $Y[n]$ are zero-mean random processes,

$$R_{XY}[n;l] = C_{XY}[n;l].$$

Two random processes are called *orthogonal* if $R_{XY}[n;l] = 0$ and *uncorrelated* if $C_{XY}[n;l] = 0$.

2. Stationarity of Random Processes

Recall that a random process is *wide-sense stationary* (WSS) if

1. the mean of the random process is a constant, $m_X[n] = m_X$, and
2. the correlation function is a function only of the spacing between samples, i.e., $R_X[n;l] = R_X[l]$.

and that two random processes are *jointly wide-sense stationary* (JWSS) if

1. they are each WSS, and
2. their cross-correlation function is a function only of the spacing between samples, i.e., $R_{XY}[n;l] = R_{XY}[l]$.

Under the assumptions of WSS and JWSS, the mean, correlation and covariance functions are summarized in Table 2.4.

3. Matrix Representations of Moments

Using the vector representation (2.5) for a random signal, a number of important concepts and properties can be defined. The first moment or mean of a random vector is defined by

$$\mathbf{m_X} = \mathcal{E}\{\mathbf{X}\} = \begin{bmatrix} \mathcal{E}\{X[0]\} \\ \mathcal{E}\{X[1]\} \\ \vdots \\ \mathcal{E}\{X[N-1]\} \end{bmatrix} = \begin{bmatrix} m_X[0] \\ m_X[1] \\ \vdots \\ m_X[N-1] \end{bmatrix}, \tag{2.25}$$

Mean Function	$m_X = \mathcal{E}\{X[n]\}$	(2.18)
(Auto)correlation Function	$R_X[l] = \mathcal{E}\{X[n]X^*[n-l]\}$	(2.19)
Covariance Function	$C_X[l] = \mathcal{E}\{(X[n]-m_X)(X[n-l]-m_X)^*\}$	(2.20)
Interrelation	$R_X[l] = C_X[l] + \lvert m_X\rvert^2$	(2.21)
Cross-correlation Function	$R_{XY}[l] = \mathcal{E}\{X[n]Y^*[n-l]\}$	(2.22)
Cross-covariance Function	$C_{XY}[l] = \mathcal{E}\{(X[n]-m_X)(Y[n-l]-m_Y)^*\}$	(2.23)
Interrelation	$R_{XY}[l] = C_{XY}[l] + m_X m_Y^*$	(2.24)

Table 2.4. Summary of definitions and relationships for stationary random processes, (After [Ref. 5]).

which is completely specified by the associated mean function $m_X[n]$ in (2.10). If the random process is WSS, then the mean function is independent of the sample index and $\mathbf{m_X}$ is defined by a vector of constants

$$\mathbf{m_X} = \begin{bmatrix} m_X \\ m_X \\ \vdots \\ m_X \end{bmatrix}. \tag{2.26}$$

The correlation matrix represents the complete set of second moments for the random vector and is defined by

$$\mathbf{R_X} = \mathcal{E}\{\mathbf{X}\mathbf{X}^{*T}\}. \tag{2.27}$$

The correlation matrix thus has the explicit form

$$\mathbf{R_X} = \begin{bmatrix} \mathcal{E}\{|X[0]|^2\} & \mathcal{E}\{X[0]X^*[1]\} & \dots & \mathcal{E}\{X[0]X^*[N-1]\} \\ \mathcal{E}\{X[1]X^*[0]\} & \mathcal{E}\{|X[1]|^2\} & \dots & \mathcal{E}\{X[1]X^*[N-1]\} \\ \vdots & \vdots & \ddots & \vdots \\ \mathcal{E}\{|X[N-1]X^*[0]\} & \mathcal{E}\{X[N-1]X^*[1]\} & \dots & \mathcal{E}\{|X[N-1]|^2\} \end{bmatrix} \tag{2.28}$$

$$= \begin{bmatrix} R_X[0;0] & R_X[0;-1] & \dots & R_X[0;-N+1] \\ R_X[1;1] & R_X[1;0] & \dots & R_X[1;-N] \\ \vdots & \vdots & \ddots & \vdots \\ R_X[N-1;N-1] & R_X[N-1;N-2] & \dots & R_X[N-1;0] \end{bmatrix}, \tag{2.29}$$

which is completely specified by the associated correlation function $R_X[n;l]$ in (2.12). If the random process is WSS, then the correlation is a function of only the sample spacing and has the form of a Toeplitz matrix:

$$\mathbf{R_X} = \begin{bmatrix} R_X[0] & R_X[-1] & R_X[-2] & \dots & R_X[-N+1] \\ R_X[1] & R_X[0] & R_X[-1] & \ddots & R_X[-N] \\ R_X[2] & R_X[1] & \ddots & \ddots & \dots \\ \vdots & \vdots & \ddots & \ddots & \vdots \\ R_X[N-1] & R_X[N-2] & \dots & R_X[1] & R_X[0] \end{bmatrix}. \tag{2.30}$$

This matrix is completely specified by the associated correlation function $R_X[l]$ in (2.19).

The cross-correlation matrix represents the complete set of second moments between two random vectors $\mathbf{X} \in \mathbb{R}^N$ and $\mathbf{Y} \in \mathbb{R}^M$ and is defined by

$$\mathbf{R_{XY}} = \mathcal{E}\{\mathbf{X}\mathbf{Y}^{*T}\}, \tag{2.31}$$

and the associated correlation matrix has the form

$$\mathbf{R_{XY}} = \begin{bmatrix} R_{XY}[0;0] & R_{XY}[0;-1] & \dots & R_{XY}[0;-M+1] \\ R_{XY}[1;1] & R_{XY}[1;0] & \dots & R_{XY}[1;-M] \\ \vdots & \vdots & \ddots & \vdots \\ R_{XY}[N-1;N-1] & R_{XY}[N-1;N-2] & \dots & R_{XY}[N-1;N-M] \end{bmatrix}, \tag{2.32}$$

which is completely specified by the associated cross-correlation function $R_{XY}[n;l]$ in (2.15). In general, $\mathbf{R_{XY}}$ is not a square matrix (unless $N = M$). If the associated random processes are JWSS, then the cross-correlation is a function of only the sample spacing

$$\mathbf{R_{XY}} = \begin{bmatrix} R_{XY}[0] & R_{XY}[-1] & \dots & R_{XY}[-M+1] \\ R_{XY}[1] & R_{XY}[0] & \vdots & R_{XY}[-M] \\ R_{XY}[2] & R_{XY}[1] & \ddots & \dots \\ \vdots & \vdots & \dots & \vdots \\ R_{XY}[N-1] & R_{XY}[N-2] & \dots & R_{XY}[N-M] \end{bmatrix}, \tag{2.33}$$

which is completely specified by the associated correlation function $R_X[l]$ in (2.22). In general, such matrices will exhibit Toeplitz structure but will not be Hermitian symmetric [Ref. 5]. Similar expressions and statements can be made concerning the cross-covariance matrix and function. The essential definitions, properties, and relations for the quantities discussed in this section are listed in Table 2.5.

4. Reversal of First and Second Moment Quantities

Since the operations of expectation and reversal commute, we have the following relations for the first and second moment quantities

$$\mathbf{m}_{\tilde{\mathbf{X}}} = \mathcal{E}\{\tilde{\mathbf{X}}\} = \tilde{\mathbf{m}}_{\mathbf{X}}, \tag{2.34}$$

and

$$\mathbf{R}_{\tilde{\mathbf{X}}} = \mathcal{E}\{\tilde{\mathbf{X}}\tilde{\mathbf{X}}^{*T}\} = \tilde{\mathbf{R}}_{\mathbf{X}} \qquad (\mathbf{C}_{\tilde{\mathbf{X}}} = \tilde{\mathbf{C}}_X). \tag{2.35}$$

Mean	$\mathbf{m_X} = \mathcal{E}\{\mathbf{X}\}$
(Auto)correlation	$\mathbf{R_X} = \mathcal{E}\{\mathbf{X}\mathbf{X}^{*T}\}$
Covariance	$\mathbf{C_X} = \mathcal{E}\{(\mathbf{X} - \mathbf{m_X})(\mathbf{X} - \mathbf{m_X})^{*T}\}$
Interrelation	$\mathbf{R_X} = \mathbf{C_X} + \mathbf{m_X}\mathbf{m_X}^{*T}$
Cross-correlation	$\mathbf{R_{XY}} = \mathcal{E}\{\mathbf{X}\mathbf{Y}^{*T}\}$
Cross-covariance	$\mathbf{C_{XY}} = \mathcal{E}\{(\mathbf{X} - \mathbf{m_X})(\mathbf{Y} - \mathbf{m_Y})^{*T}\}$
Interrelation	$\mathbf{R_{XY}} = \mathbf{C_{XY}} + \mathbf{m_X}\mathbf{m_Y}^{*T}$
Symmetry	$\mathbf{R_X} = \mathbf{R_X}^{*T}, \quad \mathbf{C_X} = \mathbf{C_X}^{*T}$
Relation of $\mathbf{R_{XY}}$ and $\mathbf{C_{XY}}$	$\mathbf{R_{XY}} = \mathbf{R_{YX}}^{*T}, \quad \mathbf{C_{XY}} = \mathbf{C_{YX}}^{*T}$

Table 2.5. Summary of useful definitions and relationships for random processes, (After [Ref. 5]).

Further, if $\mathbf{R_X}$ ($\mathbf{C_X}$) is a Toeplitz correlation (covariance) matrix corresponding to a WSS random process, it follows that

$$\tilde{\mathbf{R}}^*_{\mathbf{X}} = \mathbf{R_X}. \tag{2.36}$$

D. NUMBER THEORY

Number theory, "... the branch of mathematics concerned with the study of the properties of the integers [Ref. 55]," is a natural framework for the analysis of discrete-time systems, where the independent variables, by definition, are integers.

In particular, since in this analysis of multirate systems, notions of divisibility, factorization and congruence are integral, the ensuing discussion is provided to introduce and define these and related concepts [Ref. 55, 56, 57, 58].

1. Division Algorithm Theorem

The elementary operation of division forms the basis of much of what is to follow and is expressed by the *division algorithm theorem.*

Theorem 1. Let a and b be integers with $a > 0$. Then there exists unique integers q and r satisfying

$$b = qa + r, \qquad 0 \leq r < a, \tag{2.37}$$

where q is called the quotient and r is called the remainder.

The proof of this can be found in many texts, e.g., [Ref. 55, 56, 57].

Example 1. *A specific example demonstrating the division algorithm theorem is provided. Given integers $a = 3$ and $b = 22$, we find unique integers $q = 7$ and $r = 1$ that satisfy* (2.37)*. The quotient is $q = 7$; the remainder is $r = 1$.* ■

2. Divisibility

Definition 13. Let a and b be integers. Then a *divides* b, written $a|b$, if and only if there is some integer c such that $b = ca$. When this condition is met, the following are equivalent statements: (i) a is a factor of b, (ii) b is divisible by a, and (iii) b is a multiple of a. If a does not divide b, we write $a \nmid b$.

Example 2. *This example illustrates the concept of divisibility for a number of integer pairs.*

$$3|12, 7|21, 9|108, 12|144;$$
$$4 \nmid 5, 7 \nmid 8, 8 \nmid 7, 3 \nmid 22.$$ ■

a. Greatest Common Divisor

Definition 14. Let a and b be integers. The integer d is called the *greatest common divisor* of a and b, denoted by $\gcd(a, b)$, if and only if

1. $d > 0$,
2. $d|a$ and $d|b$,
3. whenever $e|a$ and $e|b$, we have $e|d$.

The integers a and b are said to be *relatively prime* if $\gcd(a, b) = 1$.

Example 3. *A few examples demonstrating the greatest common divisor:*

If $a = 3$ *and* $b = 4$, *then* $d = \gcd(3, 4) = 1$ (3 *and* 4 *are relatively prime*),
If $a = 12$ *and* $b = 15$, *then* $d = \gcd(12, 15) = 3$,
If $a = 25$ *and* $b = 55$, *then* $d = \gcd(25, 55) = 5$. ■

b. Least Common Multiple

Definition 15. Let a and b be positive integers. The integer m is called the *least common multiple* of a and b, denoted by $\text{lcm}(a, b)$, if and only if

1. $m > 0$,
2. $a|m$ and $b|m$, and
3. if n is such that $a|n$ and $b|n$, then $m|n$.

The least common multiple can be expressed as

$$\text{lcm}(a, b) = \frac{ab}{\gcd(a, b)}. \tag{2.38}$$

Example 4. *A few examples demonstrating the least common multiple:*

If $a = 3$ *and* $b = 4$, *then* $m = \text{lcm}(3, 4) = 12$,
If $a = 12$ *and* $b = 15$, *then* $m = \text{lcm}(12, 15) = 60$,
If $a = 25$ *and* $b = 55$, *then* $m = \text{lcm}(25, 55) = 275$. ■

Also note that the least common multiple is associative and therefore,

$$\text{lcm}(a, b, c) = \text{lcm}(\text{lcm}(a, b), c) = \text{lcm}(a, \text{lcm}(b, c). \tag{2.39}$$

3. Greatest Integer Function

The *greatest integer function*, often called the *floor function*, is defined as follows.

Definition 16. For any $x \in \mathbb{R}$, the greatest integer function evaluated at x returns the largest integer less than or equal to x. This is sometimes referred to as the *integral part of* x. The function will be denoted as $\lfloor x \rfloor$.

Example 5. *The following examples illustrate this definition,*

$$\lfloor 2.7 \rfloor = 2,$$
$$\lfloor 0.9 \rfloor = 0,$$
$$\lfloor -0.3 \rfloor = -1. \quad \blacksquare$$

Note that the floor function satisfies the following identity

$$\lfloor x + k \rfloor = \lfloor x \rfloor + k, \quad \text{for} \quad k \in \mathbb{Z}. \tag{2.40}$$

4. Congruence

If a is fixed in (2.37), then there are an infinite number of choices of b for which the remainder r is the same. In this context, a is called the *modulus*, the choices of b are said to be *congruent modulo* a, and the remainder is called the *common residue modulo* a or simply the *common residue* [Ref. 58]. This concept of congruence is formalized with the following definitions.

Definition 17. Let n be a positive integer. The integers x and y are "congruent modulo n" or "x is congruent to y modulo n", denoted $x \equiv y \pmod{n}$, provided that $x - y$ is divisible by n. If x and y are not congruent modulo n or x is not congruent to y modulo n, we write $x \not\equiv y \pmod{n}$.

Example 6. *We demonstrate the concept of congruence with a few examples.*

$$8 \equiv 5 \pmod 3,$$
$$14 \equiv 2 \pmod{12},$$
$$49 \equiv 42 \pmod 7. \qquad \blacksquare$$

Example 7. *In the following example, $n = 2$, and there are two sets of integers that are congruent modulo 2, the even integers and the odd integers.*

$$\{\ldots, -4, -2, 0, 2, 4, \ldots\} \textit{ are congruent to } 0 \pmod 2,$$
$$\{\ldots, -3, -1, 1, 3, 5, \ldots\} \textit{ are congruent to } 1 \pmod 2. \qquad \blacksquare$$

Example 8. *In this example, $n = 3$, and there are three sets of integers that are congruent modulo 2.*

$$\{\ldots, -6, -3, 0, 3, 6, \ldots\} \textit{ are congruent to } 0 \pmod 3,$$
$$\{\ldots, -5, -2, 1, 4, 7, \ldots\} \textit{ are congruent to } 1 \pmod 3,$$
$$\{\ldots, -4, -1, 2, 5, 8, \ldots\} \textit{ are congruent to } 2 \pmod 3. \qquad \blacksquare$$

Definition 18. If $x \equiv y \pmod n$, then y is called a *residue* of x modulo n. Furthermore, if $0 \leq y < n$, then y is called the *common residue* of x modulo n, or simply the common residue.

Example 9. *Referring to Example 6, we point out the associated residues.*

5 *is a residue of* 8 *modulo* 3,
2 *is the* common *residue of* 14 *modulo* 12, *and*
42 *is a residue of* 49 *modulo* 7. $\blacksquare$

Definition 19. The set of integers $\Lambda_n = \{0, 1, \ldots, n-1\}$ is called the set of "least positive residues modulo n"

At times, it is necessary to extract the common residue [Ref. 58]. This operation is denoted by $\langle \cdot \rangle_n$ and is defined as

$$y = \langle x \rangle_n = x - \left\lfloor \frac{x}{n} \right\rfloor n, \tag{2.41}$$

where y is the common residue of x modulo n, and $\lfloor \cdot \rfloor$ is the *floor* operation.

Example 10. *A few examples of extracting the common residues of x modulo n.*

$$y = \langle 22 \rangle_3 = 22 - \left\lfloor \tfrac{22}{3} \right\rfloor 3 = 22 - 21 = 1,$$
$$y = \langle 14 \rangle_4 = 14 - \left\lfloor \tfrac{14}{4} \right\rfloor 4 = 14 - 12 = 2. \qquad \blacksquare$$

E. CHAPTER SUMMARY

This chapter introduces various fundamental signal processing and mathematical concepts required for theoretic and application-related developments in subsequent chapters. Further, for the purposes of consistency, accuracy and ease of understanding, conventions and notation are also established.

The taxonomy of signals and sequences, their various definitions, and associated notations are presented. Of particular relevance is the discussion on discrete-domain signals and their sequence representation, which form the most basic constituent of any multirate system (Chapter III).

Many concepts from linear algebra are recalled, including the concept of a random vector and the reversal of a vector or matrix. Further, the linear algebraic concept of the Kronecker product is discussed, which is useful in the matrix representation of various multirate operations in Chapter III and the multirate Wiener-Hopf equations in Chapter IV. Finally, the Frobenius inner product is introduced, which provides a compact representation of the two-dimensional linear estimate required for image reconstruction (Chapter V).

In the analysis of random processes, the second-moment properties are frequently used. Since they are essential to the development of optimal estimation theory, the analysis and various definitions and relationships are reviewed in this chapter.

Finally, several topics in number theory are presented, which have great utility in developing the theory of multirate systems and characterizing the relationships between constituent signals and the related multirate system (Chapter III).

III. MULTIRATE SYSTEMS: CONCEPTS AND THEORY

In this chapter, we develop the theory of multirate systems, which establishes the fundamental relationships in a multirate system, and culminates in a systematic framework for their analysis. These results lead to representation of the various signals in a multirate system on a common domain, system and impulse response formulations at both the signal- and system-level, linear algebraic representation of multirate operations, and ultimately, as presented in Chapter IV, development of multirate signal estimation theory.

A. INTRODUCTION

In many digital signal processing (DSP) applications, the systems involved must accommodate discrete-domain signals that are not all at the same sampling rate. For instance, consider a system in which the signals at the source and destination have different sampling rate requirements. An example of this occurs when recording music from a compact disc (CD) system at 44.1 kHz to a digital audio tape (DAT) system at 48 kHz. Another application might involve systems that incorporate several signals collected at different sampling rates. Sensor networks, many military weapon and surveillance systems, and various controllers process data from various sensors, where the information from each sensor might be collected at a different rate.

Further, a system may be at a rate that is inefficient, and sampling rate conversion may be required to reduce the rate of the system because "oversampling" is wasteful in terms of processing, storage and bandwidth.

B. MULTIRATE SYSTEMS

The various ideas described in this chapter follow [Ref. 3, 59]; however, many important extensions are made to align results with the theory of multirate systems as developed here. A *multirate system* will be defined as any system involving discrete-domain signals at different rates. Recall from Chapter II that we will use sequence notation (i.e., $x[n]$) and different index values (n, m, etc.) to denote discrete-domain signals at different rates. Figure 3.1 depicts a notional multirate system where the input, output and internal signals are at different rates. A specific example of a mul-

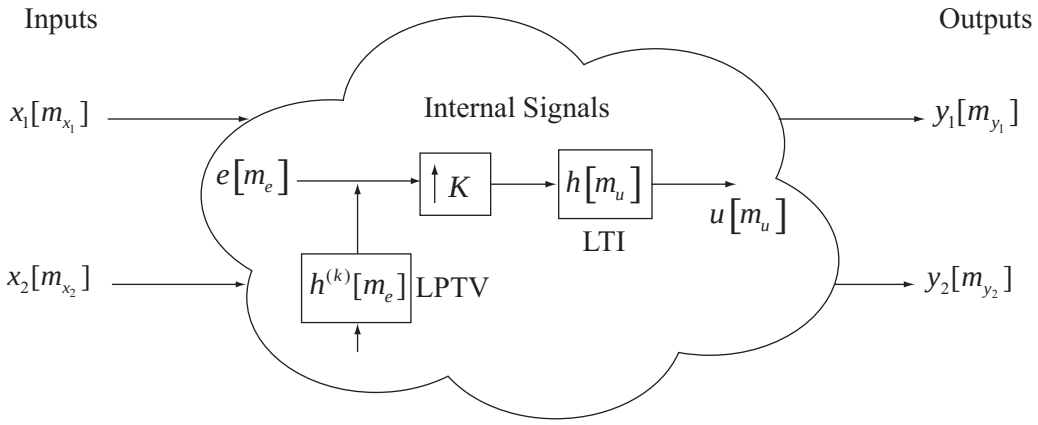

Figure 3.1. Notional multirate system where input, output, and internal signals are at different rates. (From [Ref. 3]).

tirate system is the subband coder illustrated in Figure 3.2. The signals $x[n]$ and $y[n]$ at the input and output of the system are at the original sampling rate while some of the internal signals ($y_1[m_1]$ and $y_2[m_2]$) are at lower rates produced through filtering and decimation.

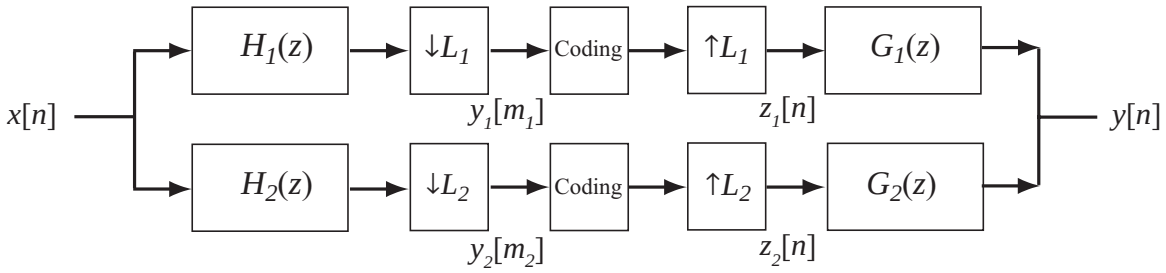

Figure 3.2. Simple subband coding system.

1. Intrinsic and Derived Rate

The notion of rate was introduced in Chapter II and is part of the description of any discrete-domain signal. The rate associated with a particular signal may be a result of sampling an analog signal or a result of operations on sequences in the system. These issues are discussed below.

a. Intrinsic Rate

A discrete-domain signal may be derived from an analog signal by periodic or uniform sampling described by

$$x[n] = x(nT_x) = x(t)|_{t=nT_x} \qquad n \in \mathbb{Z}. \tag{3.1}$$

Here, $x[n]$ is the discrete-domain sequence obtained by sampling the analog signal $x(t)$ every T_x seconds. This concept is depicted in Figure 3.3.

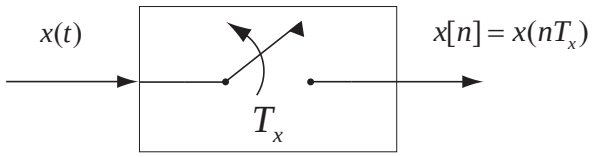

Figure 3.3. An analog signal sampled with a sampling interval of T_x.

The sampling interval T_x and its reciprocal, the sampling rate F_x, are related by

$$F_x = \frac{1}{T_x}. \tag{3.2}$$

In this context, we say $x[n]$ is at a rate F_x. The rate associated with the sequence, therefore, is the rate at which its underlying analog signal was sampled and is referred to as its *intrinsic rate*.

b. Derived Rate

The process of sampling rate conversion provides another context in considering the notion of rate or sampling rate in multirate systems. The two basic operations in sampling rate conversion are downsampling and upsampling (with appropriate filtering). These operations are depicted by the blocks shown in Figure 3.4, and they are mathematically represented by

$$y[n] = x[Mn], \tag{3.3}$$

where n is an integer, in the case of downsampling, and

$$y[n] = \begin{cases} x\left[\frac{n}{L}\right], & \text{if } n|L \ ; \\ 0, & \text{otherwise,} \end{cases} \tag{3.4}$$

in the case of upsampling. Figures 3.5 and 3.6 graphically depict the downsampling and upsampling operation, respectively, for $M = L = 2$.

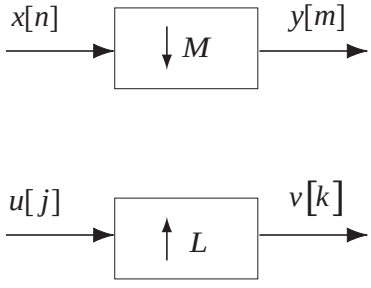

Figure 3.4. Basic operations in multirate signal processing, downsampling and upsampling.

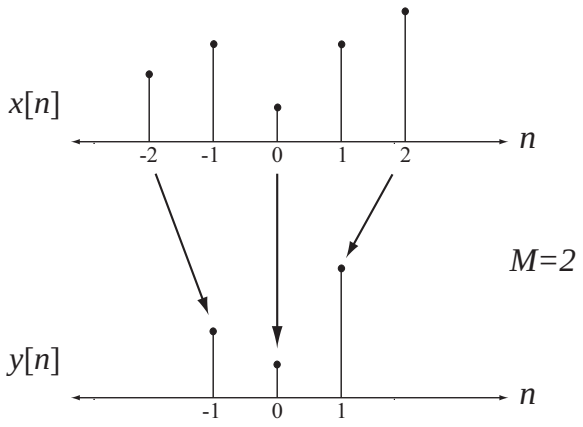

Figure 3.5. An example of the downsampling operation (3.3), $M = 2$.

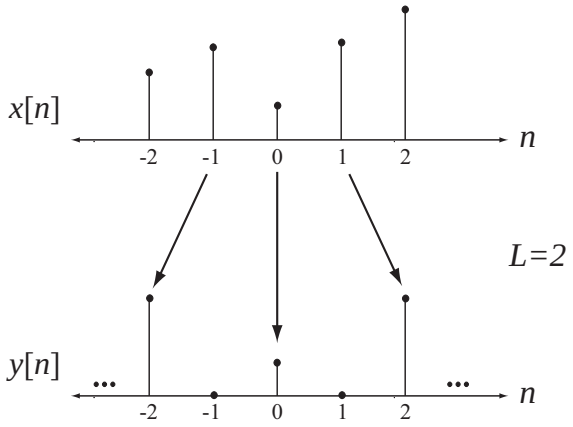

Figure 3.6. An example of the upsampling operation (3.4), $L = 2$.

Note that both operations are performed exclusively in the digital domain. The resulting signals have no intrinsic rate, but the rate is derived from the rate of the input signal. For downsampling, the output rate F_y is given by

$$F_y = \frac{F_x}{M}, \tag{3.5}$$

while for upsampling the rate is given by

$$F_y = LF_x. \tag{3.6}$$

The parameter M in downsampling is called the decimation factor while the parameter L may be called the upsampling factor. Thus, downsampling results in a reduction of sampling rate by a factor of M, and upsampling results in an increase in sampling rate by a factor of L.

It will be seen later that other operations more general than downsampling and upsampling can result in rate changes. These more general operations will be represented by linear periodically-varying filters (see Section III.D.2). The outputs of these filters have no intrinsic rate but have a derived rate associated with the operation that is performed.

C. CHARACTERIZATION OF MULTIRATE SYSTEMS

In the discussion of multirate system concepts and associated theory, it is necessary to further develop terminology, characterize such systems and develop a conceptual framework by which further analysis and extension can be based. In this section, the concepts and terms are introduced.

1. System Rate

Consider a multirate system with just two signals at different sampling rates, x_1 and x_2. Although it is not strictly necessary, the discussion can be more easily motivated if it is assumed that each signal is derived by sampling an underlying analog

signal as shown in Figure 3.7. It will be assumed that the sampling *rates* F_1 and F_2 are *integer-valued*. While the treatment could be generalized to the case where the rates are rational numbers, the assumption of integer-values simplifies the discussion and is quite realistic for practical systems. The corresponding discrete-domain signals

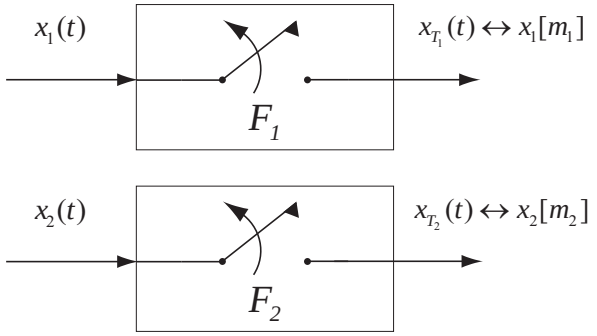

Figure 3.7. Two signals sampled at different sampling rates.

x_{T_1} and x_{T_2} at the output of the samplers are defined at points on their respective domains

$$\Psi_{T_1} = \{nT_1 \,; n \in \mathbb{Z}\}, \tag{3.7}$$

and

$$\Psi_{T_2} = \{nT_2 \,; n \in \mathbb{Z}\}, \tag{3.8}$$

where $T_1 = \dfrac{1}{F_1}$ and $T_2 = \dfrac{1}{F_2}$. The discrete-domain signals are represented in Figure 3.8 as sequences with different index values $x[n_1]$ and $x[n_2]$ indicating the different sampling rates. Note that there is some common domain

$$\Psi_{\overline{T}} = \{n\overline{T} \,; n \in \mathbb{Z}\}, \tag{3.9}$$

with some *maximum* sampling interval $\overline{T}$ in which the samples of both x_1 and x_2 can be represented. In other words, $\Psi_{T_1} \subset \Psi_{\overline{T}}$ and $\Psi_{T_2} \subset \Psi_{\overline{T}}$.

The sampling interval $\overline{T}$ in (3.9) will be called the *system sampling interval* or *clock interval*. We can state the following theorem.

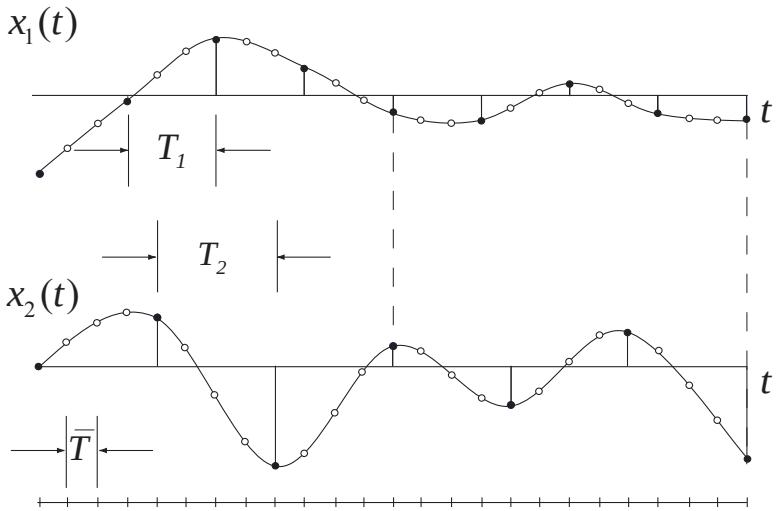

Figure 3.8. Two signals sampled at different integer-valued sampling rates. A periodic correspondence between indices can be observed (as indicated by the dashed lines). The system grid is represented by the line segment at the bottom of the figure and is derived from the set of hidden and observed samples of the associated underlying analog signals. Open circles represent "hidden" samples.

Theorem 2. The system sampling interval is given by $\overline{T} = \dfrac{1}{\overline{F}}$, where $\overline{F}$ is a positive integer, and

$$\overline{F} = \mathrm{lcm}(F_1, F_2). \tag{3.10}$$

Here, $\overline{F}$ is called the *system rate* or the *fundamental rate*.

Proof. From the definition of the least common multiple (Definition 15):

1. By definition, $\overline{F}$ must be a positive integer;
2. $\Psi_{T_1} \subset \Psi_{\overline{T}} \implies F_1 | \overline{F}, \quad \Psi_{T_2} \subset \Psi_{\overline{T}} \implies F_2 | \overline{F}$;
3. Since $\overline{T}$ is the maximum sampling interval in which samples of both x_1 and x_2 can be represented in $\Psi_{\overline{T}}$, this implies that $\overline{F} = \dfrac{1}{\overline{T}}$ is the related *minimum* sampling rate, and the third condition of Definition 15 is met.

□

We also define a *system grid* as the representation of the set $\Psi_{\overline{T}}$ on the real line, as seen in Figure 3.8. Note that the samples of a signal corresponding to the system grid can be viewed as a set of hidden and observed samples of the underlying analog signal. For example, for a given signal x_1, the observed samples are the samples of $x_1(t)$ that correspond to the set Ψ_{T_1} defined in (3.7) while the hidden samples of x_1 are the samples of $x_1(t)$ that correspond to the set $\Psi_{\overline{T}} - \Psi_{T_1}$[1].

It is frequently useful to represent all signals at the "system level" defined by $\overline{T}$ and $\overline{F}$. The system level is referred to as the "fundamental layer " in [Ref. 59]. Sequences associated with the system level will be denoted by a symbol with an overbar, as in $\overline{x}_1[n]$ and $\overline{x}_2[n]$ and a common index n. This point is developed further in Section III.C.5.

For a multirate system comprised of M signals, the definition (3.10) can be extended (see (2.39)) as

$$\overline{F} = \text{lcm}(F_1, F_2, \ldots, F_M), \tag{3.11}$$

with $\overline{T} = \dfrac{1}{\overline{F}}$.

2. Decimation Factor

Recall, from Section II.D.2(b), that the least common multiple m is a number, which is a multiple of both associated integers a and b, therefore, $a|m$ and $b|m$. Further, from Definition 13, the condition $a|m$ implies that $m = c_1 a$, and likewise $b|m$ implies that $m = c_2 b$, where c_1 and c_2 are constants.

We can apply these results to multirate systems. Since $\overline{F}$ is the least common multiple of F_1 and F_2, it follows that there exists integer constants K_1 and K_2 such that

$$\overline{F} = K_1 F_1 \quad \text{and} \quad \overline{F} = K_2 F_2. \tag{3.12}$$

[1]The "difference" $A - B$ of two sets A and B, where $B \subset A$, is defined as $A - B = \{x \in A | x \notin B\}$.

Rearranging Equation (3.12) yields an expression for these constants as

$$K_1 = \frac{\overline{F}}{F_1} \quad \text{and} \quad K_2 = \frac{\overline{F}}{F_2}. \tag{3.13}$$

Further, for a multirate system comprised of M signals, (3.13) can be extended as

$$K_i = \frac{\overline{F}}{F_i} \quad \text{where } i = 1, \ldots, M. \tag{3.14}$$

Notice that if (3.14) is rearranged to the form of (3.5):

$$F_i = \frac{\overline{F}}{K_i},$$

we explicity see that the system sampling rate $\overline{F}$ is reduced by a factor of K_i. Therefore, K_i is defined as the *system decimation factor*, or simply the *decimation factor*, for the i^{th} signal.

As a consequence, the following observation can be made and extended to any number of signals. If the underlying analog signals x_1 and x_2 are sampled at the system rate $\overline{F}$ and then are decimated by their respective decimation factors K_1 and K_2, the resultant discrete-domain signals are the signals obtained by sampling x_1 and x_2 at the original rates F_1 and F_2, respectively (see Figure 3.9). In terms of the hidden and observed samples of x_1 and x_2, the decimation factors offer a way to relate the set of observed samples to the set of all samples (hidden and observed) at the system level.

If (3.14) is expressed in terms of sampling intervals, we have

$$K_i = \frac{T_i}{\overline{T}}, \tag{3.15}$$

where the decimation factor is the ratio of the duration of the i^{th} signal's sample interval to the duration of its associated clock interval. Thus, the decimation factor K_i can also be viewed as the number of clock intervals or *system samples* between samples of the i^{th} signal when sampled at F_i.

3. System Period

Again, consider a multirate system comprised of two signals x_1 and x_2 sampled at integer-valued sampling rates F_1 and F_2, respectively. If samples of these signals

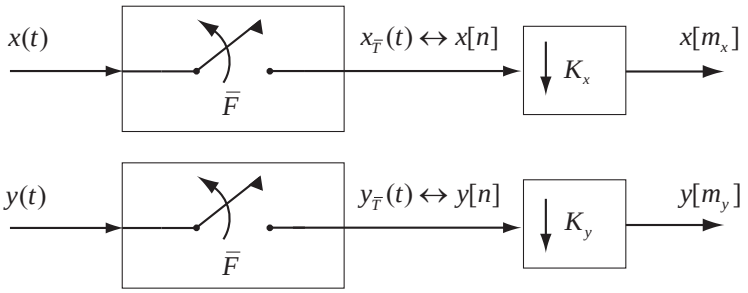

Figure 3.9. Signals sampled at the system rate and decimated by their respective decimation factors yield the original discrete-domain signals.

align on the related system grid at some time $t = t_0$, then their samples realign at some later time $t = t_1 = t_0 + T$ and at regular intervals thereafter (see Figure 3.10). The smallest positive value of T for which the realignment occurs is called the *system period* (not to be confused with the system sampling interval $\overline{T}$).Notice that $T = t_1 - t_0$ and if t_1 and t_0 are expressed in terms of their discrete-domain representations, we can write $T = (n_1 - n_0)\overline{T}$; thus, we define

$$N \equiv n_1 - n_0,$$

which is called the *discrete system period*. Observe that N represents the number of system samples between sample realignments. It relates to the system period (in seconds) as

$$T = N\overline{T}. \tag{3.16}$$

Now, we define M_i to be the number of signal samples per period. Therefore, we relate M_1 and M_2 to the discrete system period by $M_1T_1 = N\overline{T} = M_2T_2$. Recalling (3.14), we write

$$N = M_1K_1 = M_2K_2, \tag{3.17}$$

and recalling Definition (II.G.b.15), we can write

$$N = \text{lcm}(K_1, K_2), \tag{3.18}$$

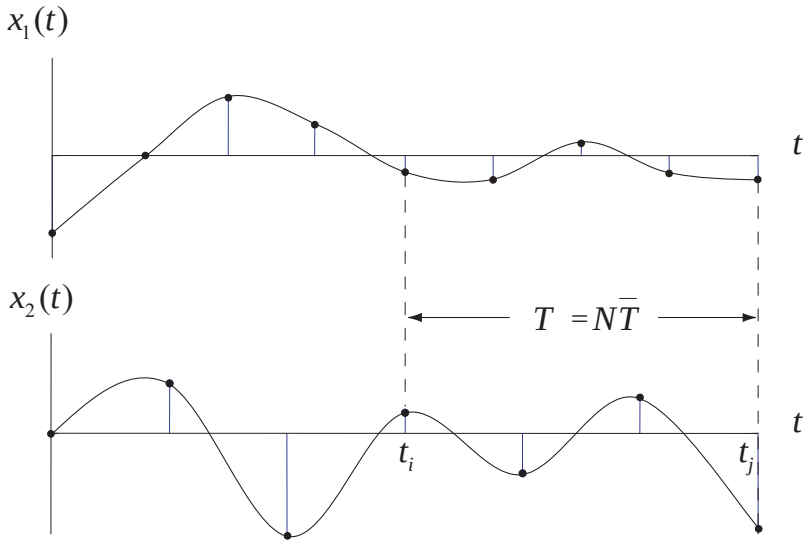

Figure 3.10. Two signals sampled at different integer-valued sampling rates. Observe the periodic alignment between indices, (After [Ref. 3]).

an explicit expression for the discrete system period. Also notice from (3.17) that

$$M_1 = \frac{N}{K_1} \quad \text{and} \quad M_2 = \frac{N}{K_2}. \tag{3.19}$$

For a multirate system comprised of M signals, the definition of (3.18) can be extended (see (2.39)) as

$$N = \text{lcm}(K_1, K_2, \ldots, K_M). \tag{3.20}$$

4. Maximally-decimated Signal Set

Consider a discrete-domain signal $y[n]$ at rate F_y. If $y[n]$ is downsampled by a factor of M, after $M-1$ successive translations, a set of related discrete-domain signals results, designated $\{x_0[m], x_1[m], \ldots, x_{M-1}[m]\}$. Note that the constituent discrete-domain signals are at rate $F_x = \dfrac{F_y}{M}$. An example is shown in Figure 3.11 for $M = 3$. If the discrete-domain signals associated with $y[n]$ are described by

$$x_i[m] = y[i + nM] \qquad i = 0, 1, \ldots, M-1, \tag{3.21}$$

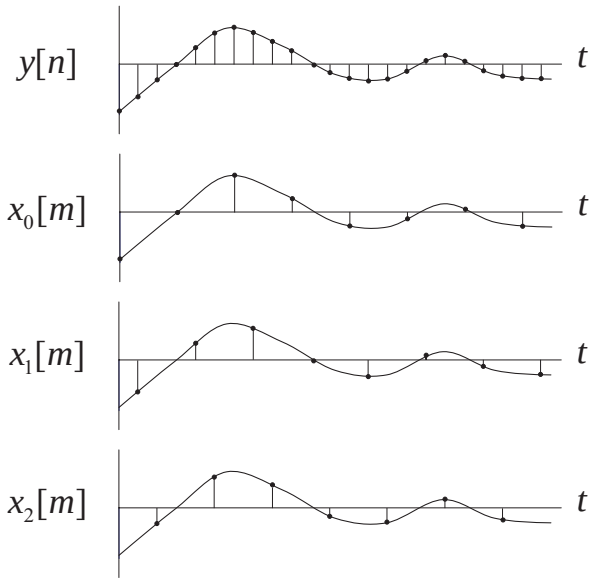

Figure 3.11. Example of a 3-fold maximally decimated signal set.

then the resultant signals will be called a *maximally-decimated* signal set with down-sampling factor M or an *M-fold maximally-decimated* signal set.

5. Representation of Signals in Multirate Systems

In the analysis of multirate systems, there is a need to relate signals to a common scale. This scale is represented by the system grid and is discussed in terms of the $\Psi_{\overline{T}}$ domain, where $\overline{T}$ is the system sampling interval. The sample indices of a signal sampled at the system rate correspond to the integer multiples of $\overline{T}$. In this context, every signal in a multirate system can be represented on the system grid.

Consider a multirate system, with a system sampling interval $\overline{T}$, containing a particular discrete-domain signal x_{T_x}, among others. This signal can be represented by the sequence

$$x[m_x] = x_{T_x}(m_x T_x),$$

where x_{T_x} is the discrete-domain signal and T_x is the associated sampling interval. Note that the sequence and its sampling rate is defined by the *discrete-domain* signal $x_{T_x}(t)$ for $t = m_x T_x$ and *not* by the analog signal $x(t)$, which may not be directly

observable or may not even exist! We refer to this as a *signal-rate* or *signal level* representation of x and, in this case, say that x is at its *native* rate. Now define $x_{\overline{T}}$ to be the associated *system-rate* or *system-level* representation of x. This signal can be represented by the sequence

$$\overline{x}[n] = x_{\overline{T}}(n\overline{T}).$$

We can relate the two representations by recalling from (3.15) that $T_x = \overline{T}K_x$ and noting that

$$x_{T_x}(m_x T_x) = x_{T_x}(m_x \overline{T} K_x) = x_{\overline{T}}(m_x K_x \overline{T}) = \overline{x}[K_x m_x].$$

Therefore, a discrete-domain signal at its native rate can be represented at the system rate or system level by

$$x[m_x] = \overline{x}[K_x m_x], \tag{3.22}$$

where K_x is the decimation factor of signal x. These concepts are illustrated in Figure 3.12 for a multirate system comprised of two signals x and y. The native rate corresponds to a signal's "original" sampling rate, and the system rate corresponds to the system rate determined from (3.10).

6. Summary of Multirate Relationships

For convenience, the representations and relationships developed in this chapter regarding multirate systems are summarized in the following tables. In Table 3.1, the various signal representations, their notations and their associated rates are indicated.

$x(t)$	Analog
$\overline{x}[n]$	System-level, system rate, $\overline{F}$
$x[m_x]$	Signal-level, native rate, F_x

Table 3.1. Signal representations in multirate systems.

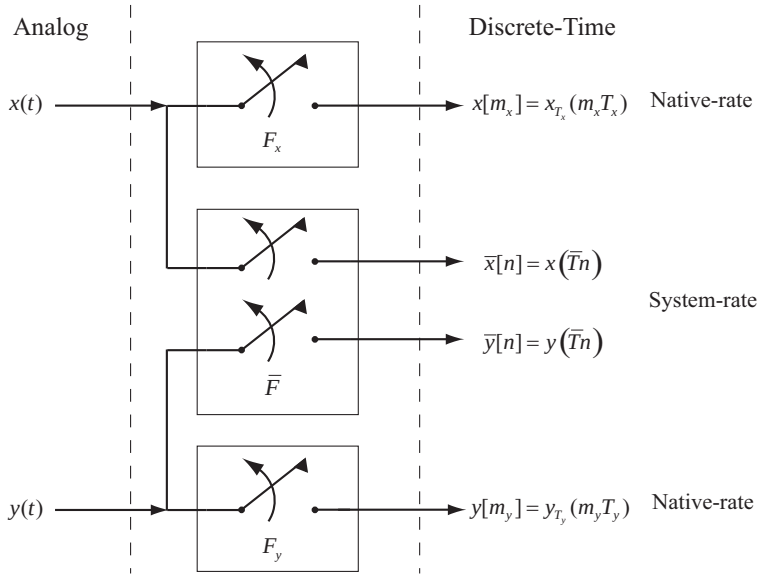

Figure 3.12. Signal representations and sampling levels in a multirate system.

In Table 3.2, the characterization of and relationship between signals in multirate systems is summarized.

Name	Relationship
System Rate	$\overline{F} = \text{lcm}(F_1, F_2, \ldots, F_M)$
System Sampling Interval	$\frac{1}{\overline{F}}$
Decimation Factor	$K_i = \frac{\overline{F}}{F_i} = \frac{T_i}{\overline{T}}$
System Sample Period	$N = \text{lcm}(K_1, K_2, \ldots, K_M)$
Samples/Period	$M_i = \frac{N}{K_i}$
System Period	$T = N\overline{T} = M_i T_i$

Table 3.2. Summary of various relationships pertaining to a multirate system (M signals).

Finally, in Table 3.3, these characterizations and relationships are summarized in relation to signal and system level representations.

	Sampling Rate	Sampling Interval	Decimation Factor	Samples per Period	System Period
Signal	F_x	T_x	K_x	M_x	$T = M_x T_x$
System	$\overline{F}$	$\overline{T}$	1	N	$T = N\overline{T}$

Table 3.3. Parameters pertaining to a multirate system, (After [Ref. 3]).

D. MULTIRATE SYSTEM THEORY

1. Description of Systems

A signal processing *system* represents the process for transforming a signal into another signal. The concept is illustrated in Figure 3.13(a), where a signal $x(t)$ is transformed into a signal $y(t)$. The input and output may be of any of the signal or sequence types discussed in Chapter II and need not be of the same type. For instance, the input may be a discrete-domain signal and the output may be an analog signal. Our primary concern, however, is the case where both the input and the output are discrete-domain signals, not necessarily with the same sampling intervals.

Since discrete-domain signals are represented by sequences together with a (known or implied) sampling rate, it is appropriate to consider the properties of "systems" that transform sequences. These will be referred to as discrete systems as shown in Figure 3.13(b), and the transformation will be represented by $\mathcal{T}_D$. In addition to performing a specified operation on the input sequence, a discrete system provides a means of determining the output sampling rate from the input sampling rate. When input and output sampling rates are not the same, it is our convention to use different letters for the index variable of the sequence.

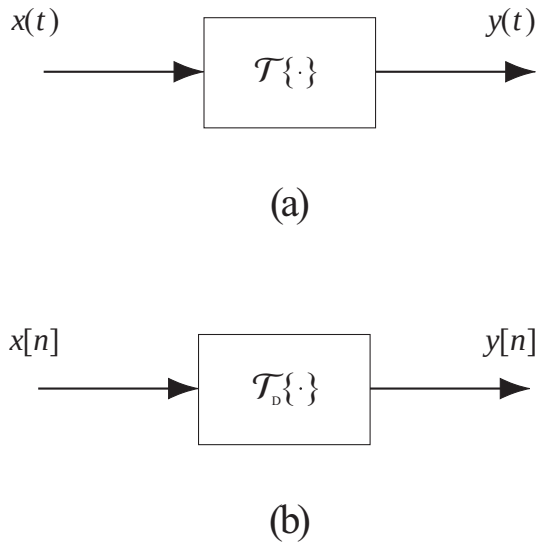

Figure 3.13. (a) Block-diagram representation of a signal processing system; (b) Block-diagram representation of a discrete system.

In general, a discrete-domain system is represented by

$$\mathbf{y}[m] = \mathcal{T}_D\{\mathbf{x}[n]\} \quad \text{or} \quad \mathcal{T}_D\{\mathbf{x}[n]\} \Rightarrow \mathbf{y}[m], \tag{3.23}$$

where $\mathcal{T}_D$ is a suitable mathematical operator and $\mathbf{x}[n]$ and $\mathbf{y}[m]$ represent the input and output sequences for such a system. Note that the sequences in general may be at different rates.

2. Classification of Discrete Systems

Discrete systems can be classified by certain restrictions or characteristics placed upon, or observed concerning them. A number of such classifications are important in signal processing, including: linear/non-linear, time-invariant/time-variant, causal/non-causal, stable/unstable, invertible/non-invertible systems, and systems

with memory/without memory. In this section, we deal with the first three of these classifications. Others are not so important to our discussion and conform to definitions used in many text books [Ref. 60, 61].

a. Linearity

A *discrete linear system* is any system that satisfies the generalized *superposition* principle. If the input to such a system consists of a weighted sum of sequences, then its output consists of the weighted sum of the system responses to each individual input sequence (superposition of responses). It is sufficient to define linearity in terms of the system's response to a weighted sum of two sequences.

Definition 20. Let $x_1[n]$ and $x_2[n]$ be two sequences at the same sampling rate. A discrete system is linear if and only if

$$\mathcal{T}_D\{\alpha_1 x_1[n] + \alpha_2 x_2[n]\} = \alpha_1 \mathcal{T}_D\{x_1[n]\} + \alpha_2 \mathcal{T}_D\{x_2[n]\}, \tag{3.24}$$

for arbitrary input sequences $x_1[n] and x_2[n]$ and constants $\alpha_1 and \alpha_2$.

Note that, while the output of a linear system may be at a different rate than the input, we make no attempt to define linearity in terms of two sequences at different rates. Indeed, the *sum* of two sequences at different rates has no obvious or unique intuitive meaning and is not necessary for our theory of multirate systems.

Any discrete system that does not satisfy Definition 20 is a nonlinear discrete system (e.g., square law system defined by $y[n] = (x[n])^2$). Time dependence is not an issue. Both downsamplers and upsamplers (see Section III.B.1(b)) are linear systems.

b. Shift-invariance

Systems can also be characterized by the variation in their input-output characteristics as time evolves, and can be subdivided into *shift-invariant* and *shift-dependent* systems (frequently called time-invariant and time-dependent).

Definition 21. Let $\mathcal{T}_D$ be a discrete system such that the input and output sequences are at the *same rate*, i.e., $\mathcal{T}_D\{x[n]\} \Rightarrow \{y[n]\}$. Then the system is *shift-invariant* if and only if

$$\mathcal{T}_D\{x[n-N]\} \Rightarrow y[n-N], \quad \text{for } \textit{all} \text{ integers } N. \tag{3.25}$$

If the system satisfies (3.25) only for a particular value N and integer multiples thereof, the system is said to be *periodic* with period N. For systems with different input and output rates, shift-invariance is not defined. Periodicity, however, can be generalized to include these systems, as shown below.

c. Periodic Shift-invariance

For discrete systems with input and output signals at different rates, i.e., $\mathcal{T}_D\{\mathbf{x}[n]\} \Rightarrow \mathbf{y}[m]$, we define a particular type of shift-invariance called *periodic shift-invariance* (PSI). A system that observes this property is called a *discrete periodically shift-invariant system*. The definition of this property follows.

Definition 22. Let $\mathcal{T}_D$ be a discrete system such that if $\mathcal{T}_D\{x[m_x]\} \Rightarrow \{y[m_y]\}$, then the system is *periodically shift-invariant* if there exists integers M_x and M_y such that

$$\mathcal{T}_D\{x[m_x - M_x]\} \Rightarrow y[m_y - M_y]. \tag{3.26}$$

Note that when the input and output are at the same rate, a *periodic* system satisfies this definition with $M_x = M_y$ and a *shift-invariant* system satisfies this definition for *all* M_x such that $M_x = M_y$. The need for the more general definition given in (3.26) will become clear further in our development.

d. Causality

In defining causality, it is important to know the rates or sampling intervals of the sequences involved. In fact, as pointed out in [Ref. 62], "Causality is intrinsically related to the ordering in time [or domain] of input and output signals of [a] system." Ordering is clear in a single-rate system as identical sample indices in each associated sequence correspond to identical points in a common domain. In

multirate systems, sequence sample indices must be referred back to their absolute scales (i.e., the discrete-domain signal) to discuss ordering.

Definition 23. A discrete system $\mathcal{T}_D$ is *causal* if and only if

$$y[m_y] \text{ depends } \textit{only} \text{ on } x[m_x - k] \quad \text{for } k = \{0, 1, \dots\}, \tag{3.27}$$

where $m_x = \left\lfloor \dfrac{K_y m_y}{K_x} \right\rfloor$, and K_x, K_y are the associated decimation factors.

A system is noncausal if it does not satisfy this definition.

It can be seen that a discrete system is causal if and only if the discrete-domain signal $y_{T_y}(t)$ at $t = m_y T_y$ depends only on values of the discrete-domain input signal $x_{T_x}(t)$ for $t = m_x T_x \leq m_y T_y$. This set of input values is known as the *region of support* of the system. The concept of causality is illustrated in Figure 3.14. The discrete multirate system depicted has a discrete-domain input signal represented by the sequence $x[m_x]$ and an output signal represented by the sequence $y[m_y]$. For a given index in the output sequence m_{y_0}, Definition 23 requires that $m_{x_0} \leq \left\lfloor \dfrac{K_y m_{y_0}}{K_x} \right\rfloor$ for causality.

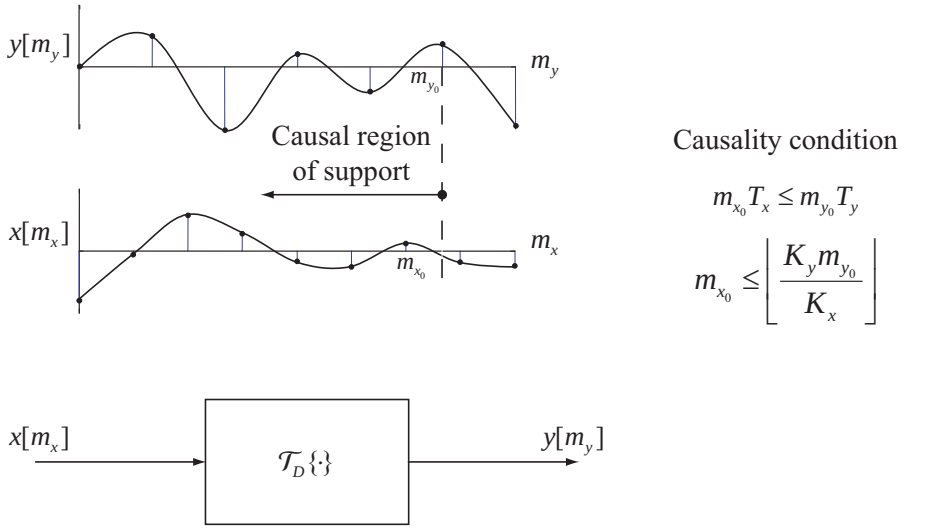

Figure 3.14. Concept of causality in a discrete multirate system comprised of a discrete-domain input signal $x[m_x]$ and output signal $y[m_y]$.

3. Representation of Discrete Linear Systems

Given a discrete linear system with input $x[m]$ and output $y[n]$, with, possibly, different sampling rates, the input-output relation or *system response* can be written as

$$y[n] = \sum_{m=-\infty}^{\infty} g[n,m]x[m]. \tag{3.28}$$

The term $g[n,m]$, called the *kernel* or *Green's function*, is the response of the system at point n in the output sequence to a unit impulse[2] applied at point m in the input sequence. This formulation is a discrete-domain version of the continuous model in [Ref. 63, 64, 62], and the corresponding kernel has been referred to as the *Green's function weighting pattern response* [Ref. 65].

a. Single-rate Systems

When the input and output rates are the same, (3.28) can be written as

$$y[n] = \sum_{m=-\infty}^{\infty} h[n;m]x[n-m], \tag{3.29}$$

where

$$h[n;m] = g[n,n-m], \tag{3.30}$$

is called the *shift-dependent impulse response*. The system is *causal* (see Section III.D.2(d)) if

$$h[n;m] = 0 \quad \text{for } m < 0. \tag{3.31}$$

The system is *periodic* (see Definition 21) if there exists N such that

$$h[n;m] = h[n+N;m] \quad \text{for all } n. \tag{3.32}$$

[2]The unit impulse, also know as the Kronecker delta function, is defined as

$$\delta[n] = \begin{cases} 1, & n = 0; \\ 0, & n \neq 0. \end{cases}$$

If in addition, the system is shift-invariant (see Definition 21), then the impulse response is necessarily independent of the first argument (n) and the output can be written as the familiar convolution summation

$$y[n] = \sum_{m=-\infty}^{\infty} h[m]x[n-m] = \sum_{m=-\infty}^{\infty} h[n-m]x[m]. \tag{3.33}$$

The system represented in (3.33) is commonly referred to as a *filter* because of its interpretation in the Fourier domain, although the term "filter" is often used to apply to any system; linear or nonlinear, shift-variant or shift-invariant, in the signal processing literature. A filter is said to be a *finite impulse response* (FIR) filter (or system) if the sequence $h[n]$ has finite support and an *infinite impulse response* (IIR) filter (or system), otherwise. The *region of support* or the *support* of a given sequence is the set of values over which the sequence is non-zero [Ref. 66].

b. Multirate Systems

In developing results for multirate systems, it is convenient to first describe the multirate system at the "system level" discussed in Section III.C.5 of this chapter. When represented at the system level, we can apply known results from the analysis of single-rate systems to the multirate system and then express those results at the signal level pertaining to the signals of interest.

(1) System-level Representation Recall the system response equation (3.28)

$$y[m_y] = \sum_{m_x} g[m_y, m_x]x[m_x], \tag{3.34}$$

where y and x are at different rates represented by m_y and m_x, respectively. Also, recall (3.22) that a discrete-domain signal $x_{T_x}(t)$ can be represented at the system level

$$x[m_x] = \overline{x}[K_x m].$$

Now define $\overline{g}$, the *system kernel* or *system Green's function*, such that

$$g[m_y, m_x] = \overline{g}[K_y m_y, K_x m_x],$$

where K_x and K_y are the decimation factors for x and y, respectively. At other values of it arguments, $\overline{g}$ is defined to be 0. Now, (3.34) can be written as

$$\overline{y}[K_y m_y] = \sum_{m_x} \overline{g}[K_y m_y, K_x m_x]\, \overline{x}[K_x m_x]. \tag{3.35}$$

If g satisfies Definition 22 for periodic shift-invariance, then a necessary and sufficient condition is that

$$\overline{g}[K_y m_y, K_x m_x] = \overline{g}[K_y(m_y + M_y), K_x(m_x + M_x)].$$

where M_x and M_y are the number of samples per system period for x and y, respectively. Then

$$\overline{g}[K_y(m_y + M_y), K_x(m_x + M_x)] = \overline{g}[K_y m_y + N, K_x m_x + N] \tag{3.36}$$

where we recall (3.17) that the system sample period is given by $N = K_y M_y = K_x M_x$; therefore, $\overline{g}$ has period N in both arguments.

Now, we define

$$\overline{h}[K_y m_y; K_x m_x] \equiv \overline{g}[K_y m_y, K_y m_y - K_x m_x], \tag{3.37}$$

or, equivalently,

$$\overline{g}[K_y m_y; K_x m_x] \equiv \overline{h}[K_y m_y, K_y m_y - K_x m_x],$$

where $\overline{h}$ is called the *system impulse response*. Notice that since $\overline{g}$ satisfies (3.36), then

$$\overline{h}[n; l] = \overline{g}[n, n - l] = \overline{g}[n + N, n - l + N] = \overline{h}[n + N; l],$$

thus $\overline{h}[n; l]$ is periodic in its first argument *only*. Note, also, that if the system is causal, then $h[n; l]$ must be 0 for $l < 0$. Now we can write

$$\overline{g}[K_y m_y; K_x m_x] = \overline{h}[K_y m_y + N; K_y m_y - K_x m_x], \tag{3.38}$$

where N is the system sample period.

Now, (3.35) can be written as

$$\overline{y}[K_y m_y] = \sum_{m_x} \overline{h}[K_y m_y; K_y m_y - K_x m_x]\, \overline{x}[K_x m_x]. \tag{3.39}$$

Since $\overline{h}$ is periodic in N, we can define

$$\overline{h}^{(p)}[l] \equiv \overline{h}[n; l] \qquad \text{where } p = \langle n \rangle_N, \tag{3.40}$$

and N is the system sample period. Substituting into (3.39) yields the general filter equation

$$\overline{y}[n] = \begin{cases} \displaystyle\sum_{m_x} \overline{h}^{(p)}[n - K_x m_x]\, \overline{x}[K_x m_x], & K_y | n, \\ \text{undefined}, & \text{otherwise} \end{cases} \tag{3.41}$$

where $p = \langle n \rangle_N$.

If we desire a causal filter (see Section III.D.2(d)), then

$$m_x T_x \leq m_y T_y \quad \text{or} \quad m_x \leq \frac{K_y m_y}{K_x}, \tag{3.42}$$

and

$$\overline{y}[n] = \begin{cases} \displaystyle\sum_{m_x=-\infty}^{\lfloor \frac{K_y m_y}{K_x} \rfloor} \overline{h}^{(p)}[n - K_x m_x]\, \overline{x}[K_x m_x], & K_y | n, \\ \text{undefined}, & \text{otherwise} \end{cases} \tag{3.43}$$

where $p = \langle n \rangle_N$. The upper limit on the sum is insured if $\overline{h}^{(p)}[l] = 0$ for $l < 0$. Notice that when $T_x = T_y \rightarrow K_x = K_y$ (single-rate system), (3.41) and (3.43) simplify to the expected convolution sums.

Example 11. *Consider Figure 3.15, where two signals are represented on their associated grids. The upper grid (a) represents a signal y that has an associated decimation factor $K_y = 3$, and the lower grid (b) represents a signal x that has an associated decimation factor $K_x = 2$. Recall* (3.18) *that the system period is given by $N = \text{lcm}(K_x, K_y)$; therefore, $N = 6$.*

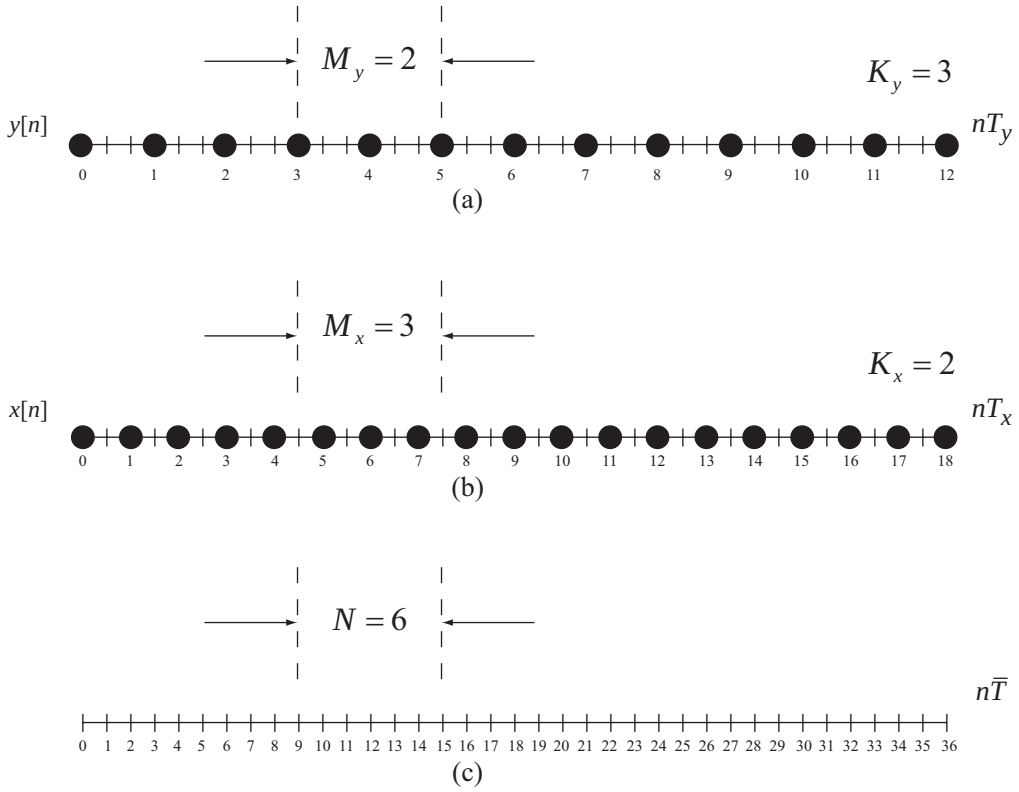

Figure 3.15. (a) Discrete-time signal $y[n]$ with decimation factor $K_y = 3$; (b) Discrete-time signal $x[n]$ with decimation factor $K_x = 2$; (c) System grid.

If we desire the estimate for y at $m_y = 4$, using a causal filter, where the filter order $P = 3$, then we can write (3.43) *as*

$$\overline{y}[12] = \sum_{m_x=3}^{\lfloor \frac{12}{2} \rfloor = 6} \overline{h}^{(0)}[12 - 2m_x]\, \overline{x}[2m_x], \qquad \textit{where } p = \langle 12 \rangle_6 = 0.$$

therefore

$$\overline{y}[12] = \overline{h}^{(0)}[4]\overline{x}[8] + \overline{h}^{(0)}[2]\overline{x}[10] + \overline{h}^{(0)}[0]\, \overline{x}[12].$$

Notice that the linear combination is in terms of the system-rate parameters (n is the system time index). Once $\overline{y}[12]$ is computed, recall that $y[m_y] = \overline{y}[m_y K_y]$; therefore, $y[4] = \overline{y}[12]$.

If we desire the estimate for y at $m_y = 5$,

$$\overline{y}[15] = \sum_{m_x=5}^{\lfloor \frac{15}{2} \rfloor = 7} \overline{h}^{(3)}[15 - 2m_x]\overline{x}[2m_x], \qquad \textit{where } p = \langle 15 \rangle_6 = 3.$$

therefore

$$\overline{y}[15] = \overline{h}^{(3)}[5]\overline{x}[10] + \overline{h}^{(3)}[3]\overline{x}[12] + \overline{h}^{(3)}[1]\overline{x}[14]. \qquad \blacksquare$$

(2) Signal-level Representation Often, it is desirable or more convenient to deal in terms of the actual signal parameters rather than system parameters; therefore, we develop (3.41) and (3.43) in terms of the individual signal parameters. To do so, we introduce the following substitutions and change of variables.

First let us examine the system impulse response $\overline{h}$,

$$\overline{h}^{(p)}[K_y m_y - K_x m_x] = \overline{h}[K_y m_y + N; K_y m_y - K_x m_x].$$

Consider the first argument, where K_y has been factored out and we recall (3.17)

$$K_y m_y + N = K_y(m_y + N/K_y) = K_y(m_y + M_y).$$

Since this argument is periodic,

$$K_y(m_y + N/K_y) \leftrightarrow K_y \langle m_y \rangle_{M_y}.$$

Now, consider the second argument, where K_x has been factored out

$$K_y m_y - K_x m_x = K_x \left(\frac{K_y m_y}{K_x} - m_x \right).$$

Recalling that

$$y[m_y] = \overline{y}[m_y K_y], x[m_x] = \overline{x}[m_x K_x],$$

and

$$\overline{h}[K_y m_y; K_x m_x] = h[m_y; m_x],$$

we can write the impulse response as

$$h^{(l)}\left[\left\lfloor\frac{K_y m_y}{K_x}\right\rfloor - m_x\right], \qquad \text{where } l = \langle m_y \rangle_{M_y},$$

and we can write

$$y[m_y] = \sum_{m_x} h^{(l)}\left[\left\lfloor\frac{K_y m_y}{K_x}\right\rfloor - m_x\right] x[m_x], \qquad \text{where } l = \langle m_y \rangle_{M_y}.$$

If we introduce the following change of variables

$$k = \left\lfloor\frac{K_y m_y}{K_x}\right\rfloor - m_x, \tag{3.44}$$

we can write the general signal-rate filtering equation as

$$\boxed{y[m_y] = \sum_{m_x} h^{(l)}[m_x] x\left[\left\lfloor\frac{K_y m_y}{K_x}\right\rfloor - m_x\right], \qquad \text{where } l = \langle m_y \rangle_{M_y}.} \tag{3.45}$$

and the signal-rate causal filtering equation as

$$\boxed{y[m_y] = \sum_{m_x=0}^{\infty} h^{(l)}[m_x] x\left[\left\lfloor\frac{K_y m_y}{K_x}\right\rfloor - m_x\right], \qquad \text{where } l = \langle m_y \rangle_{M_y}.} \tag{3.46}$$

The lower limit ($m_x = 0$) on the summation is equivalent to the causal condition $h^{(l)}[m_x] = 0$ for $m_x < 0$. Notice that M_y, the number of signal samples (y) per system period, is the period of the filters required to form $y[m_y]$, referred to as the *cyclostationary period* in [Ref. 9]. Additionally, note that when $T_x = T_y$, then $K_x = K_y$ and (3.45) and (3.46) simplify to the expected convolution sums for a single-rate system.

Example 12. *Let us illustrate with the same example previously discussed and illustrated in Figure 3.15. Recall that signals y and x have associated decimation factors* $K_y = 3$ *and* $K_x = 2$*, respectively, and that the system period* $N = 6$*. Further, recall that* $M_y = \dfrac{N}{K_y} = \dfrac{6}{3} = 2$*.*

If we desire the estimate for y at $m_y = 4$, using a causal FIR filter, where the filter order $P = 3$, then we can write (3.45) as

$$y[4] = \sum_{m_x=0}^{2} h^{(0)}[m_x]x[6 - m_x], \qquad \textit{where } l = \langle 4 \rangle_2 = 0,$$

therefore

$$y[4] = h^{(0)}[0]x[6] + h^{(0)}[1]x[5] + h^{(0)}[2]x[4].$$

If we desire the estimate for y at $m_y = 5$,

$$y[5] = \sum_{m_x=0}^{2} h^{(1)}[m_x]x[7 - m_x], \qquad \textit{where } l = \langle 5 \rangle_2 = 1,$$

therefore

$$y[5] = h^{(1)}[0]x[7] + h^{(1)}[1]x[6] + h^{(1)}[2]x[5]. \qquad \blacksquare$$

E. MATRIX REPRESENTATION

In the analysis of multirate systems, linear algebra concepts provide a useful framework to represent or model basic multirate operations, such as downsampling, upsampling and linear filtering. This section develops a systematic methodology, which is used in other sections to further represent multirate systems, an extension of work presented by [Ref. 67].

1. Decimation

Decimation is the process of digitally reducing the sampling rate of a signal [Ref. 65], and the basic element used in digital systems is the downsampler or decimator, shown in Figure 3.16. This element extracts every M^{th} sample of its input and, as a result, decreases the sampling rate by $\frac{1}{M}$. Its operation can be expressed mathematically as

$$y[n] = x[Mn] \tag{3.47}$$

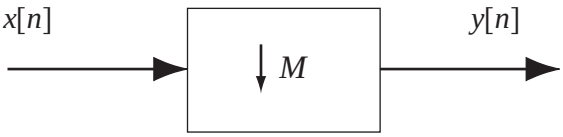

Figure 3.16. M-fold downsampler.

where n is an integer.

If the input and output signals are represented as vectors, then this operation can be expressed as a linear transformation of the form

$$\mathbf{y} = \mathcal{T}\{M, N, \mathbf{x}\} \tag{3.48}$$

where $\mathcal{T}\{\cdot\}$ represents an arbitrary linear operator that is dependent on the decimation factor M and the order of its associated vectors. If the downsampler takes input vector $\mathbf{x} \in \mathbb{R}^{NM}$ where

$$\mathbf{x} = [\ x[0] \quad x[1] \quad \dots \quad x[M] \quad x[M+1] \quad \dots \quad x[NM-1]\ ]^T$$

and produces an output vector $\mathbf{y} \in \mathbb{R}^N$ where

$$\mathbf{y} = [\ x[0] \quad x[M] \quad x[2M] \quad \dots \quad x[(N-1)M]\ ]^T,$$

then the operator can be expressed as

$$\mathcal{T} = \mathbf{D}_M, \tag{3.49}$$

and the transformation can be written as

$$\mathbf{y} = \mathbf{D}_M \mathbf{x}. \tag{3.50}$$

The constant matrix $\mathbf{D_M} \in \mathbb{R}^{N \times NM}$ is called a *decimation matrix* and is defined in terms of a Kronecker product (introduced in Section II.B.2) as

$$\mathbf{D}_M = \mathbf{I} \otimes \boldsymbol{\iota}^T \tag{3.51}$$

where $\mathbf{I}$ is the $N \times N$ identity matrix and $\boldsymbol{\iota}_k$ is an $M \times 1$ index vector with a 1 in the first position and 0's elsewhere.

As an example, consider the case where $M = 3$ and $\mathbf{x} \in \mathbb{R}^{12}$. The decimation matrix $\mathbf{D_3} \in \mathbb{R}^{4\times 12}$ is given by

$$\mathbf{D}_3 = \begin{bmatrix} 1 & 0 & 0 & 0 & 0 & 0 & 0 & 0 & 0 & 0 & 0 & 0 \\ 0 & 0 & 0 & 1 & 0 & 0 & 0 & 0 & 0 & 0 & 0 & 0 \\ 0 & 0 & 0 & 0 & 0 & 0 & 1 & 0 & 0 & 0 & 0 & 0 \\ 0 & 0 & 0 & 0 & 0 & 0 & 0 & 0 & 0 & 1 & 0 & 0 \end{bmatrix},$$

which results in $\mathbf{y} \in \mathbb{R}^4$.

2. Expansion

Expansion and decimation are dual operations. Expansion is the process of digitally *increasing* the sampling rate of a signal, and the basic element used is the upsampler or expander, shown in Fig 3.17. This element inserts $L-1$ zeros after every sample of the input and, as a result, increases the sampling rate by L. Mathematically the process is described by

$$y[n] = \begin{cases} x\left[\dfrac{n}{L}\right], & \text{if } n \text{ is an integer multiple of } L; \\ 0, & \text{otherwise,} \end{cases} \tag{3.52}$$

or

$$y[n] = \sum_{k=-\infty}^{\infty} x(k)\delta(n - kL). \tag{3.53}$$

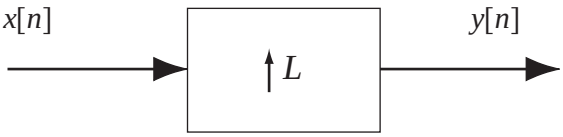

Figure 3.17. L-fold expander.

If the input and output signals are represented as vectors, then this operation can be expressed as a linear transformation of the form

$$\mathbf{y} = \mathcal{T}\{L, N, \mathbf{x}\} \tag{3.54}$$

where $\mathcal{T}\{\cdot\}$ represents an arbitrary linear operator that is dependent on the upsampling factor L and the order of its associated vectors. If the expander takes input vector $\mathbf{x} \in \mathbb{R}^N$ where

$$\mathbf{x} = [\ x[0] \quad x[1] \quad \dots \quad x[N-1]\ ]^T$$

and produces an output vector $\mathbf{y} \in \mathbb{R}^{(NL)}$ where

$$\mathbf{y} = \left[\ x[0] \ \overbrace{0 \ \dots \ 0}^{L-1} \ x[1] \ \overbrace{0 \ \dots \ 0}^{L-1} \ x[2] \quad \dots \quad x[(N-1)] \ \overbrace{0 \ \dots \ 0}^{L-1}\ \right]^T$$

then the operator can be expressed as

$$\mathcal{T} = \mathbf{U}_L, \tag{3.55}$$

and the transformation can be written as

$$\mathbf{y} = \mathbf{U}_L\mathbf{x}. \tag{3.56}$$

The constant matrix $\mathbf{U_L} \in \mathbb{R}^{NL\times N}$ is called an *expansion matrix* and is defined in terms of a Kronecker product as

$$\mathbf{U}_L = \mathbf{I} \otimes \boldsymbol{\iota} \tag{3.57}$$

where $\mathbf{I}$ is the $N \times N$ identity matrix and $\boldsymbol{\iota}$ is an $L \times 1$ index vector with a 1 in the first position and 0's elsewhere.

As an example, consider the case where $L = 3$ and $\mathbf{x} \in \mathbb{R}^4$. The expansion

matrix $\mathbf{U_3} \in \mathbb{R}^{12\times 4}$ is given by

$$\mathbf{U}_3 = \begin{bmatrix} 1 & 0 & 0 & 0 \\ 0 & 0 & 0 & 0 \\ 0 & 0 & 0 & 0 \\ 0 & 1 & 0 & 0 \\ 0 & 0 & 0 & 0 \\ 0 & 0 & 0 & 0 \\ 0 & 0 & 1 & 0 \\ 0 & 0 & 0 & 0 \\ 0 & 0 & 0 & 0 \\ 0 & 0 & 0 & 1 \\ 0 & 0 & 0 & 0 \\ 0 & 0 & 0 & 0 \end{bmatrix},$$

which results in $\mathbf{y} \in \mathbb{R}^{12}$.

Notice that, if $L = M$, the expansion matrix is related to the decimation matrix through matrix transposition as

$$\mathbf{D}_M = (\mathbf{U}_L)^T \qquad \text{for } M = L; \tag{3.58}$$

in other words, the operation of decimation and expansion are complementary processes when $M = L$.

3. Sample Rate Conversion with Delay

In the analysis of various multirate implementations, notably those involving polyphase decompositions (efficient implementations) [Ref. 68], signal delay must be incorporated in the system model and forms another basic building block of multirate systems as shown in Figure 3.18. In discrete systems, a signal delay[3] is simply a shift

[3]Despite the name, there is no restriction in considering advancement in sample index. This will be clear by the sign associated with the delay.

of the associated sequence to the right or left by some integer number of samples M and is represented by the usual

$$x[n-M] \longleftrightarrow z^{-M}$$

and

$$x[n+M] \longleftrightarrow z^{+M}$$

where z^{-M} indicates a delay or shift to the right, and z^{+M} indicates a negative delay or shift to the left.

In conjunction with signal delay, the sample rate conversion transformations of (3.50) and (3.56) can be generalized. Given a delay $k \in \{0, 1, \ldots, M-1\}$, then

$$\mathbf{y} = \mathbf{D}_M^{(k)}\mathbf{x}. \tag{3.59}$$

The constant matrix $\mathbf{D}_\mathbf{M}^{(\mathbf{k})} \in \mathbb{R}^{N \times NM}$ is called an *decimation matrix with delay* and is defined in terms of a Kronecker product as

$$\mathbf{D}_M^{(k)} = \mathbf{I} \otimes \boldsymbol{\iota}_k^T \tag{3.60}$$

where $\mathbf{I}$ is the $N \times N$ identity matrix and $\boldsymbol{\iota}_k$ is an $M \times 1$ index vector with a 1 in the $(k+1)^{th}$ position and 0's elsewhere.

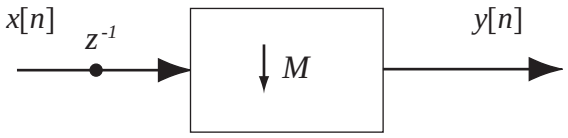

Figure 3.18. M-fold decimator with delay.

In a similar manner,

$$\mathbf{y} = \mathbf{U}_L^{(k)}\mathbf{x}. \tag{3.61}$$

The constant matrix $\mathbf{U}_\mathbf{L}^{(\mathbf{k})} \in \mathbb{R}^{NL \times N}$ is called an *expansion matrix with delay* and is defined in terms of a Kronecker product as

$$\mathbf{U}_L^{(k)} = \mathbf{I} \otimes \boldsymbol{\iota}_k \tag{3.62}$$

where $\mathbf{I}$ is the $N \times N$ identity matrix and $\boldsymbol{\iota}_k$ is an $L \times 1$ index vector with a 1 in the $(k+1)^{th}$ position and 0's elsewhere.

Consideration of (3.60) and (3.62) shows the duality of the two operators, for $M = L$, and results in the general expression

$$U_M^{(k)} = (D_M^{(k)})^T = \mathbf{I} \otimes \boldsymbol{\iota}_k \qquad \text{for } k \in \{0, 1, \ldots, M-1\}. \tag{3.63}$$

4. Linear Filtering

It is also useful to provide a matrix representation of linear filtering. Recall from (3.33) that a P length causal FIR filter is fully specified by its P filter coefficients (impulse response). If we denote these coefficients $\mathbf{h} \in \mathbb{R}^P$ as

$$\mathbf{h}_P = [\ h[0] \quad h[1] \quad \ldots \quad h[P-1]\ ]^T$$

and the related input data sequence $\mathbf{x}_P[n] \in \mathbb{R}^P$ as

$$\mathbf{x}_P[n] = [\ x[n-P+1] \quad \ldots \quad x[n-1] \quad x[n]\ ]^T,$$

then the output of the filter at index n, $y[n] \in \mathbb{R}$ can be represented by

$$y[n] = \mathbf{h}_P^T \tilde{\mathbf{x}}_P[n] = \tilde{\mathbf{h}}_P^T \mathbf{x}_P[n]. \tag{3.64}$$

F. CHAPTER SUMMARY

This chapter establishes the theory of multirate systems and provides the foundation upon which the remainder of this work is built. The concept of a multirate system is introduced, with various practical examples. A multirate system is formally defined, the notion of rate is discussed, and the basic multirate operations of downsampling and upsampling are introduced. A conceptual framework for the analysis of multirate systems is developed, which enables a systematic extension of optimal estimation and linear filtering theory to multirate systems. The characterizations of

constituent multirate signals introduced include system rate, decimation factor, system period, and maximally-decimated signal sets. Further, this chapter introduces the concept of a system grid, which allows representation of the various signals in a multirate system on a common domain.

The system theory of multirate systems is also developed, including the concepts of linearity, shift-invariance, period shift-invariance, and causality. In addition, the input-output relation of a multirate system is discussed in terms of the system response and its associated Green's function and is adapted to the multirate problem in both system-level and signal-level representations. Further, the relationship between linear periodically time-varying filters and their linear time-invariant equivalents is discussed.

Finally, the basic multirate operations are analyzed from a linear algebraic point of view, and matrix representations for the operations of downsampling, upsampling, sample rate conversion and linear filtering are presented.

THIS PAGE INTENTIONALLY LEFT BLANK

IV. MULTIRATE OPTIMAL ESTIMATION

Signal or image reconstruction can be viewed as a problem in signal estimation, where a related low-rate (low-resolution) signal or signals is used to estimate an underlying high-rate (high-resolution) signal. From this perspective, the observation signal or signals, and desired signal form a multirate system and the theory of multirate systems developed in Chapter III can be used to extend single-rate signal estimation theory to the multirate case, which is the concern of this chapter.

A. SIGNAL ESTIMATION

"Estimation is the process of inferring the value of a quantity of interest from [typically] indirect, inaccurate, and uncertain observations [Ref. 69]." A pictorial representation of this concept is depicted in Figure 4.1, where the source d represents some quantity of interest (unknown parameter, random variable, random process, etc.), $\mathbf{x}$ are the observations, related to d, and $\hat{d}(\mathbf{x})$ is the estimate. Note that, since $\mathbf{x}$ and sometimes d are considered to be *random variables*, $\hat{d}$, which is a *function* of the observations, is also a random variable. In the field of signal processing, these quantities of interest are signals, and a major emphasis of research is on signal estimation, where one signal is estimated from some other related signal or signals. The desired signal may be corrupted by distortion or interference and is usually unobservable (at least at the moment when the estimate is desired). In [Ref. 70], a number of typical signal estimation applications are presented including: the recovery of a transmitted signal from a distorted received signal, subject to amplitude and phase distortions and additive white noise over the communications channel; and image restoration of an image recorded by an imaging system that introduces blurring, nonlinear geometric distortions, and additive white noise.

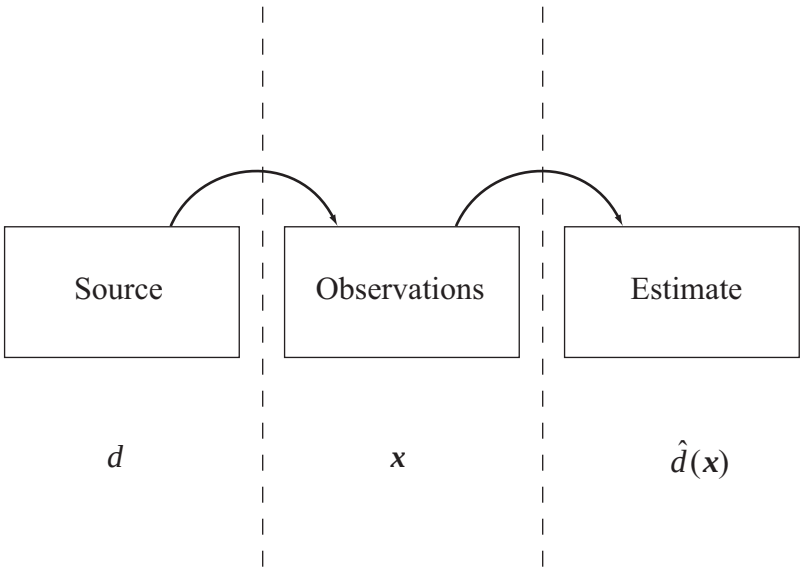

Figure 4.1. Concept of estimation.

B. OPTIMAL FILTERING

When the quantity of interest is a random signal, optimal filtering provides a framework for signal estimation. Optimal filtering is an area of signal processing study that is concerned with the design of filters to process a class of signals with statistically similar characteristics [Ref. 5] that are "best" in some sense, in terms of stated optimality criteria (i.e., minimum mean-squared error). The optimal filtering problem is posed in the following manner. Suppose that a random process $x[n]$ is observed, which is related to another random process $d[n]$ that cannot be observed directly. A general expression for the estimate is

$$\hat{d}[n] = \phi[\{x[n]\}]. \tag{4.1}$$

The optimal filtering problem is concerned with finding the appropriate *functional* $\phi[\cdot]$ that provides the best estimate of the desired signal $\hat{d}[n]$. When $\phi[\cdot]$ is linear,

the functional is commonly referred to as a (linear) *filter*. This concept is depicted in Figure 4.2.

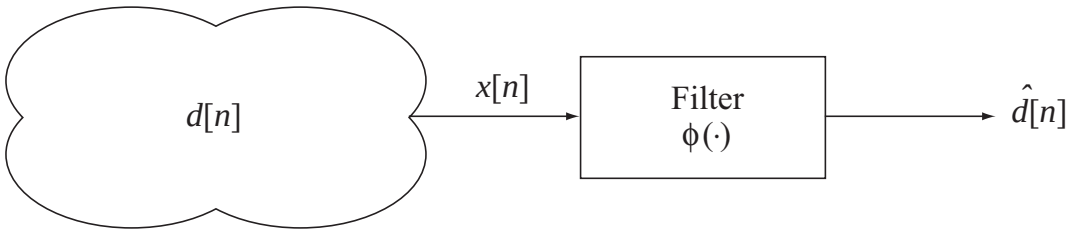

Figure 4.2. General single-rate optimal filtering problem. When $\phi[\cdot]$ is linear, the functional is commonly referred to as a linear *filter*.

Typically, these filters are constrained to be a linear function of the observations and hence can be written in the form (recall (3.28))

$$\hat{d}[n] = \sum_{m=-\infty}^{\infty} g[n;m]x[m], \tag{4.2}$$

where the sequence $g[n;m]$, which may be finite or infinite, is the familiar Green's function. This class of optimal filtering is called *optimal linear filtering*.

Often, the optimality criterion is based on minimization of the mean-square error (MSE) between the desired and estimated signals, i.e.,

$$\sigma_\varepsilon^2[n] = \mathcal{E}\{|\varepsilon[n]|^2\}, \tag{4.3}$$

where

$$\varepsilon[n] = d[n] - \hat{d}[n] \tag{4.4}$$

is the error in estimation at the n^{th} sample. When coupled with this MSE optimality criterion, optimal linear filtering is commonly referred to as *Wiener filtering* in recognition of the pioneering work of Norbert Wiener [Ref. 71, 72] in the 1940's.[1] Of great significance is that only second-order statistics are required in determination

[1]Wiener's pioneering work addressed the optimal filtering problem in continuous time, but is easily translated to discrete time, as is common now. Kolmogorov, in Russia, worked on the discrete-time problem for time series [Ref. 73] and appears to have preceded (or at least matched) Wiener in formulating and solving the problem (for discrete time).

of these optimal filters [Ref. 61]. Further, under the condition of joint wide-sense stationarity (JWSS) between the input $x[n]$ and the desired process $d[n]$, the filter is shift-invariant (see Section III.D.2(b)). For our purposes, we develop the *general* discrete FIR Wiener filtering equations, then the filtering equation for JWSS observation and estimate signals. In order to facilitate such developments, the *orthogonality principle* [Ref. 5] is stated.

1. Orthogonality Principle

Theorem 3 (Orthogonality Principle). Let $\varepsilon[n] = x[n] - \hat{x}[n]$ be the estimation error. Then,

1. the optimal linear filter with coefficients $h[0], h[1], \ldots, h[P-1]$ minimizes the error variance σ_ε^2 if the filter coefficients are chosen such that $\mathcal{E}\{\varepsilon[n]x^*[n-i]\} = \mathcal{E}\{x[n-i]\varepsilon^*[n]\} = 0$, $i = 0, 1, \ldots, P-1$, that is, if the error is orthogonal to the observations.

2. The minimum error variance is given by $\sigma_{\varepsilon_{\min}}^2 = \mathcal{E}\{\varepsilon[n]d^*[n]\} = \mathcal{E}\{d[n]\varepsilon^*[n]\}$.

The proof of this result can be found in several places [Ref. 5, 60, 74, 70].

2. Discrete Wiener Filter Equations

The equations whose solution provides the optimal filter are known as the Wiener-Hopf equations. In developing the "ordinary" (single-channel/single-rate) Wiener-Hopf equations, let us define the estimate in terms of a linear FIR filter that operates on $x[n]$ and the $P-1$ previous values of the process. The estimate (from (3.29)) is given by

$$\hat{d}[n] = \sum_{m=0}^{P-1} h[n;m]x[n-m], \tag{4.5}$$

where $h[n;m]$ is the shift-dependent impulse response sequence of the optimal filter and P is the associated filter order (length of the impulse response sequence). If $x[n-i]$ for $i = 0, 1, \ldots, P-1$ represents any one of the observations of the sequence

$x[n]$, then by applying the orthogonality principle (Theorem 3), we can write

$$\mathcal{E}\{\varepsilon[n]x^*[n-i]\} = \mathcal{E}\left\{\left(d[n] - \sum_{m=0}^{P-1} h[n;m]x[n-m]\right)x^*[n-i]\right\} = 0 \tag{4.6}$$

or

$$\sum_{m=0}^{P-1} R_x[n-m;i-m]h[n;m] = R_{dx}[n;i]; \qquad i = 0,1,\ldots,P-1. \tag{4.7}$$

This equation is the desired *discrete Wiener-Hopf equation* and can be written in matrix form. For example, for $P = 3$, we have

$$\begin{bmatrix} R_x[n;0] & R_x[n-1;-1] & R_x[n-2;-2] \\ R_x[n;1] & R_x[n-1;0] & R_x[n-2;-1] \\ R_x[n;2] & R_x[n-1;1] & R_x[n-2;0] \end{bmatrix} \begin{bmatrix} h[n;0] \\ h[n;1] \\ h[n;2] \end{bmatrix} = \begin{bmatrix} R_{dx}[n;0] \\ R_{dx}[n;1] \\ R_{dx}[n;2] \end{bmatrix}. \tag{4.8}$$

By applying the second part of the orthogonality principle, the expression for the minimum mean-square error can be found as

$$\sigma^2_{\varepsilon_{\min}}[n] = \mathcal{E}\{\varepsilon[n]d^*[n]\} = \mathcal{E}\left\{\left(d[n] - \sum_{m=0}^{P-1} h[n;m]x[n-m]\right)d^*[n]\right\} \tag{4.9}$$

or

$$\sigma^2_{\varepsilon_{\min}}[n] = R_d[n;0] - \sum_{m=0}^{P-1} h[n;m]R^*_{dx}[n;m]. \tag{4.10}$$

If the random processes are JWSS, then the statistical properties of the associated system do not change with n, the estimate can be generated by a linear shift-invariant FIR filter, and the minimum mean-square error becomes constant.

The matrix form of the Wiener-Hopf equation (4.7) can be derived directly if (4.5) is written in vector form,

$$\hat{d}[n] = (\tilde{\mathbf{x}}[n])^T\mathbf{h}, \tag{4.11}$$

where

$$\mathbf{x}[n] = \begin{bmatrix} x[n-P+1] \\ x[n-P] \\ \vdots \\ x[n] \end{bmatrix}, \tag{4.12}$$

with $\tilde{\mathbf{x}}[n]$ as defined in Section II.B.3, and

$$\mathbf{h} = \begin{bmatrix} h[0] \\ h[1] \\ \vdots \\ h[P-1] \end{bmatrix}, \tag{4.13}$$

or in the general non-stationary case

$$\mathbf{h} = \begin{bmatrix} h[n;0] \\ h[n;1] \\ \vdots \\ h[n;P-1] \end{bmatrix}. \tag{4.14}$$

Again, evoking the orthogonality principle, we can write

$$\tilde{\mathbf{R}}_{\mathbf{x}}^{*}\mathbf{h} = \tilde{\mathbf{r}}_{d\mathbf{x}}, \tag{4.15}$$

where

$$\mathbf{R}_x = \mathcal{E}\{\mathbf{x}[n]\mathbf{x}^{*T}[n]\}, \tag{4.16}$$

and

$$\mathbf{r}_{d\mathbf{x}} = \mathcal{E}\{d[n](\mathbf{x}[n])^{*}\}. \tag{4.17}$$

Equation (4.15) has the specific form (4.8) (for $P = 3$). The minimum mean-square error can be written as

$$\sigma^2_{\varepsilon_{\min}}[n] = R_d[n;0] - \tilde{\mathbf{r}}^{T}_{d\mathbf{x}}\mathbf{h}^{*}. \tag{4.18}$$

C. MULTIRATE OPTIMAL FILTERING

1. Single-channel, Multirate Estimation Problem

In the single-channel, multirate optimal filtering problem, the observation signal and the desired signal are at different rates and our goal is to form an estimate

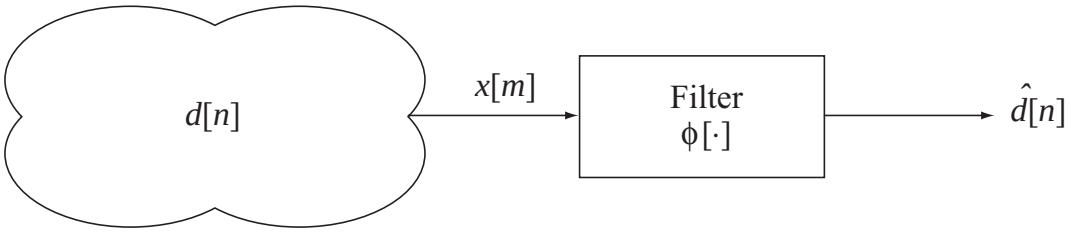

Figure 4.3. General single-channel, multirate optimal filtering problem. Note that the estimate and observation signals may be at different rates.

of the underlying desired signal from the observation signal. This notion is depicted in Figure 4.3 where $x[m]$ represents the observation signal at rate F_x, $d[n]$ represents the desired signal at some other rate F_d, and $\hat{d}[n]$ represents the estimate. A general expression for the estimate is

$$\hat{d}[n] = \phi[\{x[m]\}], \tag{4.19}$$

where the scalar estimate is a function of the sequence $x[m]$. Again, we seek the appropriate functional that provides the best estimate of $\hat{d}[n]$. When $\phi[\cdot]$ is linear, the functional is, again, referred to as a linear filter.

In this work, we have developed two approaches to formulating the required estimate. The first approach is based on a causal FIR Wiener filtering model, the second on a non-causal FIR Wiener filtering model. The latter is of particular interest since it is the basis for the two-dimensional work that follows (see Chapter V).

a. Index Mapping

The FIR linear filtering problem involves computing the linear combination of some finite number of observations to determine an estimate of a desired signal at a particular sample index, $n = n_0$.

In the single-rate case, the region of support of the filter (see Section III.D.3) is unambiguous. In the case of a causal filter, the filter uses $x[n_0]$ through $x[n_0 - P + 1]$ to estimate $d[n_0]$. In the multirate case, determining this region of support requires a way of relating corresponding sample indices between the

desired and observation sequences. Developing this methodology, referred to as *index mapping*, is the concern of this section.

Let us motivate the discussion by considering Figures 4.4 and 4.5, where

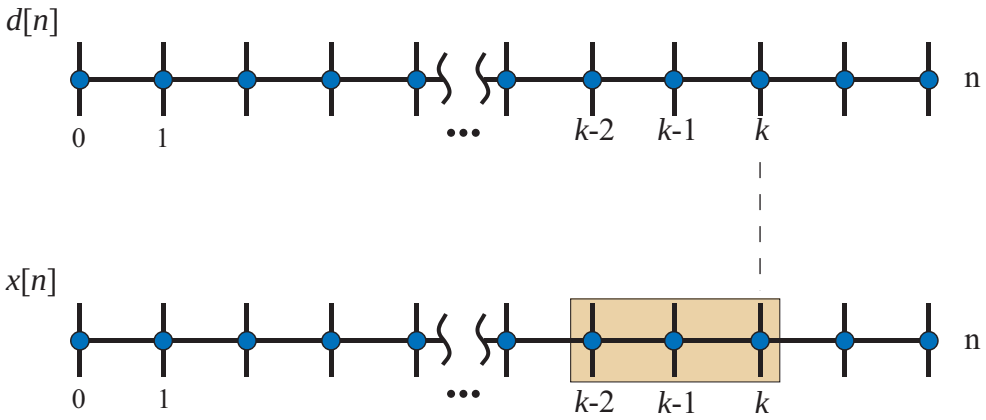

Figure 4.4. An illustration of ordinary causal FIR Wiener filtering and the relationship between samples of sequences $\hat{d}[n]$ and $x[n]$, $P = 3$.

the horizontal axes represent time. The first figure depicts single-rate estimation of the

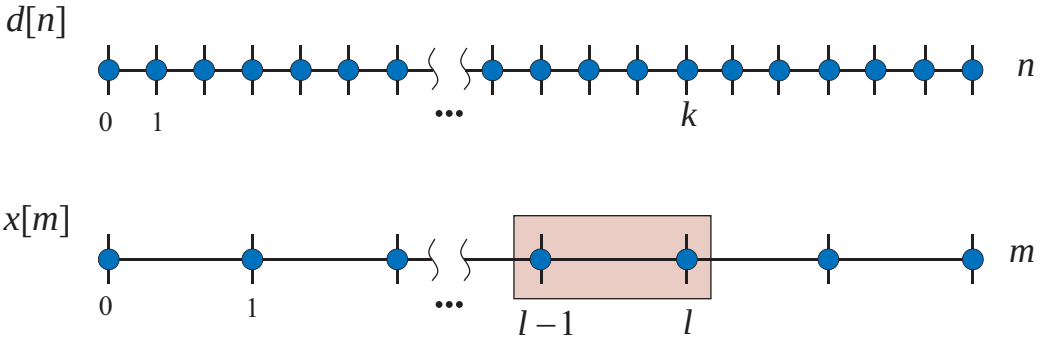

Figure 4.5. An illustration of single-channel, multirate causal FIR Wiener filtering and the relationship between samples of sequences $\hat{d}[n]$ and $x[m]$, $P = 2$.

desired sequence $d[n]$ at sample index $n = k$ with a causal FIR filter of order $P = 3$. Since both sequences are at the same rate, the region of support, the region encompassed by the rectangular "filter", corresponds to observations $x[k], x[k-1], x[k-2]$. If we consider the underlying discrete-domain signals, we notice that both signals are defined on the same "signal domain", $\Psi_{T_d} = \Psi_{T_x}$. Since both signals are defined on

the same domain, the index value k for either sequence represents the same point in time.

Figure 4.5 depicts multirate estimation of the desired sequence $d[n]$ at sample index $n = k$ with a causal FIR filter of order $P = 2$. Here, we notice that the underlying discrete-domain signals are *not* defined on the same domain. So, consider a particular index value k. In general, the time at which $d[k]$ occurs (kT_d) is not the same as the time at which $x[k]$ occurs (kT_x). There may be some other index value l (see Figure 4.5), however, such that $d[k]$ and $x[l]$ occur at the same time or very nearly at the same time. In an optimal filtering problem, we would generally like $d[k]$ and $x[l]$ to be as close as possible. In addition, we may also require the filter to be causal (see Definition 23). Establishing this correspondence is referred to as the index mapping problem.

Let $\Psi_d = \{nT_d; n \in \mathbb{Z}\}$ represent the signal domain that corresponds to an arbitrary discrete-domain signal with sampling interval T_d, and $\Psi_x = \{mT_x; m \in \mathbb{Z}\}$ represent the signal domain that corresponds to its associated observation signal with sampling interval T_x. Also, define a distance metric [Ref. 54] $D[n, m]$ called the *index metric* as

$$D[n, m] \equiv |nT_d - mT_x| = \overline{T}|K_d n - K_x m|, \tag{4.20}$$

where $\overline{T}$ is the system sampling interval. The index metric gives us a notion of distance between any two indices from different signal domains. In fact, $|K_d n - K_x m|$ is the number of system samples between such indices. Figure 4.6 illustrates this concept of distance for two arbitrary sample indices, n_0 and m_0. A normalized plot of the index metric, for $K_x = 3$ and $K_d = 1$, is depicted in Figure 4.7(a). In this case, $D[n, m] = |n - 3m|$, for $0 \leq n, m \leq 30$. Each line contains the locus of points associated with a particular value of n. Also, note that the index metric is identically zero $D[n, m] = 0$ when $n = 3m$.

The index mapping problem is now stated. Given a discrete-domain signal d at rate F_d and its associated observation signal x at a different rate F_x,

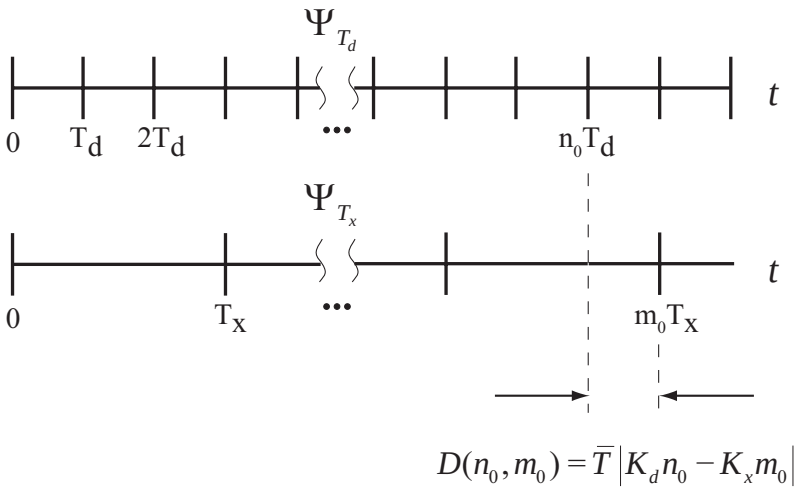

Figure 4.6. Notion of distance between indices n_0 and m_0.

for a given sample index $n = n_0$, associated with d, find the observation sample index $m = m_0$, associated with x such that the related index distance $D[n_0, m_0]$ is minimized, subject to certain constraints. Intuitively, this makes sense since the best estimate of $d[n_0]$ should typically result from the closest observation samples.

If the problem of interest involves causal filtering (see Definition 23), then the required constraint on the minimization is

$$nT_d \geq mT_x \quad \text{or} \quad n \geq \frac{K_x}{K_d} m. \tag{4.21}$$

This states that (on the system level) the output must not precede the observations. Therefore, the problem is posed as

$$\min_m D(n, m) \qquad \text{subject to } n \geq \frac{mK_x}{K_d}. \tag{4.22}$$

The solution to this minimization is expressed as a mapping from the estimation index to the observation index as

$$\mathcal{M}_{causal} : n \rightarrow \left\lfloor \frac{nK_d}{K_x} \right\rfloor, \tag{4.23}$$

or

$$m = \mathcal{M}_{\text{causal}}(n), \tag{4.24}$$

where K_d and K_x are the associated decimation factors.

This minimization is illustrated in Figure 4.7(b), which displays a plot of the index metric, again for $K_x = 3$ and $K_d = 1$, where the value of n has been specified as $n = 5$. In this case, the causality constraint requires that $n \geq 3m$, which is indicated by the shaded region in the lower figure. Thus, the minimization pertains only to that portion of $D[5, m]$ contained within this region. By inspection, we see that when $m = 1$, the index metric $D[5, m] = 2$ is at its minimum.

Continuing this example, for $K_x = 3$ and $K_d = 1$, with the causality constraint, we have the following mappings from the set of estimate signal indices to the observation signal index as shown in Table 4.1.

n	$m = \left\lfloor \frac{nK_d}{K_x} \right\rfloor$
$\{0, 1, 2\}$	0
$\{3, 4, 5\}$	1
$\{6, 7, 8\}$	2

Table 4.1. Causal mapping from a set of estimate signal indices to the associated observation signal index.

If there is no causality constraint (as in smoothing or image processing), then the minimization is unconstrained and the problem is posed as

$$\min_m D[n, m]. \tag{4.25}$$

The solution to this minimization is expressed as a mapping from the estimate signal index to the respective observation signal index as

$$\mathcal{M}_{nc} : n \rightarrow \left\lfloor \frac{(n + \lfloor \frac{K_x}{2} \rfloor)K_d}{K_x} \right\rfloor, \tag{4.26}$$

or

$$m = \mathcal{M}_{\text{nc}}(n), \tag{4.27}$$

where K_d and K_x are the associated decimation factors.

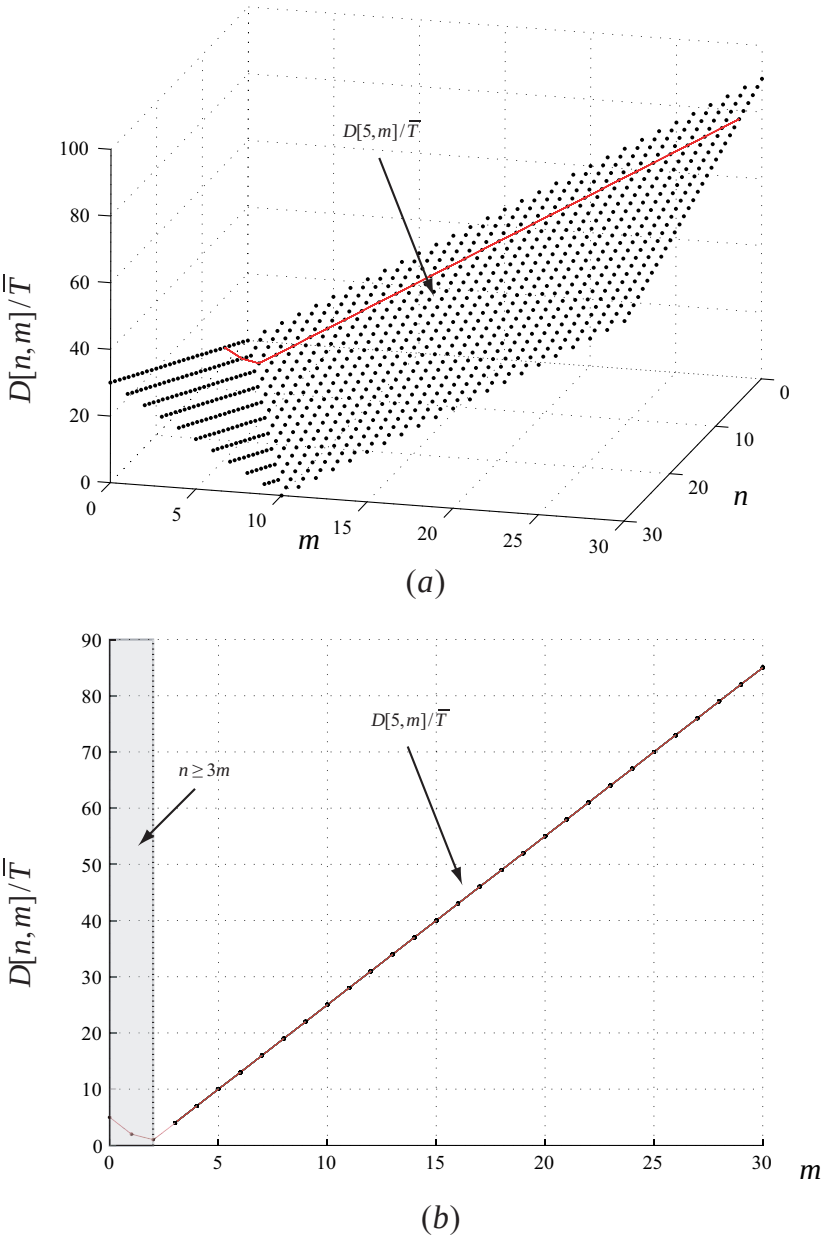

Figure 4.7. (a) Normalized plot of $D[n, m]$ in 3 dimensions. (b) Plot of $D[n, m]$ versus m for $n = 5$.

Again, from Figure 4.7(b), we can illustrate this minimization, again at $n = 5$, but now with no causality constraint. In this case, when the observation signal index is $m = 2$, the index metric is $D[5, 1] = 1$, and the index metric is a minimum. Note that this value of the observation signal index m is different from the previous solution (a consequence of the causality constraint in the former problem).

Continuing this example, for $K_x = 3$ and $K_d = 1$, without the causality constraint, we have the following mappings from the set of estimate signal indices to the observation signal index as shown in Table 4.2.

n	$m = \left\lfloor \frac{(n+\lfloor \frac{K_x}{2} \rfloor)K_d}{K_x} \right\rfloor$
$\{-1, 0, 1\}$	0
$\{2, 3, 4\}$	1
$\{5, 6, 7\}$	2

Table 4.2. Non-causal mapping from a set of estimate signal indices to the associated observation signal index.

b. Single-channel, Multirate Wiener-Hopf Equations

Recall that the input-output relationship for the general multirate filtering problem is given by (3.45) and is repeated here for convenience

$$y[m_y] = \sum_{m_x} h^{(l)}[m_x] x\Big[\Big\lfloor \frac{K_y m_y}{K_x} \Big\rfloor - m_x\Big], \qquad \text{where } l = \langle m_y \rangle_{M_y}.$$

This equation can be written in terms of the single-channel, multirate estimation problem as

$$\hat{d}[n] = \sum_{m} h^{(l)}[m] x\Big[\Big\lfloor \frac{K_d n}{K_x} \Big\rfloor - m\Big], \qquad \text{where } l = \langle n \rangle_{M_d}.$$

We can further generalize the form of the linear multirate estimate if we consider the mapping issues discussed in Section IV.C.1(a). We can write (3.45) in terms of an arbitrary mapping function as

$$\hat{d}[n] = \sum_{m} h^{(l)}[m] x\Big[\mathcal{M}[n] - m\Big], \tag{4.28}$$

where $\mathcal{M}[\,\cdot\,]$ is the appropriate mapping function (causal, non-causal), and $l = \langle n \rangle_{M_d}$.

With a finite variant of (4.28), in the usual manner, we evoke the orthogonality principle. Thus, for observations $x[\mathcal{M}[n] - i]$ for $i = 0, 1, \ldots, P-1$, we can write

$$\mathcal{E}\{\varepsilon[n] x^*\Big[\mathcal{M}[n] - i\Big]\}$$
$$= \mathcal{E}\left\{\left(d[n] - \sum_{m=0}^{P-1} h^{(l)}[m] x\Big[\mathcal{M}[n] - m\Big]\right) x^*\Big[\mathcal{M}[n] - i\Big]\right\} = 0,$$
$$\text{for i = 0,1,. . . ,P-1,} \quad (4.29)$$

or

$$\sum_{m=0}^{P-1} R_x[\mathcal{M}[n] - m; i - m] h^{(l)}[m] = R_{dx}[n; n - \mathcal{M}[n] + i]; \qquad i = 0, 1, \ldots, P-1, \quad (4.30)$$

where $l = \langle n \rangle_{M_d}$. This is called the *discrete single-channel, multirate Wiener-Hopf equation*.

Applying the second part of the orthogonality principle, we find the following expression for the minimum mean-square error

$$\sigma^2_{\varepsilon_{\min}}[n] = R_d[n; 0] - \sum_{m=0}^{P-1} h^{(l)}[m] R^*_{dx}[n; n - \mathcal{M}[n] + m]. \quad (4.31)$$

Notice that if the observation sequence is stationary, then the associated correlation function is independent of the mapping function and the Wiener-Hopf equation can be written

$$\sum_{m=0}^{P-1} R_x[i - m] h^{(l)}[m] = R_{dx}[n; n - \mathcal{M}[n] + m]; \qquad i = 0, 1, \ldots, P-1, \quad (4.32)$$

where $l = \langle n \rangle_{M_d}$.

The Wiener-Hopf equation expressed in its matrix form, for $P = 3$, when the observation process is stationary:

$$\begin{bmatrix} R_x[0] & R_x[-1] & R_x[-2] \\ R_x[1] & R_x[0] & R_x[-1] \\ R_x[2] & R_x[1] & R_x[0] \end{bmatrix} \begin{bmatrix} h^{(l)}[0] \\ h^{(l)}[1] \\ h^{(l)}[2] \end{bmatrix} = \begin{bmatrix} R_{dx}[n; n - \mathcal{M}[n]] \\ R_{dx}[n; n - \mathcal{M}[n] + 1] \\ R_{dx}[n; n - \mathcal{M}[n] + 2] \end{bmatrix}, \quad (4.33)$$

where $l = \langle n \rangle_{M_d}$. Notice that the correlation matrix is Toeplitz.

As in the ordinary Wiener filtering problem, the Wiener-Hopf equation can be derived in matrix form by writing (4.28) as

$$\hat{d}[n] = (\tilde{\mathbf{x}}\big[\mathcal{M}[n]\big])^T \mathbf{h}^{(l)}, \tag{4.34}$$

where if

$$\mathbf{x}\big[\mathcal{M}[n]\big] = \begin{bmatrix} x\big[\mathcal{M}[n] - P + 1\big] \\ x\big[\mathcal{M}[n] - P\big] \\ \vdots \\ x\big[\mathcal{M}[n]\big] \end{bmatrix}, \tag{4.35}$$

then

$$\tilde{\mathbf{x}}\big[\mathcal{M}[n]\big] = \begin{bmatrix} x\big[\mathcal{M}[n]\big] \\ x\big[\mathcal{M}[n] - 1\big] \\ \vdots \\ x\big[\mathcal{M}[n] - P + 1\big] \end{bmatrix}, \tag{4.36}$$

with $\tilde{\mathbf{x}}[\mathcal{M}[n]]$ as defined in Section II.B.3, and where $\mathbf{h}^{(l)}$ is defined as

$$\mathbf{h}^{(l)} = \begin{bmatrix} h^{(l)}[0] \\ h^{(l)}[1] \\ \vdots \\ h^{(l)}[P-1] \end{bmatrix}, \tag{4.37}$$

where $l = \langle n \rangle_{M_d}$.

Again, evoking the orthogonality principle (Theorem 3), the Wiener-Hopf equation (4.30) can be expressed in its matrix form as

$$\tilde{\mathbf{R}}^*_{\mathbf{x}} \mathbf{h}^{(l)} = \tilde{\mathbf{r}}_{d\mathbf{x}\left[\mathcal{M}[n]\right]}, \tag{4.38}$$

where $l = \langle n \rangle_{M_d}$, and

$$\mathbf{r}_{d\mathbf{x}\left[\mathcal{M}[n]\right]} = \mathcal{E}\{d[n]\mathbf{x}^*\big[\mathcal{M}[n]\big]\}. \tag{4.39}$$

Equation (4.38) has the specific form (4.33) (for $P = 3$). The minimum mean-square error can be written as

$$\sigma^2_{\varepsilon_{\min}}[n] = R_d[n;0] - \tilde{\mathbf{r}}^T_{d\mathbf{x}\left[\mathcal{M}[n]\right]}\mathbf{h}^{(l)*}, \tag{4.40}$$

where $l = \langle n \rangle_{M_d}$.

c. Matrix Approach to the Single-channel, Multirate Wiener-Hopf Equations

Another approach in developing the multirate Wiener-Hopf equations involves the matrix representation concepts of Section III.E and results presented in [Ref. 9]. Again, consider a multirate system comprised of an observation signal x at rate F_x and a desired signal d at rate F_d, and let the order of the associated filter be denoted P. Recall from (3.10), (3.14) and (3.18) that the system rate is $\overline{F} = \text{lcm}(F_x, F_d)$, the associated decimation factors are $K_i = \overline{F}/F_i$, and the system sample period is $N = \text{lcm}(K_x, K_d)$. The period of the filters required to form the estimate d (see Section III.D.3.b(2), cyclostationary period) is K, and in the case of single-channel, multirate estimation, $K = \dfrac{N}{K_d}$.

For any index n, the observation signal x, represented by the sequence $x[n]$, can be expressed

$$\tilde{\mathbf{x}}^{(k)}[n] = \mathbf{D}^{(k)}_K \tilde{\mathbf{x}}[n], \quad k = \{0, 1, \ldots, K-1\}, \tag{4.41}$$

where

$$\tilde{\mathbf{x}}[n] = \begin{bmatrix} x[n] \\ x[n-1] \\ \vdots \\ x[n - PK_x + 1] \end{bmatrix},$$

and $\mathbf{D}^{(k)}_K$ is a decimation matrix with delay (3.60). In this context, the decimation matrix with delay is a mapping or transformation that extracts the samples in the required causal region of support from the observation vector.

The optimal estimate is formed from a linear combination of the appropriate observation samples and associated filter coefficients and is given by

$$\hat{d}_k[n] = (\tilde{\mathbf{x}}^{(k)}[n])^T \mathbf{h}^{(k)}, \quad k = \{0, 1, \ldots, K-1\}, \tag{4.42}$$

where the reversal operation $\tilde{\mathbf{x}}[n]$ is defined in Section II.B.3. Note that in this formulation, all signals and computations are at the system rate, and, as a result, we are solving a more general problem since we estimate $d_{T_d}[n]$ at every point on the system grid $\Psi_{\overline{T}}$, not just on the signal domain Ψ_{T_d}. The desired estimate is recovered by decimating the result by K_d.

In the usual manner, we form the error in estimation and evoke the orthogonality principle. The Wiener-Hopf equation (4.30) can be expressed in its matrix form as

$$\tilde{\mathbf{R}}_{\mathbf{x}}^{(k)} \mathbf{h}^{(k)*} = \tilde{\mathbf{r}}_{d\mathbf{x}}^{(k)*}, \quad k = \{0, 1, \ldots, K-1\}, \tag{4.43}$$

or in terms of single-rate statistical parameters (from (4.16) and (4.17)),

$$\mathbf{D}_K^{(k)} \tilde{\mathbf{R}}_{\mathbf{x}} \mathbf{D}_K^{(k)T} \mathbf{h}^{(k)*} = \mathbf{D}_K^{(k)} \tilde{\mathbf{r}}_{d\mathbf{x}}^{*}, \quad k = \{0, 1, \ldots, K-1\}. \tag{4.44}$$

Applying the second part of the orthogonality principle yields an expression for the minimum mean-square error,

$$\sigma_k^2 = R_d[0] - \tilde{\mathbf{r}}_{d\mathbf{x}}^{(k)T} \mathbf{h}^{(k)*}, \quad k = \{0, 1, \ldots, K-1\}, \tag{4.45}$$

where the subscript k on the mean-square error reflects the periodically time-varying nature of the error.

2. Multi-channel, Multirate Estimation Problem

In the multi-channel, multirate optimal filtering problem, there are multiple observation signals and these signals are allowed to be at rates different from the desired signal. The goal is to estimate this underlying signal from the set of related multirate observation signals. This notion is depicted in Figure 4.8 where there are

M observation signals at rates denoted by m_i, which may all be different. A general expression for the estimate is

$$\hat{d}[n] = \phi\left[\{x_i[m_i]; i = 0, 1, \ldots, M-1\}\right], \tag{4.46}$$

where the scalar estimate is now a function of a set of multirate observation signals. When the functional $\phi[\cdot]$ is linear, then the estimate is formed from linear filtering.

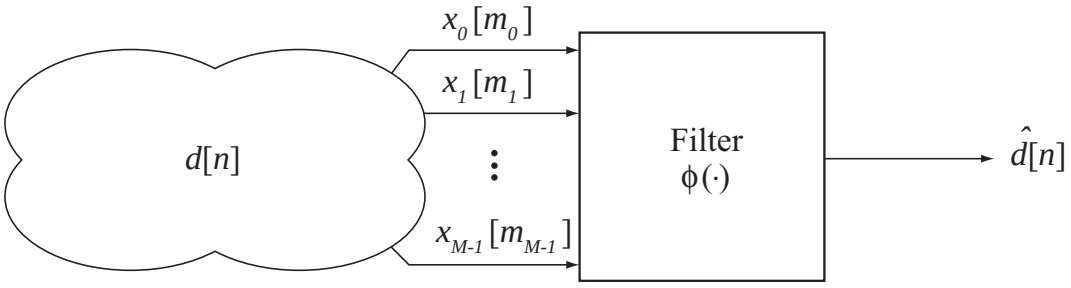

Figure 4.8. General multirate optimal filtering problem with M multirate observation signals.

a. Multi-channel Index Mapping

In this section, we develop the mapping relationship between the estimate and observation sample indices in a multi-channel, multirate system in order to determine the required regions of support in linear filtering. In doing so, we develop a set of mapping functions for the causal and noncausal FIR filtering problems. In this context, the index mapping problem is, for a given index n, associated with the estimate, to find the M observation indices m_i, such that the related index distances $D[n, m_i]$ are minimized, subject to certain constraints, where $i = 0, 1, \ldots, M-1$.

If the problem of interest involves causal filtering, then the required constraint on the minimization is

$$nT_d \geq m_i T_i \quad \text{or} \quad n \geq \frac{K_i}{K_d} m_i, \quad \text{for } i = 0, 1, \ldots, M-1. \tag{4.47}$$

Therefore, the problem is posed as

$$\min_{m_i} D(n, m_i) \qquad \text{subject to } n \geq \frac{K_i}{K_d} m_i, \quad \text{for } i = 0, 1, \ldots, M-1. \tag{4.48}$$

The solution to this minimization is expressed as a mapping from the estimate index to the observation indices as

$$\mathcal{M}_{causal} : n \rightarrow \left\lfloor \frac{nK_d}{K_i} \right\rfloor, \tag{4.49}$$

or

$$m_i = \mathcal{M}_{\text{causal}}(n), \tag{4.50}$$

where K_d and K_i are the associated decimation factors, and $i = 0, 1, \ldots, M-1$.

The multi-channel, multirate causal filtering problem is depicted in Figure 4.9.

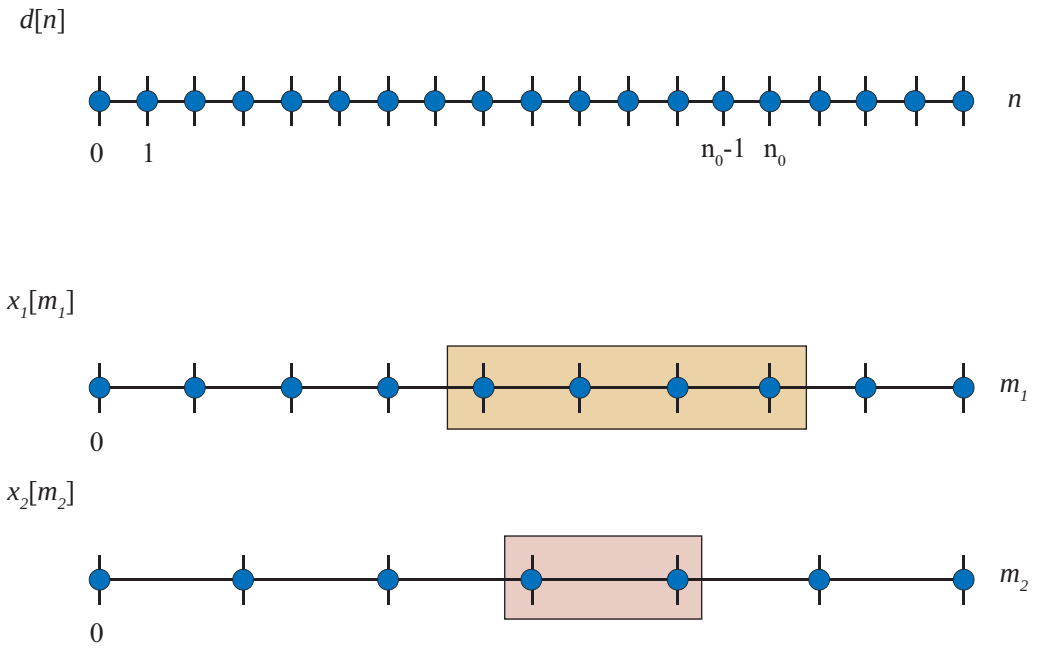

Figure 4.9. Concept of index mapping in multi-channel, multirate FIR Wiener filtering.

If the problem of interest involves noncausal FIR filtering, then there is no constraint on the minimization, and the problem is posed as

$$\min_{m_i} D[n, m_i] \quad \text{for } i = 0, 1, \ldots, M-1. \tag{4.51}$$

By examining the appropriate plots of $D[n, m_i]$, the solution to this minimization is found as a mapping from the high-rate index to the respective low-rate indices as

$$\mathcal{M}_{nc} : n \rightarrow \left\lfloor \frac{(n + \lfloor \frac{K_i}{2} \rfloor) K_d}{K_i} \right\rfloor, \tag{4.52}$$

or

$$m_i = \mathcal{M}_{\text{nc}}(n), \tag{4.53}$$

where K_d and K_i are the associated decimation factors, and $i = 0, 1, \ldots, M-1$.

b. Multi-channel, Multirate FIR Wiener Filtering model

Recall that, for the single-channel FIR Wiener filtering model (4.28), the estimate is written as

$$\hat{d}[n] = \sum_{m_x=0}^{P-1} h^{(l)}[m_x] x \left[\mathcal{M}[n] - m_x\right],$$

where $l = \langle n \rangle_{\frac{N}{K_d}}$, and $\mathcal{M}[n]$ is the required mapping function (causal, non-causal, etc.).

In the multi-channel model, we extend or generalize (4.28) to include multiple observations as

$$\hat{d}[n] = \sum_{i=0}^{M-1} \sum_{m=0}^{P-1} h_i^{(p)}[m] x_i \left[\mathcal{M}_i[n] - m\right], \tag{4.54}$$

where $p = \langle n \rangle_{\frac{N}{K_d}}$, P is the filter order, and $\mathcal{M}_i[n]$ is the mapping function associated with the i^{th} channel.

c. Multi-channel, Multirate Wiener-Hopf Equations

Using equation (4.54), we form the error in estimation and evoke the orthogonality principle. Thus, we can write

$$\begin{aligned}
&\mathcal{E}\{\varepsilon[n] x_i^*\Big[\mathcal{M}_i[n] - j\Big]\} \\
&\quad = \mathcal{E}\left\{\left(d[n] - \sum_{r=0}^{M-1} \sum_{s=0}^{P-1} h_r^{(p)}[s] x_r\Big[\mathcal{M}_r[n] - s\Big]\right) x_i^*\Big[\mathcal{M}_i[n] - j\Big]\right\} = 0, \\
&\qquad\qquad 0 \leq i \leq M-1, 0 \leq j \leq P-1
\end{aligned} \tag{4.55}$$

or

$$\sum_{r=0}^{M-1}\sum_{s=0}^{P-1} R_{x_r x_i}[\mathcal{M}_r[n]-s;\mathcal{M}_r[n]-\mathcal{M}_i[n]+j-s]h_r^{(p)}[s]$$

$$= R_{dx_i}[n; n-\mathcal{M}_i[n]+j],$$

$$0 \le i \le M-1, 0 \le j \le P-1, \quad (4.56)$$

where $p = \langle n \rangle_{\frac{N}{K_d}}$. These are called the *discrete multi-channel, multirate Wiener-Hopf equations.*

As in the ordinary Wiener filtering problem, the multi-channel, multirate Wiener-Hopf equations can be derived in matrix form by writing (4.54) as

$$\hat{d}[n] = \sum_{i=0}^{M-1} (\tilde{\mathbf{x}}_i\big[\mathcal{M}_i[n]\big])^T \mathbf{h}_i^{(p)}, \quad (4.57)$$

where if

$$\mathbf{x}_i\big[\mathcal{M}_i[n]\big] = \begin{bmatrix} x_i\big[\mathcal{M}_i[n]-P+1\big] \\ x_i\big[\mathcal{M}_i[n]-P\big] \\ \vdots \\ x_i\big[\mathcal{M}_i[n]\big] \end{bmatrix}, \quad (4.58)$$

then

$$\tilde{\mathbf{x}}_i\big[\mathcal{M}_i[n]\big] = \begin{bmatrix} x_i\big[\mathcal{M}_i[n]\big] \\ x_i\big[\mathcal{M}_i[n]-1\big] \\ \vdots \\ x_i\big[\mathcal{M}_i[n]-P+1\big] \end{bmatrix}, \quad (4.59)$$

with $\tilde{\mathbf{x}}_i\big[\mathcal{M}_i[n]\big]$ as defined in Section II.B.3, and where $\mathbf{h}_i^{(p)}$ is defined as

$$\mathbf{h}_i^{(p)} = \begin{bmatrix} h_i^{(p)}[0] \\ h_i^{(p)}[1] \\ \vdots \\ h_i^{(p)}[P-1] \end{bmatrix}, \quad (4.60)$$

where $p = \langle n \rangle_{\frac{N}{K_d}}$.

Applying the orthogonality principle yields:

$$\mathcal{E}\{\tilde{\mathbf{x}}_i\big[\mathcal{M}_i[n]\big]\varepsilon^*[n]\} = \mathcal{E}\left\{\tilde{\mathbf{x}}_i\big[\mathcal{M}_i[n]\big]\left(d^*[n] - \sum_{r=0}^{M-1}(\tilde{\mathbf{x}}_r\big[\mathcal{M}_r[n]\big])^{*T}\mathbf{h}_r^{(p)*}\right)\right\} = \mathbf{0}$$

$$0 \le i \le M-1, \quad (4.61)$$

and the Wiener-Hopf equations can be expressed in their matrix form as

$$\sum_{r=0}^{M-1}\tilde{\mathbf{R}}^*_{\mathbf{x}_i\mathbf{x}_r}\mathbf{h}_r^{(p)} = \tilde{\mathbf{r}}_{d\mathbf{x}_i\left[\mathcal{M}_i[n]\right]}, \quad 0 \le i \le M-1, \quad (4.62)$$

where $p = \langle n \rangle_{\frac{N}{K_d}}$, and

$$\mathbf{r}_{d\mathbf{x}_i\left[\mathcal{M}_i[n]\right]} = \mathcal{E}\{d[n]\mathbf{x}_i^*\big[\mathcal{M}_i[n]\big]\}. \quad (4.63)$$

Applying the second part of the orthogonality principle yields an expression for the minimum mean-square error:

$$\sigma^2_{\varepsilon_{\min}}[n]$$

$$= \mathcal{E}\{d[n]\varepsilon^*[n]\} = \mathcal{E}\left\{d[n]\left(d^*[n] - \sum_{r=0}^{M-1}(\tilde{\mathbf{x}}_r\big[\mathcal{M}_r[n]\big])^{*T}\mathbf{h}_r^{(p)*}\right)\right\},$$

$$0 \le i \le M-1, \quad (4.64)$$

or

$$\sigma_p^2 = R_d[n;0] - \sum_{r=0}^{M-1}\tilde{\mathbf{r}}^T_{d\mathbf{x}_r}\big[n; n-\mathcal{M}_r[n]\big]\mathbf{h}_r^{(p)*}, \quad 0 \le i \le M-1, \quad (4.65)$$

where $p = \langle n \rangle_{\frac{N}{K_d}}$, and its index on the mean-square error reflects the periodically time-varying nature of the error.

d. Matrix Approach to the Multi-channel, Multirate Wiener-Hopf Equations

In the multi-channel, multirate optimal filtering problem, we also develop a matrix-based method to develop the Wiener-Hopf equations. In this problem, M observation signals are available to form the desired signal d, where $M \ge 2$. The estimate $\hat{d}$ is formed by summing the output of M periodic filters of order P and is

given by

$$\hat{d}_k[n] = \sum_{i=0}^{M-1} (\tilde{\mathbf{x}}_i^{(k)}[n])^T \mathbf{h}_i^{(k)}, \quad 0 \le k \le K-1, \tag{4.66}$$

where K is the period of the filters required for estimation and is given by $K = \langle n \rangle_N$, where N is the system period. For any index n, the observation signal x_i, represented by the sequence $x_i[n]$, can be expressed as

$$\tilde{\mathbf{x}}_i^{(k)}[n] = \mathbf{D}_{K_i}^{(k)} \tilde{\mathbf{x}}_i[n], \quad 0 \le k \le K_i - 1, \tag{4.67}$$

where

$$\tilde{\mathbf{x}}_i[n] = \begin{bmatrix} x_i[n] \\ x_i[n-1] \\ \vdots \\ x_i[n-PK_i+1] \end{bmatrix},$$

with $\tilde{\mathbf{x}}_i[n]$ as defined in Section II.B.3, and $\mathbf{D}_{K_i}^{(k)}$ is a decimation matrix with delay (3.60), where K_i is the decimation factor associated with the i^{th} channel, and P is the filter order. Again, note that, in this formulation, all signals and computations are at the system rate, and, as a result, we are solving a more general problem since we estimate $d[n]_{T_d}$ at every point on $\Psi_{\overline{T}}$, not just on Ψ_{T_d}. The desired estimate can be recovered by decimating the result by K_d.

Again, in the usual manner, we form the error in estimation and evoke the orthogonality principle,

$$\mathcal{E}\{\tilde{\mathbf{x}}_i^{(k)}[n]\varepsilon^*[n]\} = \mathcal{E}\left\{\tilde{\mathbf{x}}_i^{(k)}[n]\left(d[n] - \sum_{j=0}^{M-1} (\tilde{\mathbf{x}}_j^{(k)}[n])^T \mathbf{h}_j^{(k)}\right)^*\right\} = \mathbf{0},$$

$$0 \le i \le M-1, \tag{4.68}$$

and the Wiener-Hopf equation (4.30) can be expressed in its matrix form as

$$\sum_{j=0}^{M-1} \tilde{\mathbf{R}}_{\mathbf{x}_i\mathbf{x}_j}^{(k)} \mathbf{h}_j^{(k)*} = \tilde{\mathbf{r}}_{d\mathbf{x}_i}^{(k)*}, \quad 0 \le i \le M-1, \tag{4.69}$$

and $k = \langle n \rangle_N$, or in terms of single-rate statistical parameters (see (4.16) and (4.17)),

$$\sum_{j=0}^{M-1} \mathbf{D}_{K_i}^{(k)} \tilde{\mathbf{R}}_{\mathbf{x}_i \mathbf{x}_j} \mathbf{D}_{K_j}^{(k)T} \mathbf{h}_j^{(k)*} = \mathbf{D}_{K_i}^{(k)} \tilde{\mathbf{r}}_{d\mathbf{x}_i}^{*}, \quad 0 \leq i \leq M-1. \tag{4.70}$$

Applying the second part of the orthogonality principle yields an expression for the minimum mean-square error given by

$$\sigma_{\varepsilon_{\min}}^2[n] = \mathcal{E}\{d[n]\varepsilon^*[n]\} = \mathcal{E}\left\{ d[n] \left(d[n] - \sum_{i=0}^{M-1} (\tilde{\mathbf{x}}_i^{(k)}[n])^T \mathbf{h}_i^{(k)} \right)^* \right\}, \tag{4.71}$$

or

$$\sigma_k^2 = R_d[n;0] - \sum_{j=0}^{M-1} \tilde{\mathbf{r}}_{d\mathbf{x}_i}^{(k)T} \mathbf{h}_i^{(k)*}, \quad 0 \leq i \leq M-1, \tag{4.72}$$

or in terms of single-rate statistical parameters,

$$\sigma_k^2 = R_d[n;0] - \sum_{j=0}^{M-1} \tilde{\mathbf{r}}_{d\mathbf{x}_i}^{T} \mathbf{D}_{K_i}^{(k)T} \mathbf{h}_i^{(k)*}, \quad 0 \leq i \leq M-1, \tag{4.73}$$

where the subscript k on the mean-square error reflects the periodically time-varying nature of the error.

D. CHAPTER SUMMARY

In this chapter, the problem of signal estimation is introduced from an optimal filtering perspective. Specifically, we consider linear filtering, where the optimality criterion is based on minimizing the mean-square error (Wiener filtering).

To begin the discussion, the Wiener-Hopf equations for single-rate sequences are reviewed, establishing the foundation upon which the single- and multi-channel, multirate Wiener-Hopf equations are developed. These results are important to the methods of signal and image reconstruction discussed in Chapter V.

Additionally, the concept of index mapping is proposed, which systematically describes the relationship between samples of a signal at one rate to those of a signal at another rate (indices in one signal domain to those in another signal domain). This

concept is particularly well-suited for developing the required regions of support in linear filtering. In detailing this relationship, both a causal and non-causal mapping transformation are developed, but the notion of mapping is generalized, providing a basis for the development of "generalized" multi-channel, multirate Wiener-Hopf equations.

Finally, matrix-based approaches, using the matrix representations of Chapter III, are used to develop the single- and multi-channel, multirate Wiener-Hopf equations for implementation in Chapter V.

THIS PAGE INTENTIONALLY LEFT BLANK

V. SUPER-RESOLUTION SIGNAL AND IMAGE RECONSTRUCTION

In this chapter, we apply the multirate and optimal estimation theory results of Chapters III and IV to the problem of signal and image reconstruction. We start by developing a 1-D methodology and begin the analysis of this method on a simple test signal (a triangle wave) and evaluate the performance on this known data. We then apply the procedure to image data when the image is processed along rows.

We then turn to the full problem of image reconstruction and discuss how the 1-D multirate theory and methods extend to 2-D, present an image reconstruction methodology, and provide an example of the application of this methodology, comparing results to other methods.

A. SIGNAL RECONSTRUCTION

Consider the problem of estimating a discrete random process $d[n]$, which cannot be observed directly, from a set of M related observation signals, represented by $\{x_0[m_0], x_1[m_1], \ldots, x_{M-1}[m_{M-1}]\}$. These observation signals are related to the random process $d[n]$ through various forms of distortion and interference. Further, these signals may be at rates different from that of $d[n]$, and observation signals at the same rate may also be shifted in time with respect to one another.

1. Observation Model

In order to facilitate discussion, we present the observation model depicted in Figure 5.1, which represents the i^{th} observation signal. In this model, we consider linear forms of distortion. Notice that the translation is along the system grid ($\Psi_{\overline{T}}$) and is indexed to the particular signal of interest (see e.g., s_0 and s_1 in Figure 5.2). Further, notice that the downsampling factor is also indexed to a particular signal.

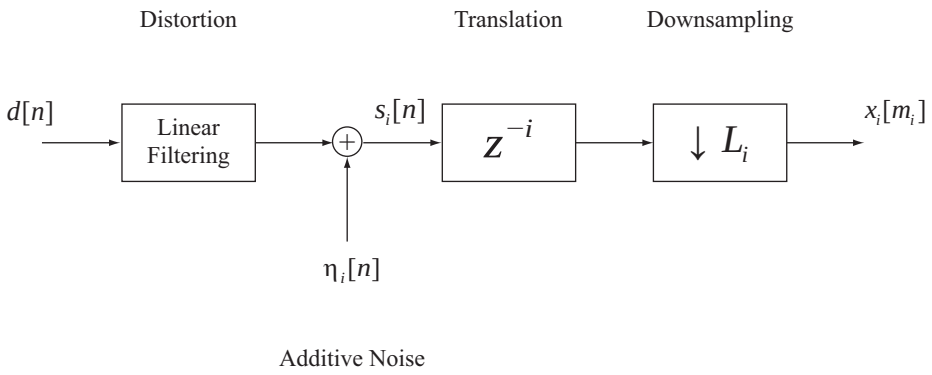

Figure 5.1. Observation model, where observation signals $x_i[m_i]$ are derived from an underlying signal d, subject to distortion, additive noise, translation, and downsampling.

If we consider signal $s_3[n]$, its associated downsampling factor is L_3, which may be different from that of other observation signals.

2. Optimal Estimation

As we have previously observed, if the desired signal $d[n]$ and its observations $\mathbf{x}_i[m_i]$ are jointly wide-sense stationary, then the linear filters required for optimal mean-square estimation are periodically time-varying [Ref. 7]. In this case, we can write the estimate as

$$\hat{d}_k[n] = \sum_{i=0}^{M-1} (\tilde{\mathbf{x}}_i^{(k)}[n])^T \mathbf{h}_i^{(k)} \tag{5.1}$$

where $\mathbf{h}_i^{(k)}$ is a set of time-varying filter coefficients of length P_i and $\tilde{\mathbf{x}}_i[n]$ is a vector of samples from the i^{th} observation sequence. The periodic time variation is denoted by the index k where $0 \leq k \leq L-1$, L is the system periodicity and $k = \langle n \rangle_L$ (see Figure 5.3). In this analysis, we consider that the observations signals are maximally decimated (see Section III.C.4) versions of $d[n]$, where $L_i = L$, and, in this case, the observation vectors can be written as

$$\tilde{\mathbf{x}}_i^{(k)}[n] = \mathbf{D}_L^{(\langle k-i \rangle_L)} \tilde{\mathbf{s}}_i[n] \tag{5.2}$$

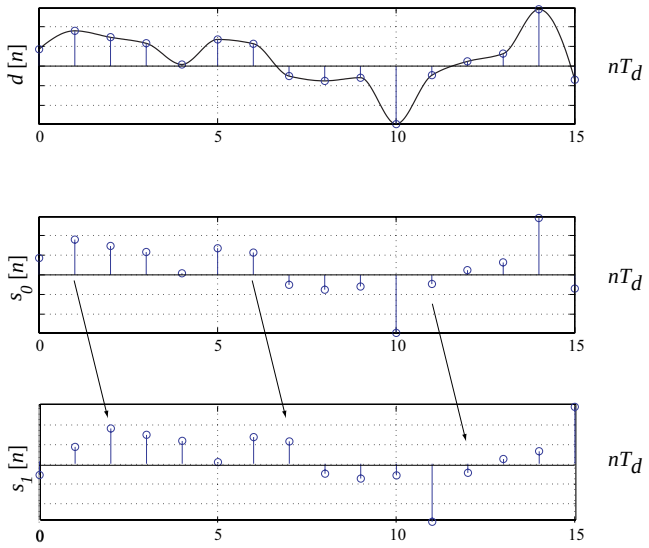

Figure 5.2. Observation sequences s_0 and s_1 shifted by a delay ($i = 0, i = 1$, respectively).

and

$$\tilde{\mathbf{s}}_i[n] = [s_i[n], s_i[n-1], \ldots, s_i[n - P_i L + 1]]^T . \tag{5.3}$$

The decimation matrix with time delay $\mathbf{D}_L^{(\langle k-i \rangle_L)}$ extracts the appropriate samples from $\mathbf{s}_i[n]$ to form each observation vector.

Minimizing the mean-square error [Ref. 9] leads to a set of Wiener-Hopf equations of the form

$$\begin{bmatrix} \tilde{\mathbf{R}}_{00}^{(k)} & \tilde{\mathbf{R}}_{01}^{(k)} & \ldots & \tilde{\mathbf{R}}_{0L-1}^{(k)} \\ \tilde{\mathbf{R}}_{01}^{(k)*T} & \tilde{\mathbf{R}}_{11}^{(k)} & \ldots & \tilde{\mathbf{R}}_{1L-1}^{(k)} \\ \vdots & \vdots & \vdots & \vdots \\ \tilde{\mathbf{R}}_{0L-1}^{(k)*T} & \tilde{\mathbf{R}}_{1L-1}^{(k)*T} & \ldots & \tilde{\mathbf{R}}_{L-1L-1}^{(k)} \end{bmatrix} \begin{bmatrix} \mathbf{h}_0^{(k)*} \\ \mathbf{h}_1^{(k)*} \\ \vdots \\ \mathbf{h}_{L-1}^{(k)*} \end{bmatrix} = \begin{bmatrix} \tilde{\mathbf{r}}_{d0}^{(k)*} \\ \tilde{\mathbf{r}}_{d1}^{(k)*} \\ \vdots \\ \tilde{\mathbf{r}}_{dL-1}^{(k)*} \end{bmatrix}$$

$$0 \leq k \leq L-1, \tag{5.4}$$

where the time average mean-square error [Ref. 9] is given by

$$\sigma_\epsilon^2 = R_d[0] - \frac{1}{L} \sum_{k=0}^{L-1} \sum_{j=0}^{L-1} \tilde{\mathbf{r}}_{dj}^{(k)T} \mathbf{h}_j^{(k)}. \tag{5.5}$$

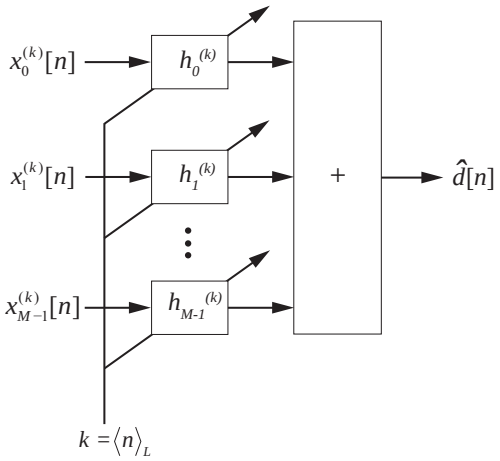

Figure 5.3. Reconstruction of the original signal from an ensemble of subsampled signals based on optimal linear filtering

Notice that this is an arithmetic mean of the set of σ_k^2, $0 \leq k \leq L-1$. The correlation terms are defined as

$$\tilde{\mathbf{r}}_{di}^{(k)} = \mathbf{D}_L^{(\langle k-i \rangle_L)} \tilde{\mathbf{r}}_{di} \tag{5.6}$$

$$\tilde{\mathbf{R}}_{ij}^{(k)} = \mathbf{D}_L^{(\langle k-i \rangle_L)} \tilde{\mathbf{R}}_{ij} \mathbf{D}_L^{(\langle k-j \rangle_L)^{*T}} \tag{5.7}$$

and

$$R_d[0] = \mathcal{E}\{d[n]d^*[n]\} \tag{5.8}$$

where

$$\tilde{\mathbf{r}}_{di} = \mathcal{E}\{d[n]\tilde{\mathbf{s}}_i^*[n]\} \tag{5.9}$$

and

$$\tilde{\mathbf{R}}_{ij} = \mathcal{E}\{\tilde{\mathbf{s}}_i[n]\tilde{\mathbf{s}}_j^{*T}[n]\}. \tag{5.10}$$

Solving the multirate Weiner-Hopf equations (5.4) yields a set of filter coefficients, which can be used in the estimation of $d[n]$ as depicted in Figure 5.3. The application of these filters to the observation data is illustrated in Figure 5.4.

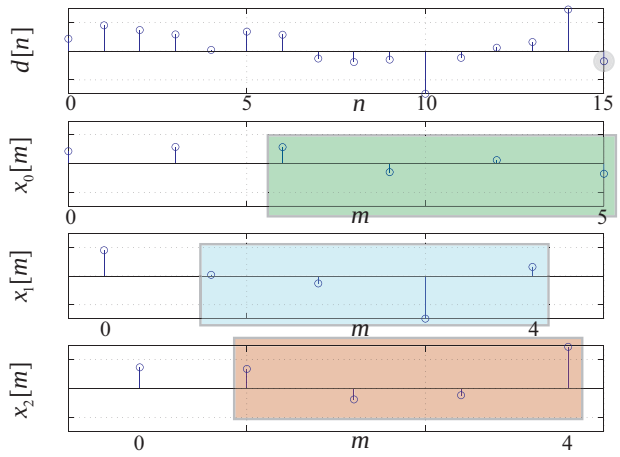

Figure 5.4. Reconstruction of the original signal from an ensemble of subsampled signals based on FIR Weiner filtering with decimation factor L = 3 and filter order P = 4. The figure illustrates the support of the time-varying filters $\mathbf{h}_i^{(k)}$ at a particular time, $n = 15$ and $k = 0$ (shaded circle).

The system equations can alternatively be derived using the appropriate mapping function. In this case, we find that the causal mapping function can be written

$$\mathcal{M}_{\text{sr}} : n \to \left\lfloor \frac{n-i}{L} \right\rfloor = \left\lfloor \frac{n}{L} \right\rfloor + \left\lfloor \frac{k-i}{L} \right\rfloor, \tag{5.11}$$

or

$$m_i = \mathcal{M}_{\text{sr}}(n), \tag{5.12}$$

where L is the decimation factor, and $k = \langle n \rangle_L$. Notice that the first term $\left\lfloor \frac{n}{L} \right\rfloor$ of the mapping function corresponds to the multirate filtering scenarios of Chapter IV; however, we require an additional corrective term $\left\lfloor \frac{k-i}{L} \right\rfloor$ to account for the translation between signals.

Notice that if

$$\left\lfloor \frac{n-i}{L} \right\rfloor = \left\lfloor \frac{n}{L} \right\rfloor + \left\lfloor \frac{k-i}{L} \right\rfloor,$$

using the definition (2.41) of the common residue $\langle n \rangle_L$, we can write

$$n = \left\lfloor \frac{n}{L} \right\rfloor L + \langle n \rangle_L.$$

Then, by direct substitution

$$\left\lfloor \frac{n-i}{L} \right\rfloor = \left\lfloor \frac{n}{L} - \frac{i}{L} \right\rfloor = \left\lfloor \frac{\left\lfloor \frac{n}{L} \right\rfloor L}{L} + \frac{\langle n \rangle_L}{L} - \frac{i}{L} \right\rfloor = \left\lfloor \left\lfloor \frac{n}{L} \right\rfloor + \frac{\langle n \rangle_L}{L} - \frac{i}{L} \right\rfloor.$$

Since $\left\lfloor \frac{n}{L} \right\rfloor$ is always an integer, it can be moved out of the floor operation (2.40), to obtain

$$\left\lfloor \frac{n-i}{L} \right\rfloor = \left\lfloor \frac{n}{L} \right\rfloor + \left\lfloor \frac{\langle n \rangle_L}{L} - \frac{i}{L} \right\rfloor.$$

By definition, $k = \langle n \rangle_L$; therefore, we can write

$$\left\lfloor \frac{n-i}{L} \right\rfloor = \left\lfloor \frac{n}{L} \right\rfloor + \left\lfloor \frac{k-i}{L} \right\rfloor.$$

Example 13. *As an example, for $L = 3$, we have the following mappings from a particular estimate index to the corresponding observation indices (recall that for the maximally decimated case with $L = 3$, $i = \{0, 1, 2\}$) as shown in Table 5.1.*

n	$m_i = \mathcal{M}_{sr}(n)$
12	$\{\lfloor \frac{12}{3} \rfloor + \lfloor \frac{0-i}{3} \rfloor\} = \{4, 3, 3\}$
13	$\{\lfloor \frac{12}{3} \rfloor + \lfloor \frac{1-i}{3} \rfloor\} = \{4, 4, 3\}$
14	$\{\lfloor \frac{12}{3} \rfloor + \lfloor \frac{2-i}{3} \rfloor\} = \{4, 4, 4\}$

Table 5.1. Causal mapping from an estimate signal index to the associated observation signal indices, for the maximally-decimated case, L=3.

These mapping transformations can be directly applied to the multi-channel, multi-rate Wiener-Hopf equations (4.62) and (4.65).

3. Reconstruction Methodology

The process used in the reconstruction of a signal from a set of subsampled observations is described as follows. First, a training signal, at the desired rate, is obtained that is representative of the class of signals that will be processed. From this signal, a maximally-decimated set of observations are derived and the single-rate statistical parameters are extracted. Then, using the Wiener-Hopf equations

developed in Section V.A.2, the filter coefficients are computed. With the class-specific filter coefficients, we are able to reconstruct signals "of the same class" by employing the estimate of (5.1). In other words, we use training data to develop the required filter coefficients from a class-representative signal at the desired rate, and apply these filters to any set of "representative" observations at a lower rate to reconstruct the desired signal.

4. Application results

a. Reconstruction of a Known Waveform

To evaluate the performance of the proposed method, two examples are presented. In the first example, a triangular waveform is considered for reconstruction. Our method was compared to the method described in [Ref. 31], which can produce an exact reconstruction of the triangular waveform if the highest frequency terms are left out. Both methods produce accurate results when there is no noise added to the observation sequences. When a small amount of noise is added to the observation sequences, the exact reconstruction method fails to reliably reproduce the signal while the method described here continues to produce a reasonably good approximation to the signal even under severely noisy conditions. The original triangular waveform is shown in Figure 5.5 (a). Also shown there are the reconstructed waveform (a) and the mean-square error (b).

The observation sequences are shown in Figure 5.6. These were constructed by shifting the original sequence, downsampling by a factor of $L = 3$, and adding white Gaussian noise. In this particular example, a signal-to-noise ratio (SNR) of -4.8dB was used. For our purposes, SNR is computed from the ratio of signal power to noise variance. Note that the underlying form of the original sequence is undetectable.

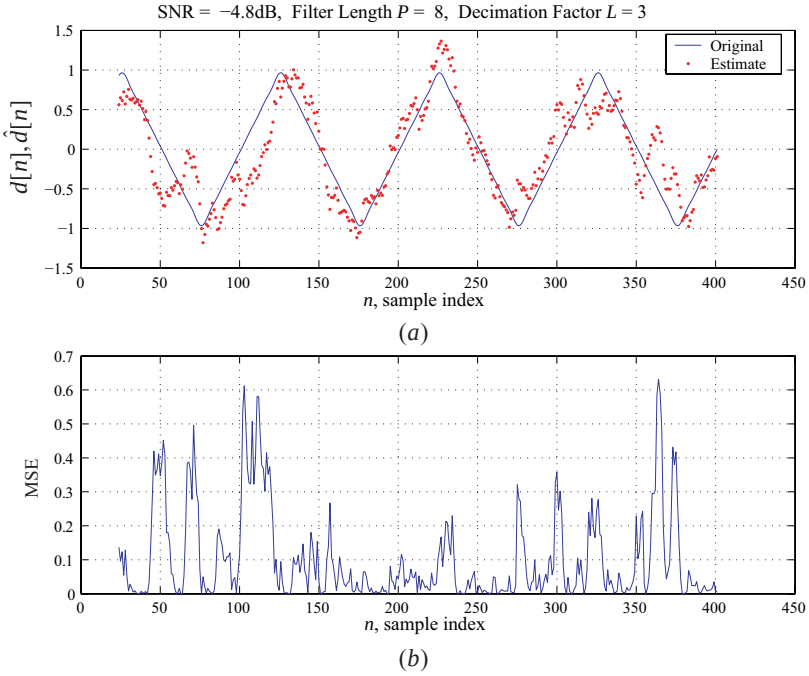

Figure 5.5. Simulation results using optimal linear filtering method for reconstruction; SNR $= -4.8$dB, $P = 8$, and $L = 3$.

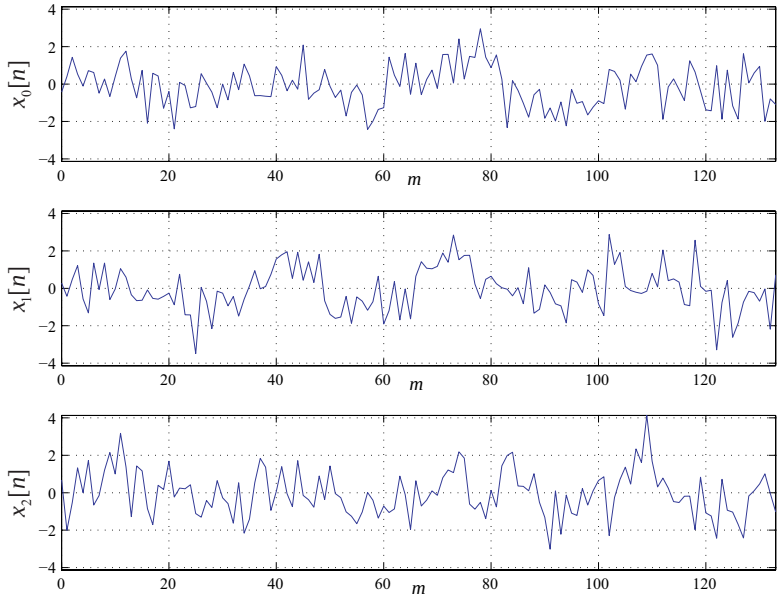

Figure 5.6. Observation sequences of an underlying triangle waveform after being subjected to additive white gaussian noise and subsampled by a factor of $L = 3$.

As a precursor to consideration of the two-dimensional image reconstruction problem, we applied the one-dimensional methods described here to image data.

b. Extension to Two-Dimensional Reconstruction

We consider each row of the observed LR images as an observation signal vector belonging to the set $\{\mathbf{x}_0[m], \mathbf{x}_1[m], \ldots, \mathbf{x}_{M-1}[m]\}$ (see Figure 5.7). Reconstruction is then accomplished line-by-line until every row of each image is processed. In this case, the original image is depicted in the left panel of Figure 5.8, and one of

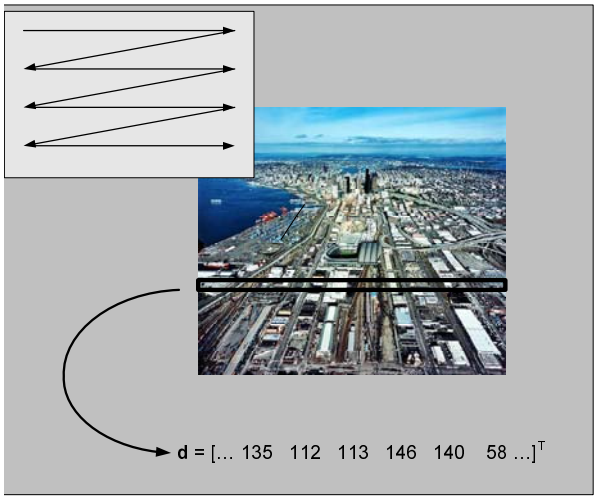

Figure 5.7. Line-by-line processing of observation images.

its three subsampled observation images with additive white Gaussian noise is given in the right panel. The image depicted in the left panel of Figure 5.9 represents the result of applying standard nearest-neighbor interpolation to one of the three noisy subsampled images, and the reconstructed image is shown on the right panel. Although the image is processed in only one direction, there is significant improvement over the interpolated image. In particular, note that edges of structures can be observed in many cases where the interpolated image does not provide such detail.

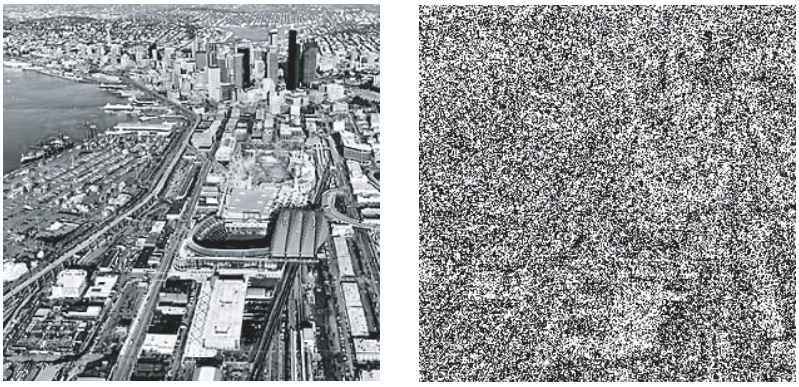

Figure 5.8. Original image (left); Subsampled observation image $L = 3$ with additive white Gaussian noise, 0dB (right).

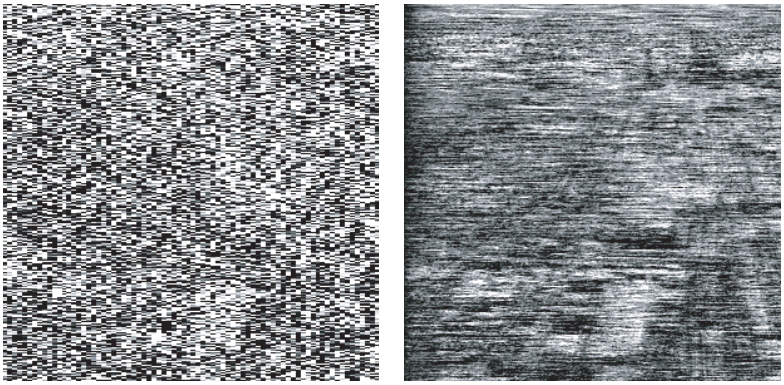

Figure 5.9. Result of applying standard nearest-neighbor interpolation to one of the three noisy subsampled images (left); Reconstructed image (right).

B. IMAGE RECONSTRUCTION

In this section, we consider the signal reconstruction problem in two dimensions, i.e., super-resolution (SR) image reconstruction. This analysis is an extension of the theory and application presented for the 1-D case. Specifically, we consider the problem of estimating a two-dimensional discrete random process, which cannot be observed directly, from a set of related observations, at a different sampling rate. Like the 1-D problem posed earlier, the observation signals are related to the random process through various forms of distortion and interference and these signals may also be shifted in time with respect to one another.

1. Observation Model

In the context of SR image reconstruction, the underlying two-dimensional signal (image) is at a high-rate (HR), and the observations are at some low-rate (LR). The relationship between the HR signal and a particular observation image ($(i,j)^{\text{th}} - \text{channel}$) is illustrated in the block diagram of Figure 5.10. This observation model shows that each LR observation is acquired from the HR image subject to distortion (typically blur), subpixel translation, downsampling, and channel noise. We can represent the observation model as

$$\mathbf{F}_{ij} = \mathbf{D}_{L_1}^{(i)} \mathbf{F} \mathbf{G}_{ij} \mathbf{D}_{L_2}^{(j)T} + \boldsymbol{\eta}_{ij}. \tag{5.13}$$

The matrix $\mathbf{F} \in \mathbb{R}^{ML_1 \times NL_2}$ represents the desired HR two-dimensional signal (image) with (MNL_1L_2) pixels. Its related LR observation is represented by the matrix $\mathbf{F}_{ij} \in \mathbb{R}^{M \times N}$. The matrix $\mathbf{G_{ij}}$ is a linear operator that accounts for channel distortion and matrix $\boldsymbol{\eta}_{ij}$ represents the channel noise. The parameters L_1 and L_2 represent the horizontal and vertical downsampling factors, respectively, and the parameters i and j represent the horizontal and vertical subpixel translation, respectively. The matrix

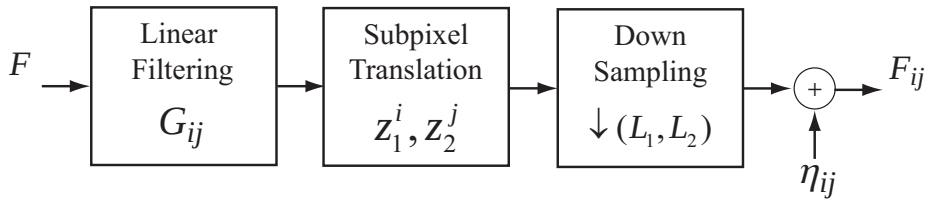

Figure 5.10. Observation model relating the HR image with an associated LR observation. Each LR observation is acquired from the HR image subject to distortion (typically blur), subpixel translation, downsampling, and channel noise.

$\mathbf{D}_L^{(k)}$ is a decimation matrix with delay, defined in (3.60), and is used to extract the appropriate pixels from the HR image to form a particular observation image. The matrix on the left incorporates the horizontal downsampling and translation (L_1, i) while the matrix on the right incorporates the vertical downsampling and translation (L_2, j). A maximally decimated set (see Section III.C.4) of images is obtained from

$$\{\mathbf{F}_{ij}\}, \quad i = 0, 1, \ldots, L_1 - 1, \; j = 0, 1, \ldots, L_2 - 1.$$

Example 14. *This example illustrates the operation of decimation matrices with delay on a HR image. Consider* $L_1 = L_2 = 3$, $i = 1$ *and* $j = 2$*; the HR image* $\mathbf{F}$ *with* $\mathbf{G}_{1,2} = \mathbf{I}$ *and* $\boldsymbol{\eta}_{1,2} = \mathbf{0}$:

$$\mathbf{F} = \begin{bmatrix} 0 & 1 & 2 & 3 & 4 & 5 \\ 6 & 7 & 8 & 9 & 10 & 11 \\ 12 & 13 & 14 & 15 & 16 & 17 \\ 18 & 19 & 20 & 21 & 22 & 23 \\ 24 & 25 & 26 & 27 & 28 & 29 \\ 30 & 31 & 32 & 33 & 34 & 35 \end{bmatrix} \begin{matrix} \mathbf{D}_3^{(1)} \begin{bmatrix} 0 & 1 & 0 & 0 & 0 & 0 \\ 0 & 0 & 0 & 0 & 1 & 0 \end{bmatrix} \\ \\ \mathbf{D}_3^{(2)} \begin{bmatrix} 0 & 0 & 1 & 0 & 0 & 0 \\ 0 & 0 & 0 & 0 & 0 & 1 \end{bmatrix} \end{matrix}$$

The product $\mathbf{F}_{1,2}$ *can be written*

$$\begin{bmatrix} 0 & 1 & 0 & 0 & 0 & 0 \\ 0 & 0 & 0 & 0 & 1 & 0 \end{bmatrix} \begin{bmatrix} 0 & 1 & 2 & 3 & 4 & 5 \\ 6 & 7 & 8 & 9 & 10 & 11 \\ 12 & 13 & 14 & 15 & 16 & 17 \\ 18 & 19 & 20 & 21 & 22 & 23 \\ 24 & 25 & 26 & 27 & 28 & 29 \\ 30 & 31 & 32 & 33 & 34 & 35 \end{bmatrix} \begin{bmatrix} 0 & 0 \\ 0 & 0 \\ 1 & 0 \\ 0 & 0 \\ 0 & 0 \\ 0 & 1 \end{bmatrix} = \begin{bmatrix} 8 & 11 \\ 26 & 29 \end{bmatrix}.$$

The observation image $\mathbf{F}_{1,2}$ *is one of nine* $(L_1 \times L_2)$ *possible configurations.* ■

2. Optimal Estimation

Consider the set of LR observations $\{\mathbf{F}_{ij}\}$ and the related HR image $\mathbf{F}$. We desire to form an estimate for the HR image by some weighted sum of the LR observations. The estimate can be written as

$$\hat{F}[n_1, n_2] = \sum_{i=0}^{L_1-1} \sum_{j=0}^{L_2-1} \langle \mathbf{f}_{ij}[n_1, n_2], \mathbf{H}_{ij}^{(k_1,k_2)} \rangle, \tag{5.14}$$

where the expression on the right represents the Frobenius inner product of the matrices , defined in Definition 12. Here, the matrix $\mathbf{f}_{ij}[n_1, n_2] \in \mathbb{R}^{P \times Q}$ is the set of pixels that form the region of support within the appropriate LR observation, required to form this estimate, and matrix $\mathbf{H}_{ij}^{(k_1,k_2)}$ is the corresponding set of filter coefficients. In this discussion, this region of support is called the *image mask* and its associated set of filter coefficients is called the *filter mask*. The filter masks are chosen to minimize the mean-square error

$$\mathcal{E}\{\|\vec{\mathbf{F}} - \hat{\vec{\mathbf{F}}}\|^2\}, \tag{5.15}$$

where the norm is the Frobenius norm; $\mathcal{E}\{\cdot\}$ is the expectation operator; $k_i = \langle n_i \rangle_{L_i}$ for $0 \leq k_i \leq L_i$; and (i, j) represent subpixel translation, with $0 \leq i \leq L_1 - 1$, $0 \leq j \leq L_2 - 1$, and $(i, j) \in \mathbb{Z}$. In the maximally-decimated case, i and j span the entire set $\{0, 1, \ldots, L_1 - 1\}$ and $\{0, 1, \ldots, L_2 - 1\}$, respectively. Both the set of LR

image masks$\{\mathbf{f}_{ij}[n_1, n_2]\}$ and filter masks $\{\mathbf{H}_{ij}^{(k_1,k_2)}\}$ are further described in Sections V.B.2(a) and V.B.2(c), respectively.

a. Index Mapping

Developing the LR image masks $\{\mathbf{f}_{ij}\}$ involves mapping indices in the HR sample index domain Ψ_F to those in the LR sample index domain Ψ_{ij}. For a given pixel intensity $F[n_1, n_2]$, the HR indices $[n_1, n_2]$ map to a set of LR sample indices $\{[m_1, m_2]_{ij}\}$, which correspond to pixel intensities $\{F_{ij}[m_1, m_2]\}$. The indices corresponding to each observation matrix $\mathbf{F}_{ij}$ are determined such that

$$|[n_1, n_2] - [m_1, m_2]_{ij}| \tag{5.16}$$

is minimized for each (i, j).

This mapping can be shown to be

$$[m_1, m_2]_{ij} = [\mathcal{M}_i(n_1), \mathcal{M}_j(n_2)], \tag{5.17}$$

where $\mathcal{M}[n]$ is defined

$$\mathcal{M} : n \rightarrow \left\lfloor \frac{n - i + \left\lfloor \frac{L}{2} \right\rfloor}{L} \right\rfloor = \left\lfloor \frac{n}{L} \right\rfloor + \left\lfloor \frac{k - i + \left\lfloor \frac{L}{2} \right\rfloor}{L} \right\rfloor, \tag{5.18}$$

$$m_i = \mathcal{M}_{\text{sr}}(n), \tag{5.19}$$

where $nT_d \in \Psi_d$, $m_i T_i \in \Psi_i$, $k = \langle n \rangle_L$, and L is the decimation factor. Notice that the first term $\left\lfloor \frac{n}{L} \right\rfloor$ of the mapping function corresponds to the multirate filtering scenarios of Chapter IV; however, we require an additional corrective term $\left\lfloor \frac{k-i}{L} \right\rfloor$ to account for the translation between signals.

b. LR Image Mask

The LR indices $[m_1, m_2]_{ij}$ for each observation represent the centroid of each of the LR image masks. Given a desired mask size of $P \times Q$, each LR image mask is comprised of the $P \times Q$ pixels closest to $\mathbf{F}_{ij}[m_1, m_2]$.

c. Filter Mask

If the desired HR image $\mathbf{F}$ and its observations $\{\mathbf{F}_{ij}\}$ are jointly homogeneous, then the linear filters $\mathbf{H}_{ij}^{(k_1,k_2)}$ required for optimal estimation are periodically

spatially-varying, an extension of [Ref. 7]. This periodicity can be described in terms of the "phase" (k_1, k_2), where $k_i = n_i \bmod L_i$. If we define the set of *least positive residues* as $\Lambda_k = 0, 1, \ldots, k-1$, then $k_1 \in \Lambda_{L_1}$ and $k_2 \in \Lambda_{L_2}$, and all possible combinations of phase can be represented as $\Lambda_{L_1} \times \Lambda_{L_2}$.

Figures (5.11) and (5.12) depict the phase variation for $L_1 = L_2 = 2$. In this case, $\Lambda_2 = \{0, 1\}$ and $\Lambda_2 \times \Lambda_2 = \{(0,0), (0,1), (1,0), (1,1)\}$. The spatial periodicity of the phase can be observed by noting the regular recurrence of phase terms.

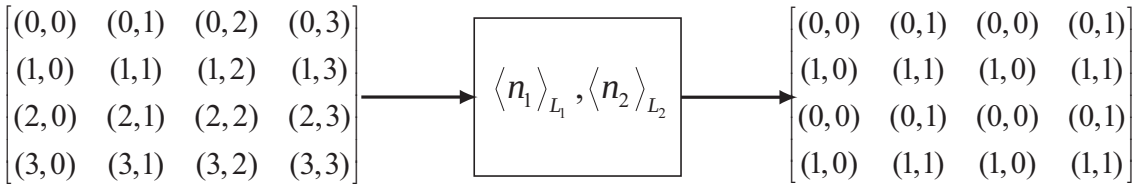

Figure 5.11. Index representation to modulo representation with $L_1 = L_2 = 2$ (note the spatial phase periodicity).

3. Reconstruction Methodology

a. Least Squares Formulation

In order to determine the filter masks $\{\mathbf{H}_{ij}^{(k_1,k_2)}\}$ required to estimate the HR image, a least squares (LS) approach is employed. We identify the set of all HR pixels that correspond to a given phase and denote this set of HR pixels as the matrix $\mathbf{F}^{(k_1,k_2)}$. This concept is depicted in Figure 5.12 where each shape corresponds to a unique phase (circle $(0,0)$, square $(0,1)$, triangle $(1,0)$, and star $(1,1)$). From (5.14), we can see that

$$\begin{bmatrix} \mathbf{F}[l_1, l_2] \\ \mathbf{F}[m_1, m_2] \\ \mathbf{F}[n_1, n_2] \\ \vdots \end{bmatrix} = \begin{bmatrix} \sum_{ij} \langle \mathbf{f}_{ij}[l_1, l_2], \mathbf{H}_{ij}^{(k_1,k_2)} \rangle \\ \sum_{ij} \langle \mathbf{f}_{ij}[m_1, m_2], \mathbf{H}_{ij}^{(k_1,k_2)} \rangle \\ \sum_{ij} \langle \mathbf{f}_{ij}[n_1, n_2], \mathbf{H}_{ij}^{(k_1,k_2)} \rangle \\ \vdots \end{bmatrix}, \tag{5.20}$$

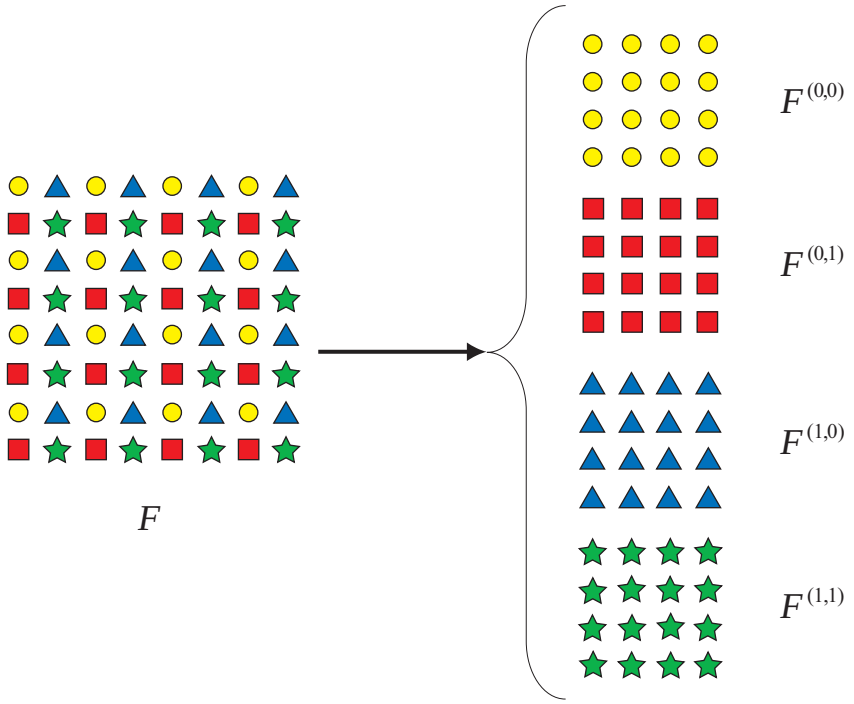

Figure 5.12. Relationship between HR pixels and spatially-varying filter masks in formulating the LS problem with $L_1 = L_2 = 2$.

where the left hand expression is $\tilde{\mathbf{F}}^{(k_1,k_2)}$. From this, we can write

$$\tilde{\mathbf{F}}^{(k_1,k_2)} \stackrel{\text{ls}}{=} \mathbf{\Phi}\tilde{\mathbf{H}}_{ij}^{(k_1,k_2)}, \tag{5.21}$$

where $\mathbf{\Phi}$ is the data matrix. This system of equations is solved in a least squares sense for the required set of filter masks at each phase $\{\mathbf{H}_{ij}^{(k_1,k_2)}\}$.

b. Processing Method

The process used in the SR image reconstruction of a set of LR observations is described as follows. First, a HR training image is obtained that is representative of the class of images that will be processed. From this image, a maximally-decimated set of LR observations are derived and then through the least squares methodology of Section V.B.3(a), filter coefficients are computed. With the class-specific filter coefficients, we are able to reconstruct images "of the same class" by employing the estimate of (5.14). In other words, we use training data to develop

filter masks from a class-representative HR image, and then apply these filters to any set of "representative" LR observations to reconstruct a HR image.

4. Application Results

In order to evaluate the performance of this method of image reconstruction, we process the "skyline" image depicted in Figure 5.13, subject to varying degrees of AWGN. The image used for the training process is the 204×204 pixel image segment depicted in this figure. From this image, a set of filter coefficients is derived that is used in SR image reconstruction.

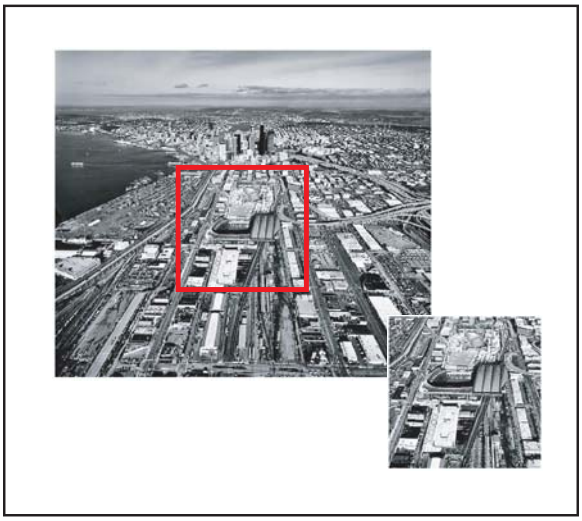

Figure 5.13. Image segment used to train filter.

The target or object of the reconstruction is depicted in Figure 5.14. From this 204×204 pixel image segment, LR observations are derived and are filtered using the class-specific filter masks. The same level of AWGN is used for the training and the target images.

Figure 5.15 depicts three members of the set of LR observations with various subpixel translations. The first image represents subpixel translation by one pixel in the horizontal direction and no translation in the vertical direction. The second represents translation by one pixel in both the vertical and horizontal directions. The third image represents translation by two pixels in both directions.

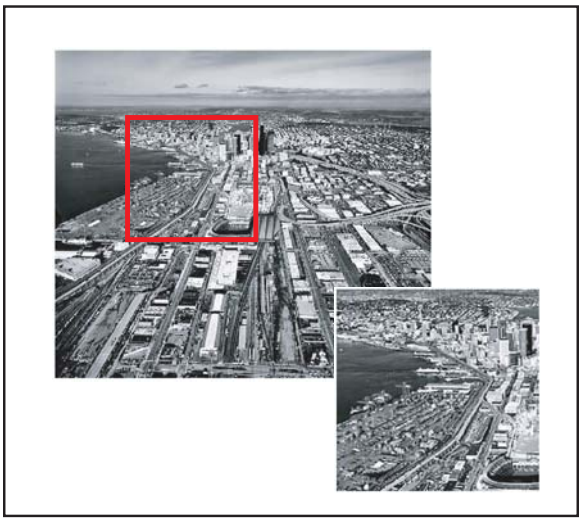

Figure 5.14. Image segment to be estimated.

In the remaining figures, the left panel depicts the SR image reconstruction using the proposed algorithm and the right panel depicts nearest-neighbor interpolation of one of the LR observations. In every case, the proposed method is superior to the interpolated result. During these experiments, other interpolation methods were considered, including bilinear and bicubic methods; again, the proposed method was found to be superior.

Figure 5.16 compares reconstructed and interpolated images for the case of no additive noise, downsampling by 3 in both the vertical and horizontal directions, and with filter mask size of 3×3. In this case, the reconstruction yields a result that is visibly indiscernible from the target image.

Figure 5.17 compares reconstructed and interpolated images for the case of an SNR $= 5$ dB, downsampling by 3 in both the vertical and horizontal directions, and with filter mask size of 3×3. In this case, we see the effects of additive noise on the reconstruction. Despite some blurring of edges, details are still discernible.

Figure 5.18 compares reconstructed and interpolated images for the case of an SNR $= -1.5$ dB, downsampling by 3 in both the vertical and horizontal directions, and with filter mask size of 3×3. In this case, the effects of additive noise on

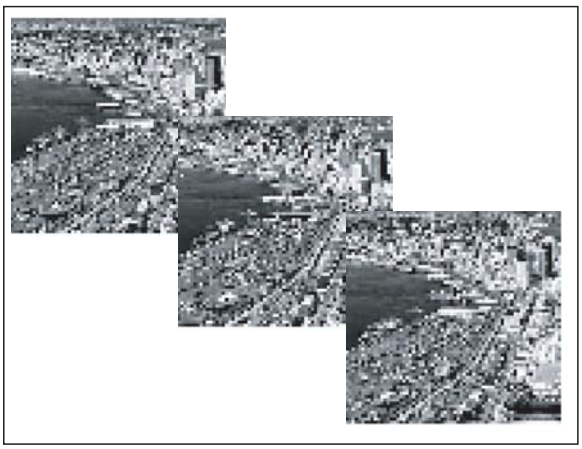

Figure 5.15. Downsampled observation images with subpixel translations $(1,0)$, $(1,1)$, and $(2,2)$, respectively; $L_1 = L_2 = 3$, $P = Q = 3$, and no AWGN.

the reconstruction are quite deleterious. Further blurring of edges is evident and details have become hard to see. However, major features in the image are still discernible. Thus, there is a significant advantage in using the proposed method over interpolation, where not even major features are discernible. Note that the poorer performance of the interpolation methods is not unexpected. In this case, *only* a single LR observation image is used for reconstruction while in the case of the proposed method, multiple, independent LR observations are used. Despite this obvious disadvantage, the interpolation methods are used throughout the literature as a benchmark [Ref. 1, 2, 28] and we follow here.

C. CHAPTER SUMMARY

In this chapter, the signal and image reconstruction problem is considered from a multirate point of view (Chapter III), using the multirate optimal estimation theory presented in Chapter IV.

First, the problem of reconstruction is posed in one dimension, in terms of a set of observation sequences that are related to a desired random sequence. An observation model is presented that models this relationship, accounting for linear

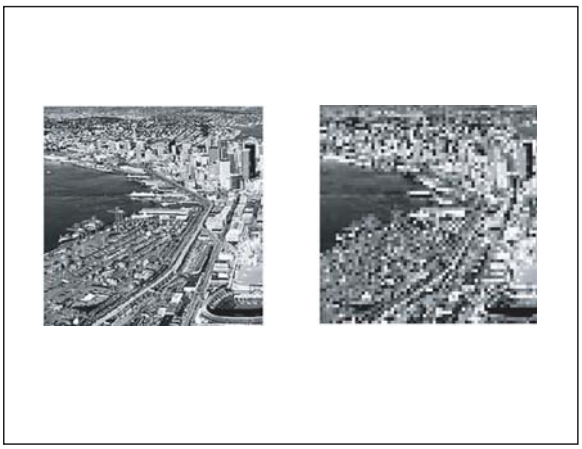

Figure 5.16. Comparison between a reconstructed image and interpolated image; $L_1 = L_2 = 3$, $P = Q = 3$, no AWGN.

distortion, additive noise, downsampling, and subsample translation. Signal reconstruction is achieved by forming an estimate comprised of a linear combination of samples of the observation sequences, and then developing and solving a set of related linear equations for the required filter coefficients. These coefficients are used to filter LR data. Finally, the results of this proposed methodology are presented and compared to other reconstruction methods.

Next, the super-resolution reconstruction problem is considered and posed in terms of a set of 2-D observation sequences that are related to a desired 2-D random sequence. Again, an observation model is presented that models this relationship, accounting for linear distortion, additive noise, downsampling, and subpixel translation. Image reconstruction is achieved by forming a linear estimate comprised of a linear combination of pixels in each LR observation image mask and developing and solving a set of related linear equations for the required filter coefficients. Formation of these image masks is based on extension of the non-causal 1-D index mapping results to two dimensions. The resultant filter masks are used to filter LR image data. Finally, the results of the proposed methodology are presented and compared to other reconstruction methods.

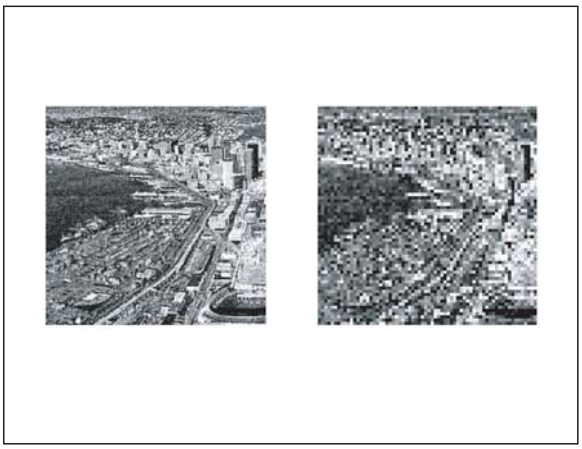

Figure 5.17. Comparison between a reconstructed image and interpolated image; $L_1 = L_2 = 3$, $P = Q = 3$, and SNR = 5 dB.

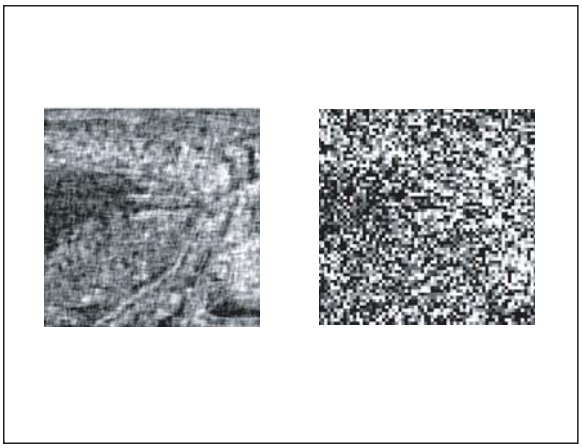

Figure 5.18. Comparison between a reconstructed image and interpolated image; $L_1 = L_2 = 3$, $P = Q = 3$, and SNR = -1.5 dB.

THIS PAGE INTENTIONALLY LEFT BLANK

VI. CONCLUSION AND FUTURE WORK

A. SUMMARY

In this dissertation, new signal processing methods for multirate signals in one and two dimensions are developed and applied to the problem of "super-resolution" signal and image reconstruction. In super-resolution processing a signal or image with high-resolution is constructed by using data from several images of a lower resolution.

A significant contribution of this work is the development of the theory of multirate systems, which provides the foundation upon which the proposed reconstruction methods are built. In developing this theory, a conceptual framework for the analysis of multirate systems is cited, which enables the extension of optimal estimation and linear filtering theory to multirate systems. Further, it leads to the concept of a system grid, which allows representation of the various signals in a multirate system on a common domain.

System theory for multirate systems, also developed here introduces multirate adaptations of the concepts of shift-invariance, periodic shift-invariance and causality. In addition, the input-output relation of a multirate system is discussed in terms of the system response and its associated Green's function and is adapted to the multirate problem in both system-level and signal-level representations. Finally, a method is adopted to provide matrix representations for the operations of downsampling, upsampling and linear filtering.

Another significant contibution of this work is the treatment of the problem of signal reconstruction from a multirate, optimal filtering perspective. Recognition that signal or image reconstruction can be viewed as a problem in signal estimation, where a related low-rate (low-resolution) signal or set of signals is used to estimate an underlying high-rate (high-resolution) signal, and that the observation signal or

signals and the desired signal form a multirate system, motivates this work. In particular, it suggests that extension of well-known results for single-rate systems could be extended to multirate signals and systems. In development of the resulting multirate forms of the Wiener-Hopf equations, the concept of index mapping is proposed. Index mapping systematically describes the relationship between samples of a signal at one rate to those of a signal at another rate and is particularly important for developing the required regions of support in linear filtering. In developing this relationship, both causal and non-causal mapping transformations are considered. The overall concept is more general, however, and provides a basis for the development of "generalized" multi-channel, multirate Wiener-Hopf equations.

In applying the multirate and optimal estimation theory results to the problem of signal and image reconstruction, a one-dimensional method is first explored. The analysis of this method starts with a simple test signal (a triangle wave) and its performance is evaluated on this known data. The procedure is then applied to image data when the image is processed along rows. Finally, the full two-dimensional problem of image reconstruction is considered and an image reconstruction methodology is developed. An example of the application of this method is provided with a comparison to results of other methods.

B. FUTURE WORK

As fundamental limits are reached in future image acquisition systems, interest in signal processing solutions will continue to intensify, and in particular, the area of super-resolution image reconstruction will likely be of great interest. During this research, advances were made in the areas of multirate signal processing and optimal

estimation theory, which led to development of the proposed reconstruction methods. With these findings, other research opportunities became apparent, and are mentioned here.

In the development of the multirate signal processing theory, several number theoretic results were obtained to describe the relationship between constituent signals in a multirate system. These results were shown to extend directly to the second moment analysis of such systems, but the second moment relationships were never entirely understood. Future work in characterizing second moments, and even higher moments, would provide further insight into the behavior of multirate systems. Furthermore, frequency-domain characterizations of such systems would also provide valuable insight, and would be a useful extension of [Ref. 12] on bifrequency and bispectrum maps.

In the analysis of performance, the 2-D method developed here was compared to standard interpolation methods, using a particular class of images. In future work, it would be beneficial to compare the proposed method to other "state of the art" algorithms [Ref. 1, 2]. Further, a more robust analysis of the proposed method's performance would be achieved if several classes of images were available for comparison. Finally, it would be useful to examine the effects of linear distortion, image rotation and non-Gaussian noise on performance.

Finally, in conducting this research, limitations were imposed on the sampling rate of constituent signals of a multirate system. For our purposes, sampling rates were constrained to be integer-valued. The theory developed in this work and in [Ref. 59] could be generalized to include cases where real-valued sampling rates are considered.

THIS PAGE INTENTIONALLY LEFT BLANK

LIST OF REFERENCES

[1] S. C. Park, M. K Park, and M. G. Kang. Super-resolution image reconstruction: A technical overview. *IEEE Signal Processing Magazine*, 20:21 – 36, May 2003.

[2] S. Chaudhuri, editor. *Super-resolution Imaging*. Kluwer Academic Publishers, 2001.

[3] C. W. Therrien. untitled. manuscript, 8 pages.

[4] A. Graham. *Kronecker Products and Matrix Calculus: with applications*. John Wiley & Sons, Inc., New York, NY, 1981.

[5] C. W. Therrien. *Discrete Random Signals and Statistical Signal Processing*. Prentice-Hall, Englewood Cliff, NJ, 1992.

[6] D. Koupatsiaris. Analysis of multirate random signals. Master's thesis, Naval Postgraduate School, Monterey, CA, 2000.

[7] C. W. Therrien. Issues in multirate statistical signal processing. In *Proc.* 35^{th} *Asilomar Conf. on Signals, Systems, and Computers*, volume 1, pages 573–576, November 2001.

[8] A. H. Hawes and C. W. Therrien. Least squares optimal filtering with multirate observations. In *Proc.* 36^{th} *Asilomar Conf. on Signals, Systems, and Computers*, volume 2, pages 1782–1786, November 2002.

[9] R. J. Kuchler and C. W. Therrien. Optimal filtering with multirate observations. In *Proc.* 37^{th} *Asilomar Conf. on Signals, Systems, and Computers*, volume 1, pages 1208–1212, November 2003.

[10] V. P. Sathe and P. P. Vaidyanathan. Effects of multirate systems on the statistical properties of random signals. In *IEEE Trans. SP*, volume 41, pages 131 – 146, January 1993.

[11] S. Akkarakaran and P. P. Vaidyanathan. New insights into multirate systems with stochastic inputs using bifrequency analysis. In *Proc. IEEE Int. Symp. on Circuits and Systems*, volume 5, pages 53 – 56, May 1998.

[12] S. Akkarakaran and P. P. Vaidyanathan. Bifrequency and bispectrum maps: a new look at multirate systems with stochastic inputs. In *IEEE Transactions on Signal Processing*, volume 48, pages 723 – 736, March 2000.

[13] O. Jahromi and P. Aarabi. Time delay estimation and signal reconstruction using multirate measurements. In *Proceedings of the 2003 International Conference on Multimedia and Expo*, volume 2, pages 597 – 600, July 2003.

[14] O. S. Jahromi, B. A. Francis, and R. H. Kwong. Multirate signal estimation. In *Proceedings of 2001 Canadian Conference on Electrical and Computer Engineering (CCECE 2001)*, volume 1, pages 147 – 152, May 2001.

[15] O. S. Jahromi. *Theory of multirate statistical signal processing.* PhD thesis, University of Toronto, Toronto, Ontario, Canada, 2002.

[16] O. S. Jahromi, B. A. Francis, and R. H. Kwong. Information theory of multirate systems. In *IEEE Int. Symp. on Information Theory (ISIT)*, page 188, June 2001.

[17] B. S. Chen and Y. L. Chen. Multirate modeling of ar/ma stochastic signals and its application to the combined estimation-interpolation problem. In *Proc. Int. Conf. Acoust., Speech, Signal Processing*, volume 43, pages 2302 – 2312, October 1995.

[18] B. S. Chen and C. W. Lin. Optimal design of deconvolution filters for stochastic multirate signal systems. *Signal Processing*, 47:287 – 305, 1995.

[19] C. W. Lin and B. S. Chen. State space model and noise filtering design in transmultiplexer systems. *Signal Processing*, 43:65 – 78, 1995.

[20] B. S. Chen and L. M. Chen. Optimal reconstruction in multirate transmultiplexer systems under channel noise: Wiener separation filtering approach. *Signal Processing*, 80:637 – 657, 2000.

[21] M. S. Spurbeck and L. L. Scharf. Least squares filter design for periodically correlated times series. *IEEE Workshop on Statistical Signal and Array Processing*, pages 267 – 270, June 1994.

[22] R. Cristi, D. A. Koupatsiaris, and C. W. Therrien. Multirate filtering and estimation: The multirate Wiener filter. In *Proc.* 34^{th} *Asilomar Conf. on Signals, Systems, and Computers*, volume 1, pages 450–454, October 2000.

[23] J. W. Scrofani and C. W. Therrien. A stochastic multirate signal processing approach to high-resolution signal reconstruction. In *Proc. Int. Conf. Acoust., Speech, Signal Processing*, 2005. Submitted.

[24] H. Ur and D. Gross. Improved resolution from sub-pixel shifted pictures. In *CVGIP: Graphical Models and Image Processing*, volume 54, pages 181 – 186, March 1992.

[25] T. Komatsu, K. Aizawa, T. Igarashi, and T. Saito. Very high-resolution imaging scheme with multiple different aperture cameras. In *Proc. IEEE*, volume 140, pages 19 – 25, February 1993.

[26] T. Komatsu, T. Igarashi, K. Aizawa, and T. Saito. Signal-processing based method for acquiring very high-resolution images with multiple cameras and its

theoretical analysis. In *Signal Processing: Image Commun.*, volume 5, pages 511 – 526, December 1993.

[27] M.S. Alam, J.G. Bognar, R.C. Hardie, and B.J. Yasuda. Infrared image registration and high-resolution reconstruction using multiple translationally shifted aliased video frames. In *IEEE Trans. on Instrum. Meas.*, volume 49, pages 915 – 923, October 2000.

[28] R. Y. Tsai and T. S. Huang. *Multiframe image restoration and registration*, pages 317 – 339. JAI Press Inc., Greenwich, CT, 1984.

[29] S. P. Kim, N. K. Bose, and H. M. Valenzuela. Recursive reconstruction of high-resolution image from noisy undersampled multiframes. In *Proc. Int. Conf. Acoust., Speech, Signal Processing*, volume 38, pages 1013 – 1027, June 1990.

[30] S. P. Kim and W.-Y. Su. Recursive high-resolution reconstruction of blurred multiframe images. In *IEEE Trans. on Image Processing*, volume 2, pages 534 – 539, October 1993.

[31] P. Vandewalle, L. Sbaiz, J. Vandewalle, and M. Vetterli. How to take advantage of aliasing in bandlimited signals. In *IEEE Conference on Acoustics, Speech and Signal Processing*, volume 3, pages 948–951, Montreal, Canada, May 2004.

[32] M. C. Hong, M. G. Kang, and A. K. Katseggelos. A regularized multi-channel restoration approach for globally optimal high-resolution video sequence. In *SPIE VCIP*, volume 3024, pages 1306 – 1317, February 1997.

[33] M. C. Hong, M. G. Kang, and A. K. Katseggelos. An iterative weighted regularized algorithm for improving the resolution of video sequences. In *Proc. Int. Conf. Image Processing*, volume 2, pages 474 – 477, October 1997.

[34] M. G. Kang. Generalized multi-channel image deconvolution approach and its applications. In *Opt. Eng.*, volume 37, pages 2953 – 2964, November 1998.

[35] N. K. Bose, S. Lertrattanapanich, and J. Koo. Advances in super-resolution using L-curve. In *Proc. Int. Symp. CAS*, volume 2, pages 433 – 436, May 2001.

[36] B. C. Tom and A. K. Katsaggelos. Reconstruction of a high-resolution image by simultaneous registration, restoration, and interpolation of low-resolution images. In *Proc. Int. Conf. Image Processing*, pages 2539–2542, 1995.

[37] R. R. Schultz and R. L. Stevenson. Extraction of high-resolution frames from video sequences. In *IEEE Trans. on Image Processing*, volume 5, pages 993 – 1011, June 1996.

[38] R. C. Hardie, K. J. Barndar, and E. E. Armstrong. Joint MAP registration and high-resolution image estimation using a sequence of undersampled images. In *IEEE Trans. on Image Processing*, volume 6, pages 1621 – 1633, December 1997.

[39] P. L. Combettes and M.R Civanlar. The foundations of set theoretic estimation. In *Proc. Int. Conf. Acoust., Speech, Signal Processing*, volume 4, pages 2921 – 2924, April 1991.

[40] H. Stark and P. Oskoui. high-resolution image recovery from image-plane arrays, using convex projections. *J. Opt. Soc. Am. A*, 6:1715 – 1726, 1989.

[41] A. M. Tekalp, M. K. Ozkan, and M. I. Sezan. High-resolution image reconstruction from lower-resolution image sequences and spaec varying image restoration. In *Proc. Int. Conf. Acoust., Speech, Signal Processing*, volume 3, pages 169 – 172, March 1992.

[42] M. K. Ozkan, A. M. Tekalp, and M. I. Sezan. POCS-based restoration of space-varying blurred images. In *Proc. Int. Conf. Image Processing*, volume 3, pages 450 – 454, July 1994.

[43] R. R. Schultz and R. L. Stevenson. A Bayesian approach to image expansion for improved definition. In *IEEE Trans. on Image Processing*, volume 3, pages 233 – 242, May 1994.

[44] M. Irani and S. Peleg. Improving resolution by image registration. In *CVGIP: Graphical Models and Image Processing*, volume 53, pages 231 – 239, May 1991.

[45] S. Mann and R. W. Picard. Virtual bellows: constructing high quality stills from video. In *Proc. Int. Conf. Image Processing*, volume 1, pages 363 – 367, November 1994.

[46] M. Irani and S. Peleg. Motion analysis for image enhancement resolution, occlusion, and transparency. In *J. Visual Commun. Image Represent.*, volume 4, pages 324 – 335, December 1993.

[47] M. Elad and A. Feuer. Restoration of a single super-resolution image from several blurred, noisy, and undersampled measured images. In *IEEE Trans. on Image Processing*, volume 6, pages 1646 – 1658, December 1997.

[48] D. Rajan and S. Chaudhuri. Generation of super-resolution images from blurred observations using an MRF model. In *J. Mathematical Imaging and Vision*, volume 16, pages 5 – 15, 2002.

[49] M. Elad and A. Feuer. Super-resolution restoration of an image sequence: adaptive filtering approach. In *IEEE Trans. on Image Processing*, volume 8, pages 387 – 395, March 1999.

[50] D. P. Simpson, editor. *Cassell's Latin Dictionary.* Wiley Publishing, Inc., New York, NY, 1968.

[51] H. B. Woolf, editor. *Webster's New Collegiate Dictionary.* G. & C. Merrian Co., Springfield, MA, 1977.

[52] A. V. Oppenheim, A. S. Willsky, and S. H. Nawab. *Signals & Systems*. Prentice Hall, Upper Saddle River, NJ, 1996.

[53] E. W. Weisstein. Mathworld. http://mathworld.wolfram.com.

[54] I. Stakgold. *Boundary Value Problems of Mathematical Physics*. Macmillan, New York, NY, 1967.

[55] W. W. Adams and L. J. Goldstein. *Introduction to Number Theory*. Prentice-Hall, Englewood Cliff, NJ, 1976.

[56] T. Nagell. *Introduction to Number Theory*. John Wiley & Sons, Inc., New York, NY, 1951.

[57] I. Niven and H. S. Zuckerman. *An Introduction to the Theory of Numbers*. John Wiley & Sons, Inc., New York, NY, 1980.

[58] J. H. McClellan and C. M. Rader. *Number Theory in Digital Signal Processing*. Prentice-Hall, Inc., Englewood Cliffs, NJ, 1979.

[59] R. J. Kuchler. *Theory of Multirate Statistical Signal Processing and Applications*. PhD thesis, Naval Postgraduate School, Monterey, CA, 2005.

[60] A. V. Oppenheim, R. W. Schafer, and J. R. Buck. *Discrete-Time Signal Processing*. Prentice Hall, Englewood Cliff, NJ, 1998.

[61] J. G. Proakis and D. G. Manolakis. *Digital Signal Processing: principles, algorithms, and applications*. Prentice-Hall, Englewood Cliff, NJ, 1996.

[62] T. A. Claasen and W. F. Mecklenbräuker. On the transposition of linear time-varying discrete-time networks and its application to multirate digital systems. *Philips J. Res.*, 23:78 – 102, 1978.

[63] L. A. Zadeh. Frequency analysis of variable networks. In *Proc. IRE*, volume 32, pages 291 – 299, March 1950.

[64] L. A. Zadeh. Time-varying networks. In *Proc. IRE*, volume 49, pages 1488 – 1503, October 1961.

[65] R. E. Crochiere and L. R. Rabiner. *Multirate Digital Signal Processing*. Prentice-Hall, Englewood Cliff, NJ, 1983.

[66] J. H. McClellan, R. W. Schafer, and M. A. Yoder. *Signal Processing First*. Pearson Prentice Hall, Upper Saddle River, NJ, 2003.

[67] D. A. Koupatsiaris. Analysis of multirate random signals. Master's thesis, Naval Postgraduate School, Monterey, CA, 2000.

[68] P. P. Vaidyanathan. *Multirate Systems and Filter Banks*. Prentice Hall, Englewood Cliffs, NJ, 1992.

[69] Y. Bar-Shalom, X. R. Li, and T. Kirubarajan. *Estimation with Applications to Tracking and Navigation*. John Wiley & Sons, Inc., Englewood Cliff, NJ, 2001.

[70] S. J. Orfanidis. *Optimum Signal Processing: An Introduction*. McGraw-Hill, New York, NY, 1988.

[71] N. Wiener. *Extrapolation, Interpolation, and Smoothing of Stationary Time Series*. MIT Press (formerly Technology Press), Cambridge, MA, 1949.

[72] N. Wiener. *Time Series*. MIT Press, Cambridge, MA, 1949.

[73] A. N. Kolmogorov. Interpolation and extrapolation von stationaren zufalligen folgen. *Bull. Acad. Sci. USSR*, 5:3 – 14, 1941.

[74] A. Papoulis. *Probability & Statistics*. Prentice Hall, Englewood Cliff, NJ, 1990.

INITIAL DISTRIBUTION LIST

1. Defense Technical Information Center
   Fort Belvoir, Virginia

2. Dudley Knox Library
   Naval Postgraduate School
   Monterey, California

3. Dr. Jeffrey B. Knorr, Code EC/Ko
   Department of Electrical and Computer Engineering
   Naval Postgraduate School
   Monterey, California

4. Dr. Charles W. Therrien, Code EC/Ti
   Department of Electrical and Computer Engineering
   Naval Postgraduate School
   Monterey, California

5. Dr. Carlos Borges, Code MA/Bc
   Department of Mathematics
   Naval Postgraduate School
   Monterey, California

6. Dr. Roberto Cristi, Code EC/Cx
   Department of Electrical and Computer Engineering
   Naval Postgraduate School
   Monterey, California

7. Dr. Robert Hutchins, Code Ec/Hu
   Department of Electrical and Computer Engineering
   Naval Postgraduate School
   Monterey, California

8. Dr. Murali Tummala, Code EC/Tu
   Department of Electrical and Computer Engineering
   Naval Postgraduate School
   Monterey, California

9. CDR James W. Scrofani
   Naval Postgraduate School
   Monterey, California